Development of Pavement Structural Analysis Tool (PSAT) for Iowa Local Roads

Final Report
March 2023

IOWA STATE UNIVERSITY
Institute for Transportation

Sponsored by
Iowa Highway Research Board
(IHRB Project TR-762)
Iowa Department of Transportation
(InTrans Project 18-670)

About the Program for Sustainable Pavement Engineering and Research

The overall goal of the Program for Sustainable Pavement Engineering and Research (PROSPER) is to advance research, education, and technology transfer in the area of sustainable highway and airport pavement infrastructure systems.

About the Institute for Transportation

The mission of the Institute for Transportation (InTrans) at Iowa State University is to save lives and improve economic vitality through discovery, research innovation, outreach, and the implementation of bold ideas.

Iowa State University Nondiscrimination Statement

Iowa State University does not discriminate on the basis of race, color, age, ethnicity, religion, national origin, pregnancy, sexual orientation, gender identity, genetic information, sex, marital status, disability, or status as a US veteran. Inquiries regarding nondiscrimination policies may be directed to the Office of Equal Opportunity, 3410 Beardshear Hall, 515 Morrill Road, Ames, Iowa 50011, telephone: 515-294-7612, hotline: 515-294-1222, email: eooffice@iastate.edu.

Disclaimer Notice

The contents of this report reflect the views of the authors, who are responsible for the facts and the accuracy of the information presented herein. The opinions, findings and conclusions expressed in this publication are those of the authors and not necessarily those of the sponsors.

The sponsors assume no liability for the contents or use of the information contained in this document. This report does not constitute a standard, specification, or regulation.

The sponsors do not endorse products or manufacturers. Trademarks or manufacturers' names appear in this report only because they are considered essential to the objective of the document.

Iowa DOT Statements

Federal and state laws prohibit employment and/or public accommodation discrimination on the basis of age, color, creed, disability, gender identity, national origin, pregnancy, race, religion, sex, sexual orientation or veteran's status. If you believe you have been discriminated against, please contact the Iowa Civil Rights Commission at 800-457-4416 or the Iowa Department of Transportation affirmative action officer. If you need accommodations because of a disability to access the Iowa Department of Transportation's services, contact the agency's affirmative action officer at 800-262-0003.

The preparation of this report was financed in part through funds provided by the Iowa Department of Transportation through its "Second Revised Agreement for the Management of Research Conducted by Iowa State University for the Iowa Department of Transportation" and its amendments.

The opinions, findings, and conclusions expressed in this publication are those of the authors and not necessarily those of the Iowa Department of Transportation.

Technical Report Documentation Page

1. Report No.	2. Government Accession No.	3. Recipient's Catalog No.
IHRB Project TR-762		

4. Title and Subtitle	5. Report Date
Development of Pavement Structural Analysis Tool (PSAT) for Iowa Local Roads	March 2023
	6. Performing Organization Code

7. Author(s)	8. Performing Organization Report No.
Nazik Citir (orcid.org/0000-0001-5163-7421), Halil Ceylan (orcid.org/0000-0003-1133-0366), Sunghwan Kim (orcid.org/0000-0002-1239-2350), Danny Waid (orcid.org/0000-0002-1652-2028), Brian P. Moore (orcid.org/0000-0003-1746-009X), and In-Ho Cho (orcid.org/0000-0002-2265-9602)	InTrans Project 18-670

9. Performing Organization Name and Address	10. Work Unit No. (TRAIS)
Program for Sustainable Pavement Engineering & Research (PROSPER) Iowa State University 2711 South Loop Drive, Suite 4700 Ames, IA 50010-8664	11. Contract or Grant No.

12. Sponsoring Organization Name and Address	13. Type of Report and Period Covered
Iowa Highway Research Board Iowa Department of Transportation 800 Lincoln Way Ames, IA 50010	Final Report
	14. Sponsoring Agency Code IHRB Project TR-762

15. Supplementary Notes

Visit https://prosper.intrans.iastate.edu/ for color pdfs of this and other research reports.

16. Abstract

Iowa has three classes of public roads: state primary highways, county (secondary) roads, and city streets. Among these, Iowa county roads serve rural Iowa transport needs by assuring a public road connection (i.e., to local access roads) for serving as conduits that channel the flow of people and commodities to and from towns and terminals (i.e., farm-to-market roads). Many Iowa county pavement systems are multilayered structures that have experienced multiple cycles of construction and renewal that make it more complex to estimate pavement structures' current structural capacities.

This study developed a Microsoft Excel macro and Visual Basic for Applications (VBA)-based automated Pavement Structural Analysis Tool (PSAT) with three analyzing options—asphalt concrete (AC) pavement systems with 1 to 10 layers on a (1) stabilized base, (2) granular base, and (3) stabilized base and granular base—to estimate the current structural capacities of in-service pavement systems by following consecutive sections within the user-friendly platform. To address this aim, a systematic approach to develop a highly realistic annotated synthetic database was created for use in artificial neural network (ANN)-based pavement response prediction models that required inputs of pavement materials and structural features and outputs of pavement responses, deflections, and strains at critical locations within the pavement structure. In addition, the equivalent layer theory (ELT) concept was integrated into the PSAT to simplify multilayered pavement systems into three-layered systems—an asphalt layer, a base layer, and a subgrade layer. Thus, it could make it easier for an Iowa county engineer to understand the current structural capacities of in-service county pavements. Mechanistic- and empirical-based approaches were also integrated into the tool to estimate the remaining service life (RSL) associated with two types of major failures for flexible pavements, namely fatigue and rutting failures, by relating pavement responses predicted by the ANN models through transfer functions. The PSAT is expected to be used as part of routine pavement analysis, design, and asset management practices for better prioritization and allocation of resources, as well as to support effective communication related to pavement needs both with the public and with elected officials.

17. Key Words	18. Distribution Statement
artificial intelligence—artificial neural networks—Iowa county pavements—pavement performance prediction—pavement structural capacity—PSAT—remaining service life	No restrictions.

19. Security Classification (of this report)	20. Security Classification (of this page)	21. No. of Pages	22. Price
Unclassified.	Unclassified.	142	NA

DEVELOPMENT OF PAVEMENT STRUCTURAL ANALYSIS TOOL (PSAT) FOR IOWA LOCAL ROADS

Final Report
March 2023

Principal Investigator
Halil Ceylan, Director
Program for Sustainable Pavement Engineering and Research (PROSPER)
Institute for Transportation, Iowa State University

Co-Principal Investigators
Sunghwan Kim, Research Scientist
In-Ho Cho, Associate Professor
Iowa State University

Danny Waid and Brian P. Moore
Iowa County Engineers Association Service Bureau (ICEASB)

Research Assistant
Nazik Citir

Authors
Nazik Citir, Halil Ceylan, Sunghwan Kim, Danny Waid, Brian P. Moore, and In-Ho Cho

Sponsored by
Iowa Highway Research Board and Iowa Department of Transportation
(IHRB Project TR-762)
Preparation of this report was financed in part through funds provided by the Iowa Department of Transportation through its Research Management Agreement with the
Institute for Transportation
(InTrans Project 18-670)

A report from
Program for Sustainable Pavement Engineering and Research (PROSPER)
Iowa State University
2711 South Loop Drive, Suite 4700
Ames, IA 50010-8664
Phone: 515-294-8103 / Fax: 515-294-0467
https://prosper.intrans.iastate.edu

TABLE OF CONTENTS

LIST OF FIGURES

LIST OF TABLES

ACKNOWLEDGMENTS

The authors gratefully acknowledge the Iowa Highway Research Board (IHRB) and Iowa County Engineers Association Service Bureau (ICEASB) for supporting this study. The Iowa county engineers who served on the technical advisory committee (TAC) for this project, including Lee Bjerke (Winneshiek County), Zach Gunsolley (Local Systems Bureau at Iowa Department of Transportation [DOT], previously at Union County), Todd Kinney (Clinton County), Mark Nahra (Woodbury County), John Riherd (Butler County), Brad Skinner (Appanoose County, previously at Montgomery County), Jacob Thorius (Washington County), and Karen Albert (Montgomery County), are also gratefully acknowledged for their guidance, support, and direction throughout the research. Special thanks are due to Steve De Vries (ICEASB) and Danny Waid (ICEASB), who developed the original concept of this study, and to Brian P. Moore (ICEASB), for his guidance, support, and direction throughout the research.

The authors would like to express their sincere gratitude to Ben Hull and Sean Malcolm from Lee County for their full support during the data collection and processing used to develop the models and tools resulting from this study. The authors would also like to express their sincere gratitude to Dr. M. Emin Kutay at Michigan State University, and other research team members from the Institute for Transportation's Program for Sustainable Pavement Engineering and Research (PROSPER) at Iowa State University for their assistance during the course of this project.

EXECUTIVE SUMMARY

In Iowa, most paved county roads are farm-to-market roads that connect vehicles to rural areas along area service roads. These roads were built decades ago and have been maintained ever since. About 70% of the road network consists of secondary roads, of which more than 20% are paved and hard surfaced. County road departments in each state have included future projects in both the County Five-Year Program and the federal-aid Transportation Improvement Program, and 30% of these road projects in Iowa are planned to be paved with hot-mix asphalt (HMA) and portland cement concrete (PCC). Considering that the paved and hard-surfaced roadways in Iowa counties that provide public and private access to property require constant maintenance and reconstruction, and that a considerable budget is allocated to them, these roads play a critical role in county engineers' job performance.

Many Iowa county pavement systems are comprised of several layers of pavement, each different with respect to age, thickness, stress level, material, condition, modulus, and impact of prior traffic; these layers have commonly been added and replaced multiple times over the years of pavement construction and renewal projects. As a result of the complexity of these pavement structures, Iowa county engineers face challenges in estimating their structural capacities to determine when or whether to manage, maintain, or rehabilitate county pavements in a cost-effective manner. Such challenges created a need to develop reliable and convenient-to-use methods and tools for Iowa county engineers to use in their routine pavement analysis, design, and asset management practices, as well as to support effective communication related to pavement needs both with the public and with elected officials.

The primary objective of this study was to develop a macro-enabled Microsoft Excel and Visual Basic for Applications (VBA)-based Pavement Structural Analysis Tool (PSAT) to help engineers predict the structural capacity, damage, and remaining service life (RSL) of Iowa county pavement systems in terms of fatigue and rutting failures by providing analysis options for three pavement types: asphalt concrete (AC) pavement systems with 1 to 10 layers on a (1) stabilized base, (2) granular base, and (3) stabilized base and granular base.

The PSAT considers the material and structural properties of the pavement layers (e.g., modulus, Poisson's ratio, and thickness) and traffic capacities of the roadway (equivalent single axle load [ESAL] or average daily traffic [ADT]). The tool is comprised of several successive sections, including capacities for predicting critical pavement responses, calculating equivalent thickness, converting traffic data from ADT to ESAL, identifying failure due to fatigue and rutting, determining a structural number (SN) of each layer, calculating damage, and a resulting RSL estimate.

This report includes an overview and evaluation of a new, systematic approach for generating a highly realistic annotated synthetic database for training deep neural networks in regression tasks and using this generated synthetic database to establish a detailed methodology for developing computational pavement structural analysis models and tools to represent field data characterizations. The field data were obtained from the Iowa Department of Transportation (DOT) Pavement Management Information System (PMIS) and Iowa County Engineers

Association Service Bureau (ICEASB). Ranges of pavement characteristics representing real pavement cases were selected from historical pavement databases and field investigations and based on past experiences.

To develop approaches for estimating the current structural capacities of pavement systems, artificial intelligence (AI)-based neural network (ANN) models were initially developed to predict critical pavement responses. A generated synthetic database that contains inputs of pavement layer properties and outputs of pavement responses computed by a high-performance layered elastic analysis program, MatLEA (MATLAB-based Layered Elastic Analysis), was used to train and test the ANN-based models.

The study performed a comprehensive investigation based on equivalent layer theory (ELT), a simplified method of approximation used in pavement structural analysis that combines overlaid pavement layers with different thicknesses and moduli into a single layer of equivalent thickness, to facilitate understanding of the structural capacities of pavement systems. The study also describes algorithms used to evaluate the structural capacities of in-service pavements in terms of allowable numbers of load repetitions, representing a mechanistic-based pavement design approach, and an SN resulting from an empirical design approach. The outcomes resulting from this project will facilitate decision-making in managing county paved road assets, improve overall pavement network performance levels, and enhance pavement preservation and rehabilitation practices.

The key findings from this study and recommendations for implementation are as follows:

- Developing a synthetic database proved to be a successful systematic approach that was used to boost the data set size; the current Iowa county pavement system lacks field data regarding inputs and outputs required for structural analysis.

- The ANN-based models were highly accurate in predicting critical pavement responses (e.g., deflections and strains) based on the pavement type, and this method requires no complex input parameters.

- The proposed ELT successfully simplified multilayered pavement systems into three-layered pavement systems with one AC layer, one base layer, and one subgrade layer. This simplified pavement system has the same stiffness as the original multilayered pavement system, making it easier for an Iowa county engineer to (1) understand the current structural capacities of in-service county pavements and (2) determine overlay design options for future cycles of rehabilitation.

- The proposed algorithms used transfer functions to estimate damage and RSL of in-service pavement systems and successfully related pavement responses (i.e., tensile strains at the bottom of an asphalt/stabilized base and compressive strains at the top of the subgrade) to fatigue and rutting failure. Then, by defining the current traffic capacities, damage and RSL for a given pavement section can be estimated.

- The user-friendly PSAT developed in this study makes it simple to follow consecutive sections after inputting the required information. AI-based models and mechanistic- and empirical-based design approaches that help predict pavement structural capacity and RSL, and thereby facilitate decision-making and managing of county pavement systems, have been successfully integrated into the tool.

- The Microsoft Excel-based PSAT could be integrated into Iowa county pavement asset management procedures comprised of data collection, data processing, data analysis, and data-driven decision-making steps.

- Future research directions were identified and recommended for the next phase of this study; they include fully implementing the pavement asset management procedure into the PSAT to better fulfill county engineers' needs. Other future research guidance can be divided into two categories: (1) short-term actions and (2) long-term actions. Short-term actions might include developing (a) a structural performance tool for rigid (concrete) pavements and (b) a structural overlay design tool. Long-term actions might include developing (a) an approach for relating mechanistic-based failures to pavement distresses, (b) a smartphone application version of the PSAT, (c) a platform integrating the Iowa Pavement Analysis Techniques (IPAT), PSAT, and CyROID (for road performance data collection) tools developed by the research team, and (d) a functional overlay design tool.

CHAPTER 1. INTRODUCTION

Problem Statement

Iowa has three classes of public roads: state primary highways, county (secondary) roads, and city streets (ICEA 2022). Among these, Iowa county roads serve rural Iowa transport needs by ensuring a public road connection (i.e., to local access roads) for every parcel of land and serving as conduits that collect the flow of people and commodities, channeling them to and from towns and terminals (i.e., farm-to-market roads). According to the Iowa County Engineers Association (ICEA) (2022), "Even though county roads are considered 'low volume,' the daily travel they carry is equivalent to a single vehicle making 60 round trips to the moon." Iowa has more than 19,000 miles of paved and hard-surfaced secondary roads to support significant traffic levels, heavy truck movement, and year-round service.

Many Iowa county pavement systems have multilayered pavement structures resulting from multiple cycles of pavement construction and renewal projects. Each such layer has a particular age, thickness, stress level, material, physical condition, modulus, and prior traffic impact. Such complex pavement structures challenge the capabilities of Iowa county engineers to estimate structural capacities of in-service pavements and to develop cost-effective decision-making strategies for management, maintenance, and rehabilitation of county pavement systems. This challenge creates a need to develop reliable and accessible methods and tools for Iowa county engineers to use in their routine pavement analysis, design, and asset management practices, as well as to support effective communication related to pavement needs both with the public and with elected officials.

Since the early 1960s, mechanistic-empirical (ME) methods for designing and analyzing pavement structures have been developed. The fundamental premise of such methods is that traffic-induced structural responses (e.g., deflection, strain, and stress) determined by mechanistic analysis are, through transfer functions (or empirical distress models), predictive of pavement distresses such as fatigue cracking and rutting, the primary structural failure modes in flexible pavements. Multilayered elastic analysis is the primary method used in current ME pavement design procedures to determine pavement response to traffic loading and environmental factors. Alternatively, while nondestructive evaluation (NDE) and structural health monitoring (SHM) techniques—such as falling weight deflectometer (FWD) tests as an external NDE method for surface deflection and *in situ* pavement sensors for strain measurements—can be utilized to determine pavement responses, such approaches can be computationally or economically costly and create additional challenges for county engineers.

Research Objectives and Scope

The primary objective of this research was to develop an easy-to-use Pavement Structural Analysis Tool (PSAT) for use by county engineers in routine pavement analysis, design, and asset management practices, as well as to support effective communication regarding pavement needs, both to the public and to elected officials. To accomplish this objective, the PSAT required the following specific features:

- Analysis capacity for a multilayered pavement system in which each layer has a unique age, thickness, material, physical condition, modulus, and prior traffic impacts
- No complex input preparation
- Real-time computation capability
- End-user friendliness with respect to inputs and outputs

Report Organization

This report consists of eight chapters and an appendix as described in the following paragraphs.

Chapter 1 provides an introduction, including problem statement, research objectives, and scope of the project.

Chapter 2 presents a review of the equivalent layer theory (ELT) concept that includes evaluation of different ELTs and compares them in terms of pavement responses.

Chapter 3 describes the detailed step-by-step methodology for development of a synthetic database derived from real pavement data obtained from the Iowa Department of Transportation (DOT) and the ICEA Service Bureau (ICEASB). Developing an artificial intelligence (AI)-based neural network (ANN) model requires a reliable and comprehensive database that correctly characterizes different pavement scenarios, and input and output parameters of ANN models were prepared in this section. First, input parameters for structural design and mechanical properties such as the modulus of elasticity, Poisson's ratio, and thickness of the pavement layers, were used to compute output parameters and critical pavement responses such as deflection and strain using the MatLEA (MATLAB-based Layered Elastic Analysis) program. Next, the generated input data set and corresponding output data set were used to train the ANN models, with a total of 30 different pavement systems divided into 3 major groups: pavements with (1) a stabilized base, (2) a granular base, and (3) both a stabilized base and granular base/subbase. Each group was comprised of 10 different pavement types, each with 1 to 10 layers of hot-mix asphalt (HMA) and representing 50,000 different pavement cases.

Chapter 4 describes a methodology for the development of ANN models using the generated synthetic database. A total of six ANN models were developed for each major pavement system including those with (1) a stabilized base, (2) a granular base, and (3) a stabilized base and granular base/subbase for both (a) deflection and (b) strain prediction.

Chapter 5 explains the methodology of the development of an algorithm for estimating the current structural capacities of Iowa county roads. It presents and compares current techniques for calculating structural capacities based on the primary structural failure modes of flexible pavement (e.g., fatigue and rutting). A combination of a mechanistic-based pavement design approach (e.g., allowable number of load repetitions) and an empirical design approach (e.g., structural number [SN]) was utilized to define the structural capacities of pavement systems. Based on the synthetic database used to develop the ANN models, the existing failure algorithms were calibrated where needed.

Chapter 6 presents the methodology of the macro-enabled Microsoft Excel-based PSAT by describing inputs and outputs for all types of pavement systems involved in pavement analysis.

Chapter 7 presents the overall research conclusions emerging from the entire study, including specified findings.

Chapter 8 summarizes recommendations for implementation and future research directions suggested by this study.

The appendix provides examples of the MATLAB software source code for computing pavement responses for multiple multilayered pavement systems (modified MatLEA code) and the Python source code for developing the ANN models.

In addition, as part of this project, the research team also developed a user guide on how to use the PSAT described in Chapter 6.

CHAPTER 2. BACKGROUND

Review of the ELT Concept

An infinite half-space model is characterized by pavement layers represented by their moduli, thicknesses, and Poisson's ratios, over a subgrade of infinite thickness. Theoretical assumptions generally used to idealize a pavement structure include the following:

- Pavement layers are assumed to be linear elastic, so after some simplification the Boussinesq equations will be valid and can be adapted to calculate stresses and strains at random locations in the model
- Material properties in each layer are homogeneous and isotropic, meaning that elastic properties are the same at all points and in all directions in a given material
- Each layer, except for the infinitely thick subgrade layer, has finite thickness in the longitudinal dimension, and all are infinite in extent in the lateral dimension

In ELT, which is used as a simple method of approximation in pavement structural analysis, overlaid pavement layers with different thicknesses and moduli are combined into a single layer of equivalent thickness (h_{eq}). It is based on the principle that the equivalent layer has the same stiffness as the original layer and has the same pressure distribution under the layer. Figure 1 shows a representation of ELT, where pavement layers with different thicknesses (h_i), moduli (E_i), and Poisson's ratios (ν_i) on subgrade are transformed into a single layer with an equivalent thickness (h_{eq}) on subgrade.

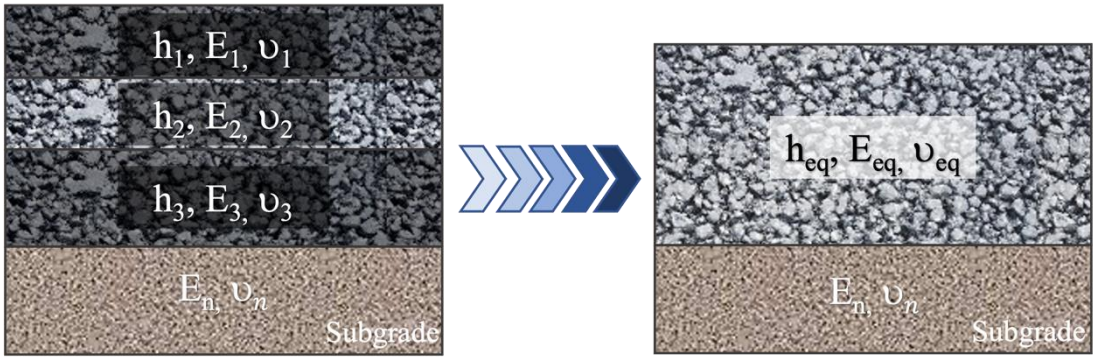

Figure 1. ELT application to transform a multilayered pavement system into a single layer

There are many equations and theories to more accurately determine h_{eq}, and some will be presented in the following sections.

Odemark's Equivalent Layer Thickness Theory

The ELT was originally proposed by Odemark (1949). It assumes that the strains and stresses below a layer depend on the stiffness of that layer only. In other words, changing the thickness,

modulus, and Poisson's ratio of layers without changing their stiffness should keep the stress and strains below the layer unchanged. Based on this concept, ELT can be used to convert a multilayered system consisting of layers with different moduli and Poisson's ratios into a single equivalent-layer system in which all layers have the same modulus.

The stiffness of a structure can be calculated using equation 1.

$$D = \frac{\mathrm{E}h^3}{12(1-\mu^2)} \quad \textbf{(1)}$$

where:

D = Stiffness
E = Modulus of elasticity
h = Layer thickness
μ = Poisson's ratio

For a two-layered system, the equivalent thickness can be expressed by equating the stiffnesses of both layers (i.e., $D_1 = D_2$), as shown in equation 2, representing a first layer with modulus (E_1), thickness (h_1), and Poisson's ratio (μ_1) and a second layer with modulus (E_2), thickness (h_2), and Poisson's ratio (μ_2).

$$\frac{E_1 h_1^3}{12(1-\mu_1^2)} = \frac{E_2 h_2^3}{12(1-\mu_2^2)}$$

Or, after rearranging the equation, it is as follows:

$$h_{equivalent} = h_2 = h_1 \left[\frac{E_1}{E_2}\left(\frac{1-\mu_2^2}{1-\mu_1^2}\right)\right]^{1/3} \quad \textbf{(2)}$$

where:

$h_{equivalent}$ = Equivalent thickness
$E_{1,2}$ = Actual elastic modulus of asphalt layer 1 and 2
$h_{1,2}$ = Actual thickness of asphalt layer 1 and 2
$\mu_{1,2}$ = Actual Poisson's ratio of asphalt layer 1 and 2

For a multilayered system, equation 3 can be used, resulting in an equation similar to equation 2 but applicable to more than two layers.

$$h_{eqi} = \sum_{i=1}^{n-1}\left(h_{\mathrm{i}}\left[\frac{E_{\mathrm{i}}}{E_{\mathrm{n}}}\left(\frac{1-\mu_{\mathrm{n}}^2}{1-\mu_{\mathrm{i}}^2}\right)\right]^{1/3}\right) \quad \textbf{(3)}$$

where:

h_{eqi} = Equivalent thickness of ith layer
E_i = Elastic modulus of ith layer
h_I = Thickness of ith layer
μ_I = Poisson's ratio of ith layer
E_n = Elastic modulus of nth layer
h_n = Thickness of nth layer
μ_n = Poisson's ratio of nth layer

Nijboer's Equivalent Layer Thickness Theory

Nijboer (1955) developed his theory using the same approach as Odemark in which the bending moments (expressed by the quantity Eh^3) of the original multiple layers and the equivalent layer are the same, but there is a second condition for the location of the neutral axis. This second condition requires that the actual depth of the neutral axis should also be the same. Using this approach, the equivalent layer thickness and modulus can be calculated using equation 4. In this theory, the Poisson's ratios ($\mu_1 = \mu_2 = \mu_0$) of all layers are assumed equal.

$$E_{equivalent\ (I)} = \left(\frac{h_2}{h_1} + \frac{E_1}{E_2}\right)^2 \times \frac{\left(\frac{h_2}{h_1}\right)^4 + 4\times\left(\frac{h_2}{h_1}\right)^3\times\left(\frac{E_1}{E_2}\right) + 6\times\left(\frac{h_2}{h_1}\right)^2\times\left(\frac{E_1}{E_2}\right) + 4\times\left(\frac{h_2}{h_1}\right)\times\left(\frac{E_1}{E_2}\right) + \left(\frac{E_1}{E_2}\right)^2}{\left(\left(\frac{h_2}{h_1}\right)^2 + 2\times\frac{h_2}{h_1} + \frac{E_1}{E_2}\right)^3} \times E_2$$

$$h_{equivalent\ (I)} = \left[\frac{\left(\frac{h_2}{h_1}\right)^2 + 2\times\left(\frac{h_2}{h_1}\right) + \left(\frac{E_1}{E_2}\right)}{\left(\frac{h_2}{h_1} + \frac{E_1}{E_2}\right)\times\left(1 + \frac{E_1}{E_2}\right)}\right]^{1/3} \times (h_1 + h_2) \quad \textbf{(4)}$$

where:

$E_{equivalent\ (I)}$ = Equivalent modulus by Nijboer (I) method
$h_{equivalent\ (I)}$ = Equivalent thickness by Nijboer (I) method
$E_{1,2}$ = Actual elastic modulus of asphalt layer 1 and 2
$h_{1,2}$ = Actual thickness of asphalt layer 1 and 2

It should be noted that, in contrast with ordinary beams that have one neutral axis, multilayered pavement systems have several neutral surfaces. In Nijboer's second method (II), the condition on the placement of the neutral axis was eliminated and replaced by the condition that the equivalent layer thickness was equal to the sum of the layer thicknesses of two actual layers. Using this approach, the equivalent layer thickness and modulus can be calculated using equation 5.

$$E_{equivalent\ (II)} = \frac{\left(\frac{h_2}{h_1}\right)^4 + 4\times\left(\frac{h_2}{h_1}\right)^3\times\left(\frac{E_1}{E_2}\right) + 6\times\left(\frac{h_2}{h_1}\right)^2\times\left(\frac{E_1}{E_2}\right)+4\times\left(\frac{h_2}{h_1}\right)\times\left(\frac{E_1}{E_2}\right)+\left(\frac{E_1}{E_2}\right)^2}{\left(\left(\frac{h_2}{h_1}\right)+1\right)^3\times\left(\left(\frac{h_2}{h_1}\right)+\left(\frac{E_1}{E_2}\right)\right)} \times E_2$$

$$h_{equivalent\ (II)} = h_1 + h_2 \quad \textbf{(5)}$$

where:

$E_{equivalent\ (II)}$ = Equivalent modulus by Nijboer (II) method
$h_{equivalent\ (II)}$ = Equivalent thickness by Nijboer (II) method

The neutral axis of the pavement structure was calculated using the equivalent layer modulus method proposed by Albayati et al. (2018). Moduli differences in multiple layers of asphalt pavement under wheel load will cause a shift in the neutral axis toward the stiffer layer. Since the neutral axis of this pavement overlaps with the center of gravity of its transformed equivalent section, all calculations must be made relative to this neutral axis position. The three-layered system shown in Figure 2a was analyzed.

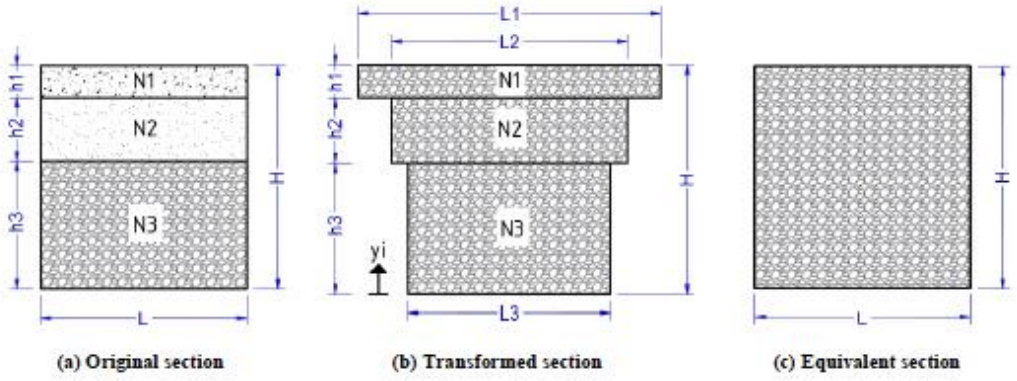

Albayati et al. 2018 / CC BY 4.0

Figure 2. Section properties of (a) multilayered pavement system, (b) transformed section, and (c) single layer pavement system

First, transformation factors are used to replace the layer moduli, E_1 and E_2, with the last layer modulus, E_3, using moduli ratios of $N_1, N_2, and\ N_3$ in equation 6a.

$$N_1 = \frac{E_1}{E_3},\ N_2 = \frac{E_2}{E_3},\ N_3 = \frac{E_3}{E_3} = 1$$

Then, $N_3 L_3 = L,\ L_1 = N_1 L,\ L_2 = N_2 L$ **(6a)**

The location of the centroid of the transformed equivalent section shown in Figure 2b is then calculated using equation 6b.

$$\mathrm{Y} = \frac{\sum_{i=1}^{n} y_i A_i}{\sum_{i=1}^{n} A_i} \quad \textbf{(6b)}$$

Next, the moment of inertia for each layer is calculated using equation 6c.

$$\mathrm{I}_i = \frac{L_i h_i^3}{12} + A_i d_i^2 \quad \textbf{(6c)}$$

Using calculated moments of inertia of each layer, the rigidity of equivalent layer can be expressed as in equation 6d.

$$\mathrm{E}_{equivalent}\mathrm{I}_{equivalent} = \sum_{i=1}^{n} E_i I_i \quad \textbf{(6d)}$$

Finally, the equivalent modulus and equivalent moment of inertia can be calculated using equation 6e, basically using it to transform the multilayered moduli into an equivalent modulus of a single layer.

$$\mathrm{E}_{equivalent} = \frac{\sum_{i=1}^{n} E_i I_i}{\mathrm{I}_{equivalent}} ; \mathrm{I}_{equivalent} = \frac{LH^3}{12} \quad \textbf{(6e)}$$

where:

$N_{1,2,3}$ = Ratio of 1st, 2nd, and 3rd layer modulus to last (3rd) layer modulus
$L_{1,2,3}$ = Lateral axis of the 1st, 2nd, and 3rd layer's cross-sectional area
$E_{1,2,3}$ = Modulus of the 1st, 2nd, and 3rd layers
$h_{1,2,3}$ = Thickness of the 1st, 2nd, and 3rd layers
$I_{1,2,3}$ = Moment of inertia of the 1st, 2nd, and 3rd layers
L = Lateral axis of the equivalent section
Y = Location of the centroid of the equivalent section
H = Thickness of the equivalent section
y_i = Distance from the centroid of each layer to the origin (0,0) axis
A_i = Cross-sectional area of each layer
d_i = Distance from the centroid of each layer to the neutral axis, Y
$E_{equivalent}$ = Equivalent modulus of the equivalent section
$I_{equivalent}$ = Equivalent moment of inertia of the equivalent section

Thenn de Barros's Equivalent Layer Thickness Theory

De Barros (1966) developed his theory by replacing Nijboer (II)'s equivalent layer modulus while maintaining the equivalent layer thickness formula, as shown in equation 7.

$$E_{equivalent} = \left(\frac{h_1 \sqrt[3]{E} + h_2 \sqrt[3]{E}}{h_1 + h_2}\right)^3$$

$$h_{equivalent} = h_1 + h_2 \quad \textbf{(7)}$$

Ullidtz and Peattie's Equivalent Layer Thickness Theory

The equivalent layer thickness theory allows for the application of Boussinesq's theory in a multilayered system so that stresses, strains, and deflections at any point in an elastic half-space can be determined. However, to obtain similar stresses, strains, and deflections calculated by the Boussinesq approximation and those from the fully elastic theory, Ullidtz and Peattie (1982) suggested applying correction factors to Odemark's equivalent thickness theory. When the load is uniformly distributed, equation 8—which involves the correction factor, *f*—is used to calculate equivalent thickness. A value of 0.9 is taken for *f* if the system has two layers. For multilayered systems, *f* is considered to be 1.0 for the first layer and 0.8 for the remainder.

$$h_{eqi} = f * \sum_{i=1}^{n-1} \left(h_{\mathrm{i}} \left[\frac{E_{\mathrm{i}}}{E_{\mathrm{n}}} \left(\frac{1-\mu_{\mathrm{n}}^2}{1-\mu_{\mathrm{i}}^2} \right) \right]^{1/3} \right) \quad \textbf{(8)}$$

where:

f = Correction factor

Ullidtz (1987) pointed out the following limitations of the use of Odemark's ELT:

- The moduli should decrease with depth, preferably at least twofold between consecutive layers
- The equivalent thickness of a layer should be larger than the radius of the loaded area

El-Badawy and Kamel (2011) investigated the accuracy of the Odemark method when the correction factor is included. Based on their results, the correction factor should not be constant, and it was found to be a function of the modular ratio, layer thickness, and depth. Using a correction factor within the range of 0.8 to 0.9 results in agreement between Odemark's concept and the elasticity theory, as shown in Figure 3.

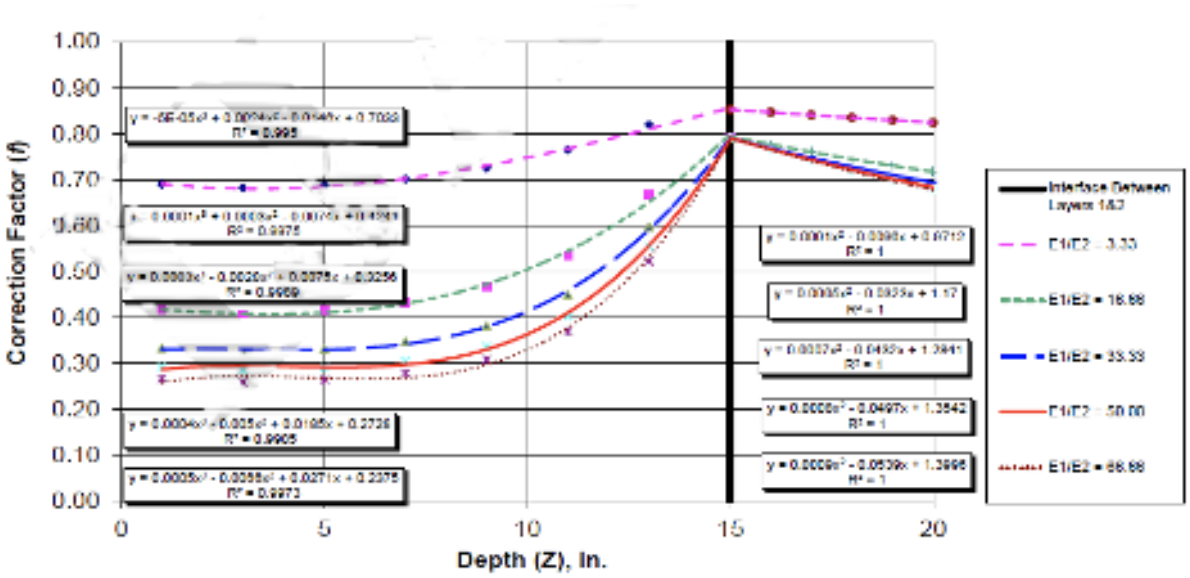

Figure 3. Correlation between the correction factor (*f*) and depth (*Z*)

Note in Figure 3 that the pavement system has a first layer depth of 15 in.

Pronk's Equivalent Layer Thickness Theory

Pronk (1993) reinforced the methodology of Nijboer (1955) by suggesting that the equivalent layer modulus should be equal to the modulus of the lower original layer. Based on this approach, equation 9 can be used to calculate equivalent thickness. This equation more closely conforms to Odemark's equivalency theory.

$$E_{equivalent} = E_2$$

$$h_{equivalent} = \left[\frac{\left(\frac{h_2}{h_1}\right)^4 + 4\times\left(\frac{h_2}{h_1}\right)^3\times\left(\frac{E_1}{E_2}\right) + 6\times\left(\frac{h_2}{h_1}\right)^2\times\left(\frac{E_1}{E_2}\right)+4\times\left(\frac{h_2}{h_1}\right)\times\left(\frac{E_1}{E_2}\right)+\left(\frac{E_1}{E_2}\right)^2}{\left(\left(\frac{h_2}{h_1}\right)+1\right)^3\times\left(\left(\frac{h_2}{h_1}\right)+\left(\frac{E_1}{E_2}\right)\right)}\right]^{1/3} \times (h_1+ h_2) \quad \textbf{(9)}$$

Van Gurp's Equivalent Layer Thickness Theory

A study conducted by Van Gurp (1995) presented a method for dealing with temperature variations within the total asphalt thickness. Many equivalency criteria can be utilized to determine equivalent layer thickness or stiffness, and most use the criterion of equal curvature or the criterion of equal strains at the lowest layer of a multilayered pavement system in substituting a solid system. The equal curvature method does not necessarily result in equal strains when specifically considering temperature gradients. Based on his work, Pronk's model was improved to more closely reflect temperature-related conditions. The approach uses the bottom layer's

stiffness in a two-layered system to substitute a solid beam so that multilayered and single layered systems have the same curvature under bending. He divided the total thickness into three sub-layers (Figure 4) and defined an equivalent asphalt thickness by first converting a three-layered system to a two-layered system and then converted the resulting two-layered system into a one-layered system with equivalent asphalt thickness ($h_{1,eq}$), as shown in the Figure 5.

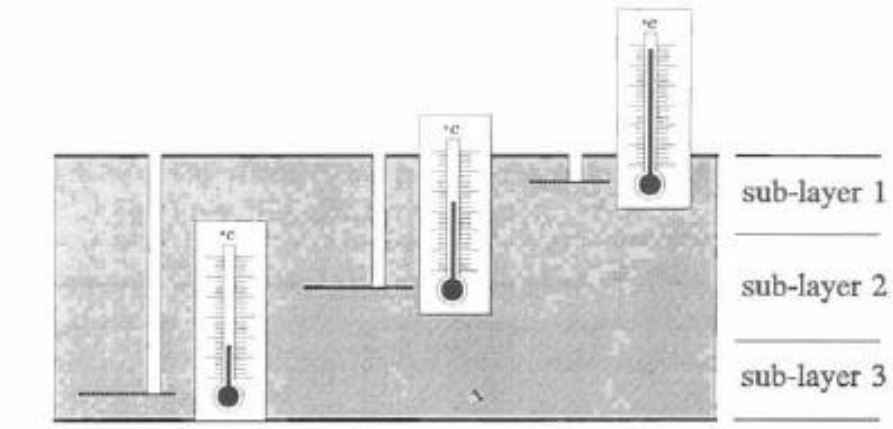

Van Gurp 1995

Figure 4. Total thickness divided into three sub-layers

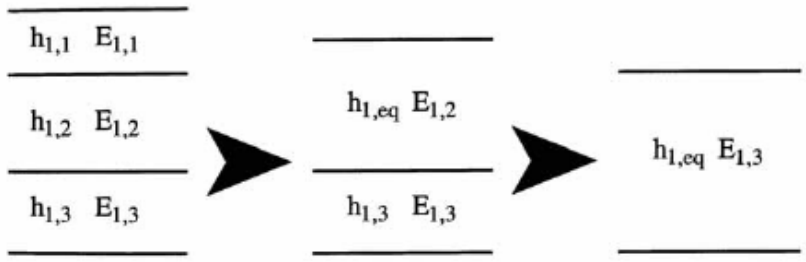

Van Gurp 1995

Figure 5. Conversion of three sub-layers into an equivalent asphalt thickness

Using the following equation 10, the equivalent layer thickness can be calculated in one step.

$$h_{equivalent} = \left[\frac{n_1^2 n_2^2 + 64 n_1 n_2^2 + 110 n_1 n_2 + 16 n_2^2 + 64 n_2 + 1}{n_1 n_2 + 2 n_2 + 1}\right]^{1/3} \times \frac{h_1}{4} \quad \textbf{(10)}$$

where:

$h_{equivalent}$ = Equivalent thickness
h_1 = Actual thickness of asphalt layer
n_1 = $E_{1,1}/E_{1,2}$
n_2 = $E_{1,2}/E_{1,3}$

Evaluation of ELTs

Proof-of-Concept: Using Odemark's Theory to Identify a Simplified Approach

A proof-of-concept demonstration on the use of ELT for analyzing representative Iowa county pavement structures with multiple cycles of pavement construction and renewal history was conducted by the Iowa State University research team (see Figure 6 and Figure 7).

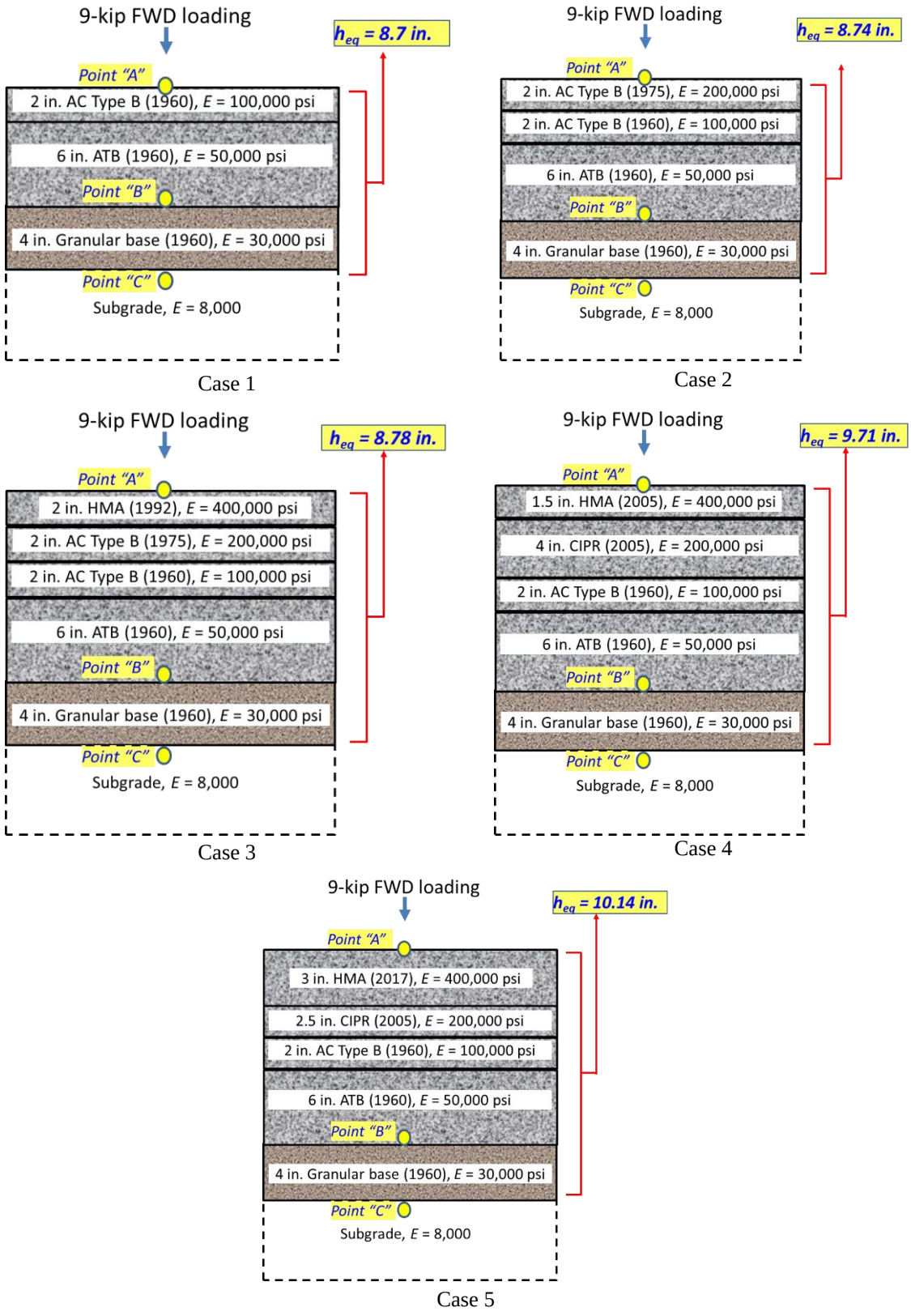

Figure 6. Simplifying multilayered pavement systems into two layers consisting of asphalt concrete (AC) on subgrade

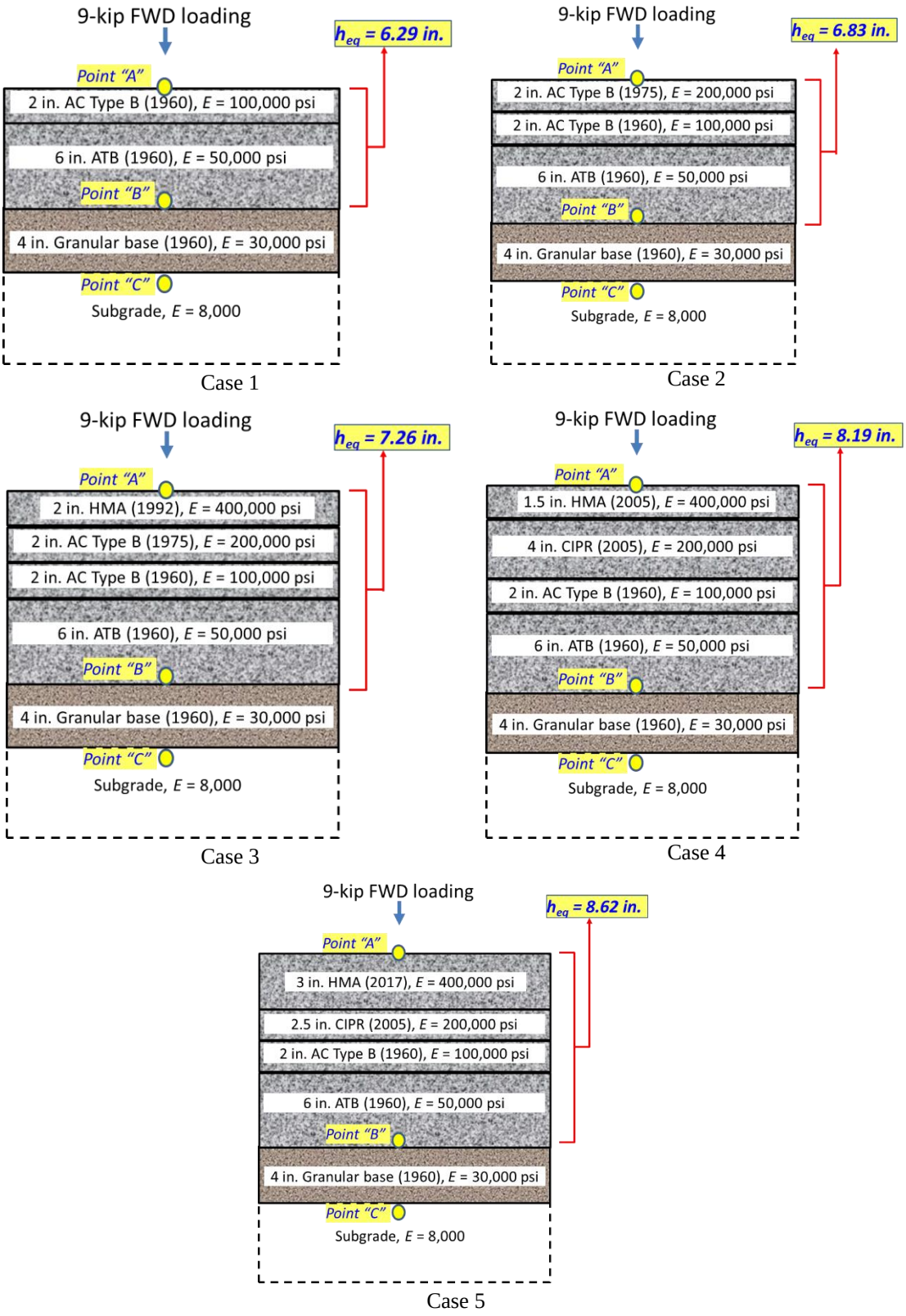

Figure 7. Simplifying multilayered pavement systems into three layers consisting of AC, granular base, and subgrade

The procedure formulated for this proof-of-concept demonstration is given in the following steps:

- Step 1: Identify equivalent thickness (h_{eq}) for a representative pavement structure
- Step 2: Compute critical pavement responses by using a mechanistic pavement structural analysis program for (1) multilayered pavement structure (i.e., original pavement structure) and (2) simplified pavement structures (i.e., equivalent thickness [h_{eq}]-based pavement structures)
- Step 3: Evaluate the resulting accuracy

A set of cases that demonstrated the use of the original Odemark theory can be categorized into two groups based on simplified pavement structure types (i.e., h_{eq}-based pavement structures). One is a two-layered pavement structure consisting of an asphalt layer on subgrade, while the other is a three-layered pavement structure consisting of an asphalt layer and a granular base layer on subgrade. The critical pavement responses calculated and compared include the following:

- Vertical deflection and horizontal strain at the top of the asphalt material surface (denoted by point A in Figure 6 and Figure 7)
- Vertical deflection and horizontal strain at the bottom of the last asphalt material layer (denoted by point B in Figure 6 and Figure 7)
- Vertical deflection and vertical strain at the top of the subgrade layer (denoted by point C in Figure 6 and Figure 7)

Figure 6 demonstrates cases where various multilayered pavement structures can be transformed into simplified two-layered pavement structures using ELT. The calculated h_{eq} values for each pavement structure are also presented in Figure 6. In each case, the calculated equivalent layer was placed on subgrade.

Figure 7 demonstrates cases where various multilayered pavement structures can be transformed into simplified three-layered pavement structures using ELT. The calculated h_{eq} values for each pavement structure are also presented in Figure 7. In each case, the calculated equivalent layer was placed on a granular base and subgrade.

Table 1 summarizes the critical pavement response results for each case when a (1) multilayered pavement structure, (2) simplified two-layered pavement structure, and (3) simplified three-layered pavement structure were examined using a mechanistic pavement structural analysis program.

Table 1. Critical pavement response comparisons for different cases

Location/ Response	Case 1			Case 2			Case 3			Case 4			Case 5		
	h_{total} = 12 in. multi-layer	h_{eq} = 8.7 in. ACC on SG	h_{eq} = 6.29 in. ACC on 4 in. GB & SG	h_{total} = 14 in. multi-layer	h_{eq} = 8.74 in. ACC on SG	h_{eq} = 6.83 in. ACC on 4 in. GB & SG	h_{total} = 16 in. multi-layer	h_{eq} = 8.78 in. HMA on SG	h_{eq} = 7.26 in. HMA on 4 in. GB & SG	h_{total} = 17.5 in. multi-layer	h_{eq} = 9.71 in. HMA on SG	h_{eq} = 8.19 in. HMA on 4 in. GB & SG	h_{total} = 17.5 in. multi-layer	h_{eq} = 10.14 in. HMA on SG	h_{eq} = 8.62 in. HMA on 4 in. GB & SG
Point A/ Deflection, in.	0.037	0.034	0.036	0.030	0.026	0.028	0.024	0.021	0.023	0.021	0.019	0.020	0.021	0.018	0.020
Point A/ Strain, µ-strain	-555	-495	-554	-402	-305	-353	-260	-181	-212	-216	-158	-183	-218	-149	-171
Point B/ Deflection, in.	0.031	0.031	0.033	0.025	0.025	0.027	0.019	0.020	0.022	0.017	0.018	0.020	0.017	0.018	0.019
Point B/ Strain, µ-strain	442	529	469	330	170	340	233	198	218	192	110	188	187	105	175
Point C/ Deflection, in.	0.028	0.031	0.030	0.022	0.025	0.025	0.018	0.020	0.020	0.016	0.018	0.018	0.016	0.017	0.018
Point C/ Strain, µ-strain	-1,453	-1,571	-1,609	-992	-1,027	-1,113	-665	-649	-734	-543	-550	-614	-527	-511	-568

Note: h_{total} = total thickness of layers on subgrade; h_{eq} = equivalent thickness; ACC = asphalt cement concrete; HMA = hot-mix asphalt; GB = granular base; SB = subgrade; "+" = tensile for strain/downward for deflections; "-" = compressive for strain/upward for deflections

As shown in Table 1, the simplified pavement structures obtained using ELT provide critical pavement response results similar to those of the multilayered pavement structure.

Based on the findings shown in Table 1, a three-layered pavement structure consisting of an asphalt layer and granular base layer on subgrade was selected as the simplified pavement structure throughout this study, since the critical pavement responses of the simplified pavement structure were closer to the pavement responses of the multilayered pavement structure's deflections and strains on the surface, at the bottom of the asphalt layer, and on top of the subgrade.

Proof-of-Concept: Selecting an ELT

There are many possible equations or theories that can be used to more accurately determine equivalent thickness for a given multilayered pavement structure, and while almost all these methods transform a three-layered pavement system to an equivalent two-layered system, this methodology can easily be extended to more than three layers using the following procedure:

1. The first simplification transforms the first and second upper pavement layers into an equivalent layer to be used as the first upper layer for the next simplification
2. The next simplification transforms the first (calculated equivalent thickness) and next upper pavement layers into a new equivalent layer to be used as the first upper layer for the next simplification
3. Steps 1 and 2 are repeated until all layers above the subgrade are transformed into a single equivalent layer

Four-layered and five-layered models were considered in Pronk's research (1994) for simplifying pavement systems into a two-layered model by using Nijboer (I), Nijboer (II), Pronk, and Ullidtz's ELT methods. Table 2 shows the material and structural properties of those four-layered and five-layered models.

Table 2. Layer properties (inputs) and critical strains (outputs)

Inputs				Outputs					
Layer	E_i, MPa	μ_i, m/m	h_i, m		BISAR	Nijboer (I)	Nijboer (II)	Pronk	Ullidtz
Full depth asphalt									
Asphalt 1	2,000	0.35	0.04	ε_h	168	127	196	171	221
Asphalt 2	4,000	0.35	0.04	ε_v	530	320	561	525	535
Asphalt 3	6,000	0.35	0.10	$E_{equivalent}$, MPa		1,374	3,951	6,000	100
Subgrade	100	0.35	∞	$h_{equivalent}$, m		0.405	0.180	0.1591	0.6369
Asphalt on top of an unbound base									
Asphalt 1	2,000	0.35	0.04	ε_h	122	85	138	126	112
Asphalt 2	4,000	0.35	0.04	ε_v	385	212	377	373	280
Asphalt 3	6,000	0.35	0.10	$E_{equivalent}$, MPa		1,374	3,951	6,000	100
Base 4	400	0.35	0.20	$h_{equivalent}$, m		0.405	0.180	0.1591	0.6369
Subgrade	100	0.35	∞						

Source: Adapted from Pronk 1994

Using Bitumen Stress Analysis in Roads (BISAR) software, the vertical strain at the top of the subgrade and the horizontal strain at the bottom of the asphalt layer were computed, with results showing that the Pronk method yielded strain values closer to BISAR values for both four- and five-layered models.

Existing and adapted theories were compared based on computed deflections and strains on the surface, at the bottom of the asphalt, and on top of the subgrade. In those computations, a total of 500 different pavement cases were considered, with 4-layered pavement systems (2 HMA layers, 1 base layer, and 1 subgrade layer) transformed into 3-layered simplified pavement systems (1 HMA layer, 1 base layer, and 1 subgrade layer). Table 3 provides a summary of the variables used for the simplified pavement systems after the application of different ELTs.

Table 3. Different ELTs used for simplified pavement systems

Simplified pavement system	Modulus	Thickness	Poisson's ratio
Theory I—Ullidtz's Equivalent Thickness Theory (El-Badawy and Kamel 2011)			
Asphalt layer (L_1)	$E_{subgrade}$	$h_{equivalent}$ (by using asphalt and subgrade layers properties in the equation)	$\mu_{subgrade}$
Base layer (L_2)	$E_{subgrade}$	$h_{equivalent\_base}$	$\mu_{subgrade}$
Subgrade layer (L_3)	$E_{subgrade}$	-	$\mu_{subgrade}$
Theory II—Ullidtz's Equivalent Thickness Theory			
Asphalt layer (L_1)	E_{base}	$h_{equivalent}$ (by using asphalt and base layers properties in the equation)	μ_{base}
Base layer (L_2)	E_{base}	h_{base}	μ_{base}
Subgrade layer (L_3)	$E_{subgrade}$	-	$\mu_{subgrade}$
Theory III—Ullidtz's Equivalent Thickness Theory			
Asphalt layer (L_1)	E_{base}	$h_{equivalent}$ (by using asphalt and base layers properties in the equation)	μ_{base}
Base layer (L_2)	$E_{subgrade}$	$h_{equivalent\_base}$	$\mu_{subgrade}$
Subgrade layer (L_3)	$E_{subgrade}$	-	$\mu_{subgrade}$
Theory IV—Ullidtz's Equivalent Thickness Theory			
Asphalt layer (L_1)	$E_{lastlayer\_HMA}$	$h_{equivalent}$ (by using asphalt layer(s) properties in the equation)	$\mu_{lastlayer\_HMA}$
Base layer (L_2)	E_{base}	h_{base}	μ_{base}
Subgrade layer (L_3)	$E_{subgrade}$	-	$\mu_{subgrade}$
Theory V—Ullidtz's Equivalent Thickness Theory			
Asphalt layer (L_1)	$E_{subgrade}$	$h_{equivalent}$ (by using asphalt and subgrade layers properties in the equation)	$\mu_{subgrade}$
Base layer (L_2)	$E_{subgrade}$	$h_{equivalent\_base}$	$\mu_{subgrade}$
Subgrade layer (L_3)	$E_{subgrade}$	-	$\mu_{subgrade}$
Theory VI—Albayati's Equivalent Modulus Theory (Albayati et al. 2018)			
Asphalt layer (L_1)	$E_{equivalent\_HMA}$	$h_{equivalent}$	$\mu_{lastlayer\_HMA}$
Base layer (L_2)	E_{base}	h_{base}	μ_{base}
Subgrade layer (L_3)	$E_{subgrade}$	-	$\mu_{subgrade}$
Theory VII—Pronk's Equivalent Thickness Theory			
Asphalt layer (L_1)	$E_{lastlayer\_HMA}$	$h_{equivalent}$ (by using asphalt layer(s) properties in the equation)	$\mu_{lastlayer\_HMA}$
Base layer (L_2)	E_{base}	h_{base}	μ_{base}
Subgrade layer (L_3)	$E_{subgrade}$	-	$\mu_{subgrade}$

Ullidtz's theory, improved from Odemark's theory, used as the first method (El-Badawy and Kamel 2011) is designated Theory I in Table 3. The equivalent thickness was calculated using the asphalt layer and base layer properties in equation 4. For the simplified pavement system, the

subgrade modulus was used as an equivalent modulus for the asphalt layer, the subgrade modulus was taken as the as base layer modulus, and the base layer thickness was converted into an equivalent base layer thickness as the modulus changed. In Theory I, all layers' Poisson's ratios were taken as that of the subgrade layer. The different alternative theories, from Theory II to Theory V, in Table 3 were slightly adapted from the original concept to compute pavement responses of the simplified pavement systems. Theory VI uses the approach presented by Albayati et al. (2018), while Theory VII uses Pronk's ELT (Pronk 1993).

Figure 8 shows comparisons of the pavement responses (i.e., deflection on the surface, deflection at the bottom of the asphalt, deflection on the top of the subgrade, horizontal strain at the bottom of the asphalt, and vertical strain on the top of the subgrade) by the statistical measurement of the line-of-equality coefficient of correlation (R^2) when using different ELTs, as noted in Table 3.

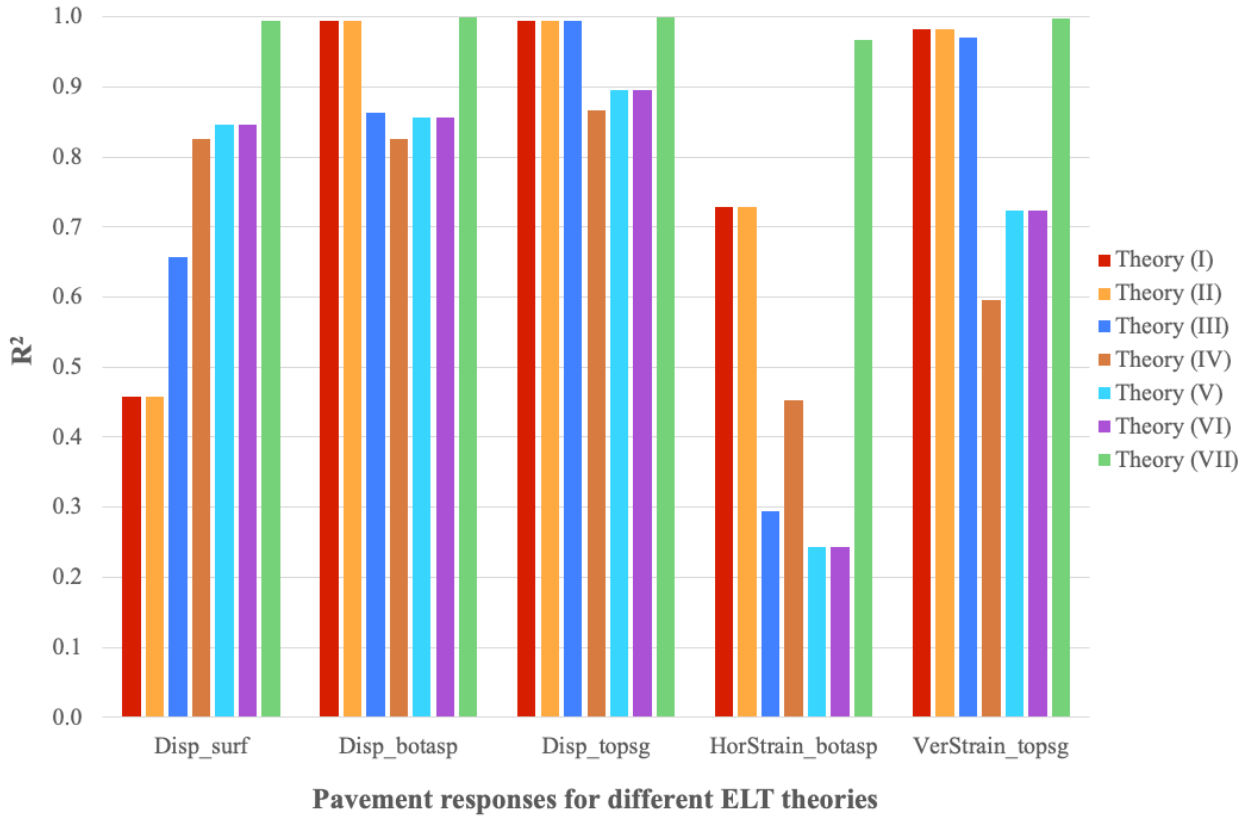

Figure 8. Comparison of pavement responses for different ELTs

Of all the ELT models evaluated, Pronk's model was found to perform best in terms of applicability and accuracy.

Review of Pavement Structural Analysis Models

Mechanistic-Based Pavement Structural Analysis Models

Mechanistic models can be used to mathematically represent pavement physics and compute critical pavement responses (like deflections, stresses, and strains) in response to idealized loading and climactic inputs. Recent advances in computing hardware (e.g., high-performance computing) have created many available choices of models and procedures (including those that can consider dynamic and viscoelastic properties) to study pavement behavior. By narrowing down the list to those that can utilize readily available data and be easily executed on personal computers (PCs), the available procedures for generating a synthetic database can broadly be classified into two categories as follows:

- Finite element analysis (FEA)
- Layered elastic analysis (LEA)

FEA models involve dividing the pavement structure into a large number of small elements and obtaining approximate numerical solutions for each such element. FEA requires fewer assumptions to be made, since it works with a more complex mathematical model than an LEA method. While a significant advantage of FEA methods over layered elastic design methods is their capability for modeling the stress-dependent behavior of unbound aggregates and fine-grained soils, FEA methods require a quantity of input data that are often not readily available. ILLI-PAVE (Raad and Figuerona 1980), a two-dimensional (2D) FEA program developed at the University of Illinois Urbana-Champaign for modeling flexible and composite pavements, has been validated and widely used for analyzing and designing flexible highway and airport pavements. Similarly, ISLAB 2000 is a versatile 2D FEA program for analyzing rigid pavements.

LEA models typically assume pavements to be homogenous, isotropic, and linearly elastic, and they support the calculation of theoretical deflections, stresses, and strains in response to the application of a surface load. In an LEA method, the pavement structure is modeled as a system of horizontal layers with constant properties that only allows elastic deformation within each layer assigned to pavement materials. Nonlinearity of pavement materials can be approximated to some extent by sub-layering the pavement layers and assigning different properties to each sub-layer (Rodway 1995). Pavement designers are interested in obtaining responses at certain critical locations, such as horizontal tensile strain at the bottom of the HMA layer (to predict bottom up HMA fatigue failure), vertical compressive strain at the top of the intermediate layer, base or subbase identity (to predict rutting failure in the base or subbase), or vertical compressive strain at the top of the subgrade (to predict rutting failure in the subgrade).

A number of LEA-based computer programs have been developed over the years, including the following:

- WESLEA (Waterways Experiment Station Elastic Layer Analysis)

- KENPAVE (Kentucky pavement analysis tool)
- CIRCLY (developed by the Australian company Mincad)
- CHEVPC (PC version of the Fortran-based Chevron Elastic Layer Analysis Program)
- WinJULEA (Jacob Uzan Layered Elastic Analysis, which is used in the AASHTOWare Pavement ME/Mechanistic-Empirical Pavement Design Guide [MEPDG] methods)
- BISAR
- MnLayer (Minnesota Layered Elastic Analysis)
- MatLEA

Almost all these packages use similar methodology, with some variations and enhancements in terms of simplification, computational efficiency, etc. In this study, KENPAVE, MnLayer, and MatLEA were specifically examined for analyzing structural responses of various pavement design options.

The Microsoft-based KENPAVE software developed by Dr. Y. H. Huang can be used for analysis and design of both flexible and rigid pavements; it is comprised of two programs, KENLAYER and KENSLAB, used for both pavement types, respectively (Huang 2004). The home screen of the KENPAVE software program is depicted in Figure 9.

Figure 9. Home screen of the KENPAVE software program

Damage analysis can be performed using the KENPAVE software on pavements with up to 19 layers and various loading conditions, such as tridem, tandem, single, or a combinations thereof. KENPAVE requires input parameters such as layer thicknesses, material properties (modulus of elasticity and Poisson's ratios), load group, tire pressure, and number of stress points for

pavement analysis to compute output parameters such as maximum allowable number of loading repetitions from calculated microstrains and stresses.

Srikanth (2015) examined the effects of surface layer thickness and modulus of elasticity using KENPAVE to evaluate horizontal tensile strain and vertical compressive stress on pavement performance; it resulted in reducing compressive and tensile microstrains and distresses in pavements with increasing surface thickness. The performance of asphalt pavement was compared by Muniandy et al. (2013), using different distress models and two different software programs—CHEVPC and KENLAYER—who concluded that strain results obtained from KENLAYER were more accurate than those from CHEVPC. Another study was conducted on damage analysis using KENLAYER to compute rutting and fatigue distresses (Adil Mutlag 2012). This study examined the effects of binder layer and wearing layer thicknesses on pavement design life by computing horizontal tensile strain and vertical compressive strains, concluding that increasing binder moduli increased fatigue damage, while decreasing it decreased rutting damage, and increasing the wearing layer thickness up to 3.94 in. extended design life. Rind et al. (2019) used KENLAYER to analyze the effects of asphalt wearing and base thicknesses on pavement performance and found that an increase in asphalt wearing and base thicknesses resulted in a decrease in microstrains and an increase in the allowance for the number of loading repetitions, or vice versa.

The MnLayer software program developed by Drs. Lev Khazanovich and Qiang Wang can be used for analysis and design of flexible pavements (Khazanovich and Wang 2007). The home screen of the MnLayer software program is depicted in Figure 10.

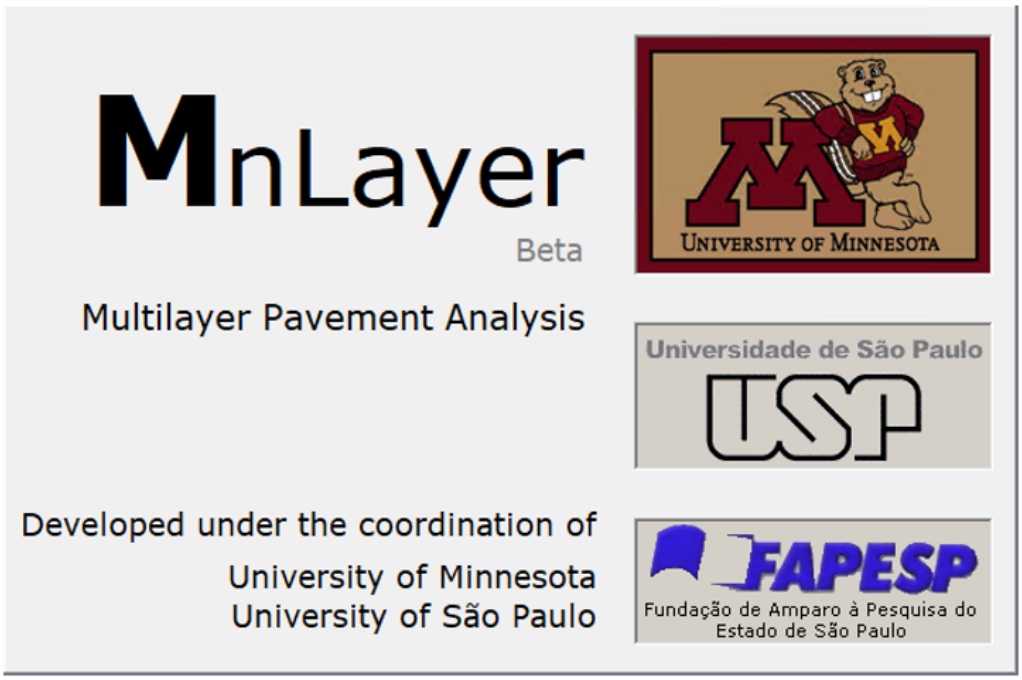

Figure 10. Home screen of the MnLayer software program

MnLayer is based on the Burmister's solution, the same theory that the JULEA program incorporated into the MEPDG but with an improved numerical integration scheme. This numerical implementation of the inverse Hankel transform led to a significant reduction in computation time, 20 times faster than other widely used LEA programs (e.g., BISAR and JULEA). The MnLayer software program requires input parameters such as layer thicknesses, material properties (modulus of elasticity and Poisson's ratios), friction number, loads (tire pressure, load, radius), and the number and locations of analysis points for pavement analysis to compute output parameters such as displacements, strains, and stresses.

Kleizienė et al. (2016) investigated the elastic and viscoelastic behavior of asphalt layers in flexible pavement systems by calculating pavement responses using MnLayer (Khazanovich and Wang 2007) and Viscoroute2 (Chabot et al. 2010) programs. In the resulting pavement response and performance analysis, it was determined that the effects of the viscoelastic properties of the asphalt mixture on pavement responses decrease with increasing pavement age. Higher horizontal strains due to bitumen aging and asphalt fatigue were predicted for the aged pavement. Another study performed an analysis of different tire footprints from a set of agricultural vehicles (Salles et al. 2022). To compute pavement responses on rural roads, different load parameters were simulated in the MnLayer program.

The MatLEA, the MATLAB-based Layered Elastic Analysis, program developed by Dr. Emin Kutay can be used for analysis and design of pavements (Kutay and Lanotte 2020). While MatLEA has no home screen, an example of a result screen is shown in Figure 11.

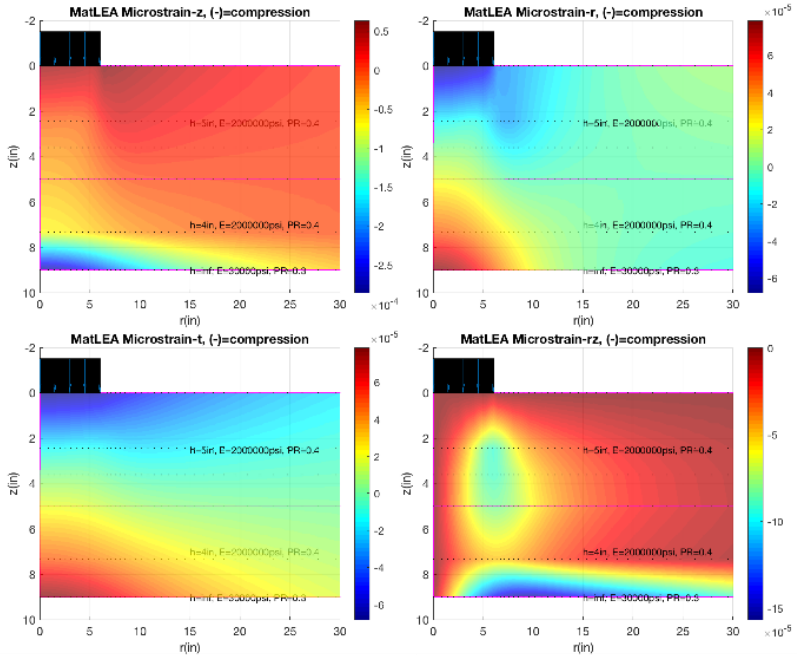

Figure 11. Sample result screen of the MatLEA software program

MatLEA has a function in the MATLAB environment software program that was used to compute pavement responses. It provides a default code for single-layer pavement analysis. The MatLEA formulations and computational steps are nearly identical to those of MnLayer. Loads are applied in a circular area with uniform pressure. Its basic concept is based on Burmister's multilayered elastic theory. Since three-dimensional (3D) matrix inversion is utilized for computing parameters, and the inverse Henkel transform is performed using bulk matrix operations, it requires much less computational time (e.g., 137 milliseconds run time for computing the responses of 315 analysis points).

Another study investigated the fatigue performance of the long-life and standard pavement sections through performance analysis using a web-based Mechanistic-Empirical Asphalt Pavement Analysis (MEAPA) tool, in which the main analysis engines were coded in MATLAB including the LEA algorithm, called MatLEA (Ghazavi et al. 2020). It concluded that long-life pavement sections had lower critical strains and a higher number of cycles-to-failure (N_f) values when compared to those of standard pavement sections.

ANN-Based Pavement Structural Analysis Models

Pavement response analysis requires complicated and time-consuming calculations. To overcome this challenge, some recent research has developed more computationally efficient models to replace traditional analysis methods. As soft computing techniques have become more prevalent in recent years, ANNs have been used to estimate pavement structure condition and response analysis, because they can identify relationships among variables of interest independent of their physical nature. ANNs are highly recommended for three reasons: less error, high efficiency, and output uniqueness.

Ceylan et al. (1999) used ANN models with two hidden layers to investigate factors affecting pavement responses by predicting maximum bending stresses and the maximum vertical deflection for jointed concrete airfield pavements. To determine the size and shape of the 3D response pulse under the asphalt layer, they developed a framework for describing the multiple-layer perceptron neural network (MLPNN) and the response, providing the basis for the coating design, including the thickness and stiffness of the layers (Fakhri and Ghanizadeh 2014). Ziyadi and Al-Qadi (2017) developed an MLPNN model by improving its generalization ability using a k-fold cross-validation technique. The model accurately predicted 11 critical pavement responses as computed by a 3D finite element (FE) model to investigate the effects of wide-base tires. Another study for predicting critical pavement responses correlated with top-down cracking failure was conducted by developing ANN models with different numbers of hidden layers and neurons (Rezaei-Tarahomi et al. 2019).

As a working practice, the authors used MnLayer to develop ANNs for predicting deflections. They also simplified multilayered pavement structures into three-layered pavement structures using the Odemark theory. In a subsequent step, the predicted deflections were used to train another ANN model (backcalculation equivalent thickness [B-EQT], and bakcalculation equivalent modulus [B-M] models) to estimate the equivalent thickness of an asphalt multilayered pavement. Ultimately, equivalent thickness and deflection predictions were

compared with outcomes from Odemark and MnLayer, respectively, and as shown in Figure 12, the results indicated that ANN models are candidates to be a useful alternative for estimating equivalent thickness and surface deflections (Citir et al. 2020).

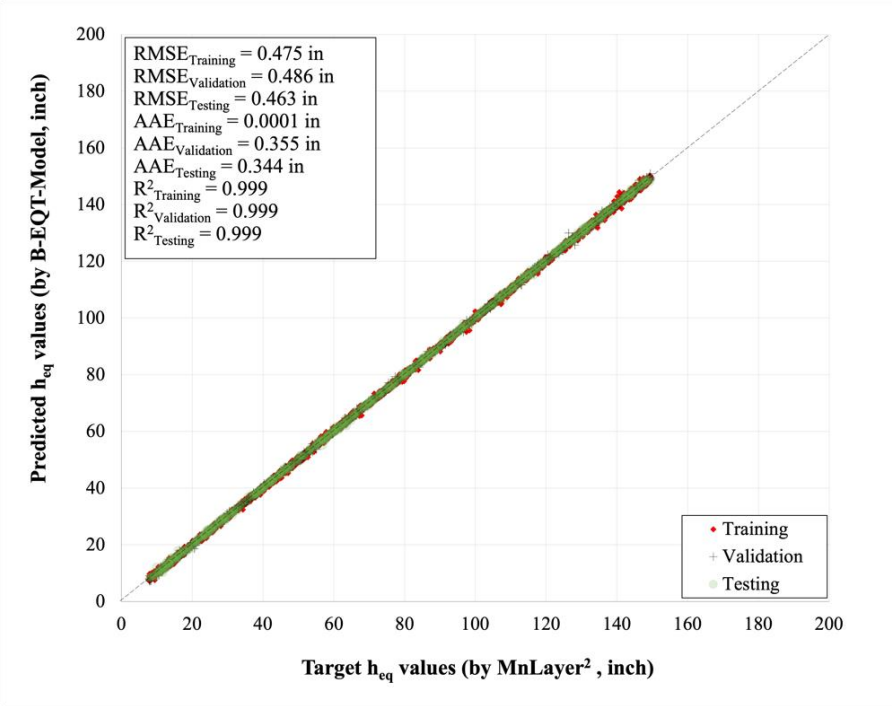

(a) Equivalent thickness

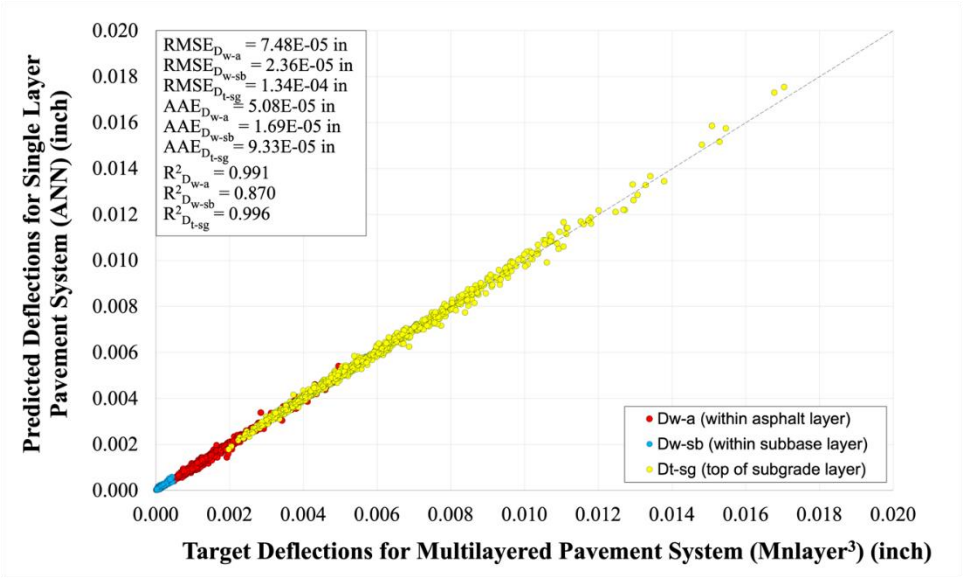

(b) Deflections

Figure 12. Accuracy of ANN models to predict (a) equivalent thickness and (b) deflections

CHAPTER 3. DEVELOPMENT OF SYNTHETIC DATABASE

Description of Overall Approaches and Data Preparation

Typical Iowa county pavement systems have multilayered pavement structures resulting from multiple cycles of pavement construction and renewal. Such complex pavement structures make it difficult for Iowa county engineers to estimate the current structural capacities of in-service pavements and develop appropriate cost-effective strategies for managing, maintaining, and rehabilitating county pavement systems. This challenge creates a need to establish reliable and accessible methods and tools for Iowa county engineers to use in their routine pavement analysis, design, and asset management practices.

In this study, a detailed step-by-step methodology was established and deployed to develop a framework for predicting structural capacities of in-service pavements by using a synthetic pavement characterization and response database, based on real-world field data from the Iowa DOT Pavement Management Information System (PMIS) and the ICEASB.

Because the quality of deep learning models is heavily dependent on data quality, the first step in establishing the framework was to develop a reliable database. Data preparation is a set of procedures that helps make a database more suitable for use by ANN models, and synthetic data generation is a valuable step before developing any such models. There are two advantages to using synthetic data. First, it entails less security risk from a data breach, even while the data set resembles real data. Second, it is scalable, meaning that it can include a limitless amount of data based on a relatively small sample of real data. Because of the lack of data in Iowa county pavement systems, this study benefited most from the second advantage by boosting the data set size to provide adequate training for an ANN model.

Synthetic data generation can generally be divided into two classes, process-driven and data-driven methods (Goncalves et al. 2020). Process-driven methods derive synthetic data using mathematical and/or computational models of a fundamental physical process, while data-driven methods generate such data using generative models trained on real data by building relationships between input and output data through statistical and machine learning techniques.

Based on the fact that this study uses LEA for computing pavement responses, statistical analysis for determining pavement characteristics within the defined range, and machine learning techniques for modeling, both process-driven and data-driven methods were used to generate the synthetic database for pavement formed of 1 to 10 HMA layer(s), a stabilized base and/or granular base/subbase, and a subgrade layer.

Different structural design and mechanical properties—including thickness, elastic modulus, and Poisson's ratio for each layer excluding the thickness of the subgrade layer—were initially produced for ranges defined for a pavement system. The literature, including both experimental data and other agencies' inventories and reports, was comprehensively reviewed to develop a general idea about the mechanical features of pavement systems. The pavement's characteristic

ranges per each layer could therefore be defined based on a historical pavement database, field investigations, and practical experience. Saltan et al. (2002), using a backcalculation procedure and developed ANN models, investigated the effect on pavement life of the elastic modulus for each layer. For this purpose, this study used the database for a typical flexible pavement shown in Figure 13.

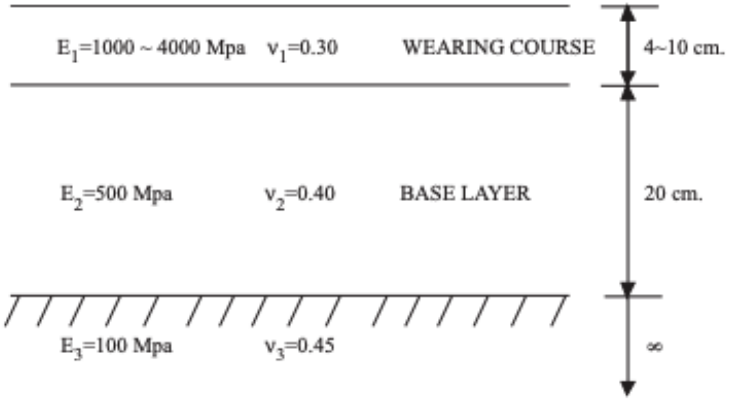

Figure 13. A typical flexible pavement used in ANN model development

In another study, surface deflections using elastic modulus and pavement layer thickness were predicted using ANN models developed using two-layered (granular surface and subgrade), three-layered (bituminous surface, granular base, and subgrade), four-layered (bituminous surface, granular base, granular subbase, and subgrade), and five-layered (bituminous overlay, bituminous surface, granular base, granular subbase, and subgrade) pavement systems. The ranges of this database are shown in Table 4 (Rakesh et al. 2006).

Table 4. Data ranges of flexible pavement characterizations used in literature

		Pavement layer and characteristics										
		Asphalt layer			*Base layer*			*Subbase layer*			*Subgrade layer*	
Data ranges by study		*Thickness, mm (in.)*	*Poisson's ratio*	*Elastic modulus, MPa (psi)*	*Thickness, mm (in.)*	*Poisson's ratio*	*Elastic modulus, MPa (psi)*	*Thickness, mm (in.)*	*Poisson's ratio*	*Elastic modulus, MPa (psi)*	*Poisson's ratio*	*Elastic modulus, MPa (psi)*
Lav et al. (2009)	*Min.*	50 (2.0)	0.35	1,000 (145,038)	150 (5.9)	0.35	35 (5,076)	-	-	-	0.35	30 (4,350)
	Max.	200 (7.9)		15,000 (2,175,566)	500 (19.7)		300 (43,511)	-	-	-		200 (29,008)
Tsai et al. (2009)	*Min.*	100 (3.9)	0.35	2,068 (299,938)	400 (15.7)	0.4	345 (50,000)	-	-	-	0.45	69 (10,000)
	Max.			3,447 (499,945)			1,379 (200,000)	-	-	-		345 (50,000)
Rakesh et al. (2006)	*Min.*	50 (2.0)	0.3	400 (58,015)	100 (3.9)	0.3	100 (14,504)	50 (2.0)	0.3	100 (14,504)	0.3	20 (2,900)
	Max.	500 (19.7)	0.5	2,000 (290,076)	600 (23.6)	0.5	600 (87,023)	300 (11.8)	0.5	500 (72,520)	0.5	100 (14,504)
Saltan et al. (2002)	*Min.*	40 (1.6)	0.3	1,000 (145,038)	200 (7.9)	0.4	500 (72,520)	-	-	-	0.45	100 (14,504)
	Max.	100 (3.9)		4,000 (580,151)				-	-	-		
Li et al. (1999)	*Min.*	-	0.2	10 (1,450)	-	-	-	-	-	-	-	-
	Max.	-	0.3	1,000 (145,038)	-	-	-	-	-	-	-	-
Davies and Mamlouk (1985)	*Min.*	25.4 (1)	0.35	690 (100,000)	76.2 (3)	0.4	345 (50,000)	152.4 (6)	0.4	69 (10,000)	0.45	27.6 (4,000)
	Max.	102 (4)		13,790 (2,000,000)	305 (12)		1,379 (200,000)	610 (24)		276 (40,000)		110.3 (16,000)
Southgate et al. (1976)	*Min.*	-	0.25	1,000 (145,038)	-	0.3	-	-	0.3	-	0.3	20 (2,900)
	Max.	-	0.35	12,000 (1,740,453)	-	0.4	-	-	0.4	-	0.4	400 (58,015)

Another study was conducted to determine the optimal genetic algorithm parameters for backcalculating pavement layer elastic moduli using a typical three-layered pavement system shown in Figure 14 (Reddy et al. 2004).

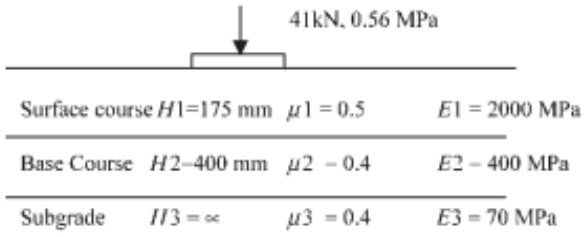

Figure 14. A typical three-layered flexible pavement used in ANN model development

Southgate et al. (1976) described a model in which the structural adequacy of flexible pavement systems can be achieved using the Chevron program that requires inputs of the elastic characteristics of the materials specified in Table 4 to determine stresses, strains, and deflections.

Another study used the four-layered flexible pavements described in Table 4 to investigate the effects of dynamic phenomena of resonance and inertial damping within subgrade on pavement responses under static and dynamic loading. Table 4 indicates the data ranges of the flexible pavement characterizations used in literature (Davies and Mamlouk 1985).

After determining the characteristic ranges of flexible pavement systems from the literature based on field investigations and experiences, historical pavement databases were examined. Figures 15 and 16 show example thickness distributions for the PMIS 2019 and Lee County, Iowa databases, respectively.

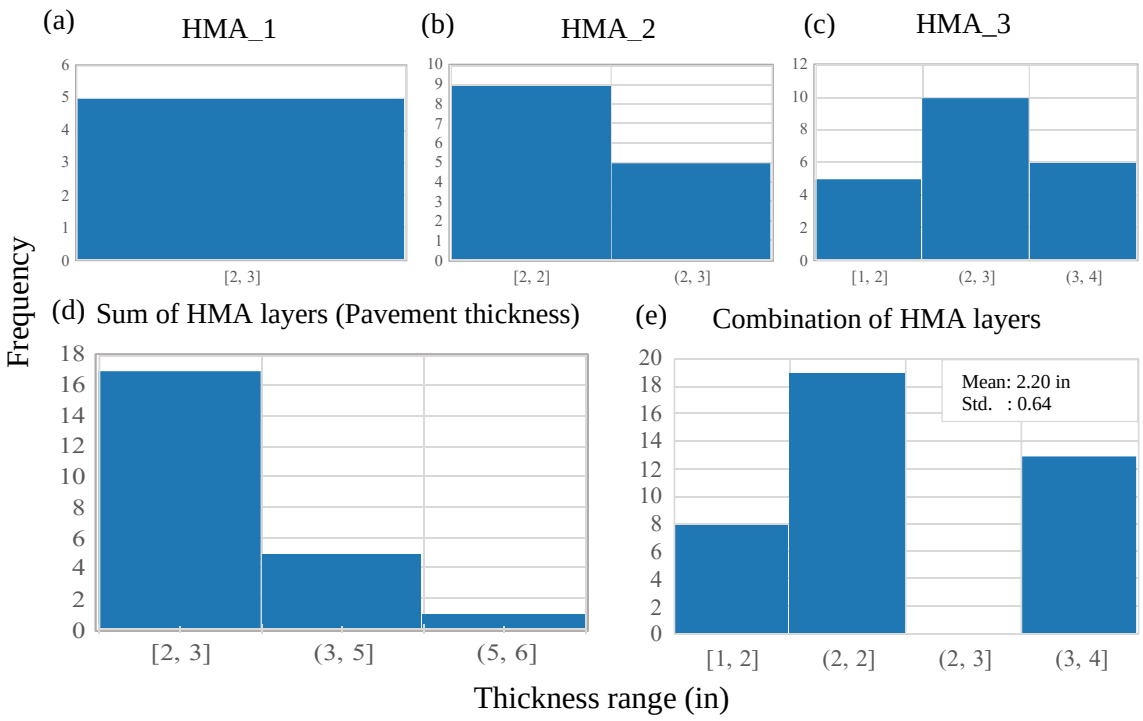

Figure 15. Thickness distributions of secondary roads, Lee County database

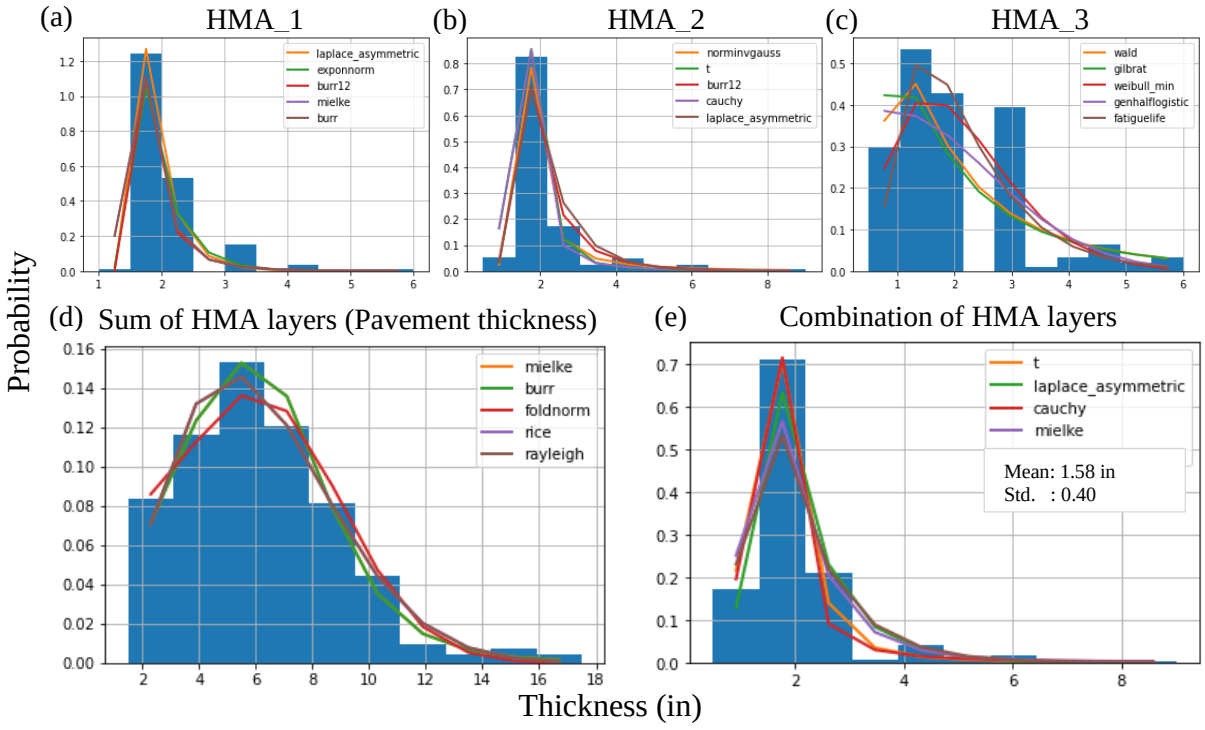

Figure 16. Thickness distributions of primary roads, PMIS 2019 database

For the desired purpose, the Fitter package from SciPy, a scientific computation library that provides utility functions for optimization, stats, and signal processing, was used to identify the distribution that best fit the PMIS data. Fitter uses 80 distributions from SciPy and allows users to plot the results to check for the most likely distribution and the best parameters.

Figures 15a–c show the thickness distributions for the first, second, and third HMA layers of secondary road sections from the Lee County database, while Figures 15d and 15e depict the sum of those HMA layers (from 1 to 10) as a total pavement thickness and the combination of those HMA layers (from 1 to 10) without summarization, respectively. Note that there was a maximum of three HMA overlays in the Lee County database, and a total of 23 secondary road sections were examined for each HMA layer. The histogram of the combination of HMA layers, Figure 15e, reveals the mean thickness and standard deviation of the distribution to be 2.2 in. and 0.64, respectively, and it was also found that minimum and maximum thicknesses in the Lee County database were 1 in. and 3.5 in. Because of the lack of data for county road sections, primary road sections were examined.

Figures 16a–c show the thickness distributions of primary road sections from the PMIS 2019 database for the first, second, and third HMA layers, while Figure 16d and 16e depict the sum of those HMA layers (from 1 to 10) as a total pavement thickness and the combination of those HMA layers (from 1 to 10) without summarization, respectively. A total of 273 primary road sections were examined for each HMA layer. Examining the histogram of the combination of HMA layers, Figure 16e, reveals the mean thickness and standard deviation of distribution to be 1.58 in. and 0.40, respectively, and it was also found that minimum and maximum thicknesses were 0.5 in. and 9 in. in the PMIS database. Since there is limited data inventory for county road sections in Iowa, an approach for developing a synthetic database for county roads was proposed in this study.

Using results from the above investigations on flexible pavement properties, the data ranges of the synthetic database used to develop the ANN models in this study were determined and are presented in Table 5, showing the minimum and maximum values of thickness, Poisson’s ratio, and elastic moduli for each layer in the pavement system.

Table 5. Data ranges of flexible pavement characterizations used in this study

Pavement layers	Pavement characteristics	Min.	Max.	Unit
Asphalt layer (max. 10 in. for individual layer)	*Thickness*	13 (0.5)	635 (25)	mm (in.)
	Poisson's ratio	0.25	0.45	-
	Elastic modulus	400 (58,000)	15,000 (2,175,000)	MPa (psi)
Stabilized base layer	*Thickness*	25 (1)	510 (20)	mm (in.)
	Poisson's ratio	0.25	0.45	-
	Elastic modulus	400 (58,000)	15,000 (2,175,000)	MPa (psi)
Granular base layer (or subbase layer)	*Thickness*	25 (1)	510 (20)	mm (in.)
	Poisson's ratio	0.30	0.40	-
	Elastic modulus	69 (10,000)	1,379 (200,000)	MPa (psi)
Subgrade	*Poisson's ratio*	0.30	0.45	-
	Elastic modulus	21 (3,000)	400 (58,000)	MPa (psi)

For example, the minimum and maximum values of asphalt thickness used in the database were determined to be 0.5 in. and 25 in., where the maximum total asphalt thickness of 25 in. is the sum of all the overlays. Individual asphalt layer thicknesses ranged between 0.5 in. and 10 in. (i.e., each asphalt layer shall not be larger than 10 in.). Likewise, the total base layer thickness bound was set to between 1 in. and 20 in. The ranges of elastic modulus of asphalt layers and stabilized base layers (asphalt treated) were determined to be 58,000 psi and 2,175,000 psi, while they were 10,000 psi and 200,000 psi for the granular base/subbase layer and 3,000 psi and 58,000 psi for the subgrade layer. Similarly, the ranges of Poisson's ratios of asphalt layers and stabilized base layers (asphalt treated) were determined to be 0.25 and 0.45 and set to 0.30 and 0.40 for the granular base/subbase layer and 0.30 and 0.45 for the subgrade layer.

It should be noted that there is a lack of field data, most specifically for county roads. The input parameters used in the models to consider the structural design and mechanical properties of pavement systems were initially determined to be thickness, Poisson's ratio, and elastic modulus. While field data for thickness could be examined as described previously, there were no available data for Poisson's ratio and elastic modulus in these field databases. In other words, the lack of field data was evident in the limited inventory of thickness data, and of other mechanical properties data, due to no recorded data. This study has thus proposed an approach on generating a synthetic database for use in model development.

Generation of Input Database for Models Using Data-Driven Methods

Flexible pavement sections from the Iowa DOT and Lee County Engineer through the ICEASB were adopted in this study for analysis. The obtained data were categorized as PMIS data for primary roads and county data for secondary roads. Using PMIS data, a total of 273 road sections were utilized to examine the field pavement history, while the Lee County database included only 27 road sections.

Explanatory Data Analysis (EDA)

A total of 30 different pavement systems divided into three major groups: those with a (1) stabilized base, (2) granular base, and (3) stabilized base and granular base/subbase, were investigated, as shown in Figure 17.

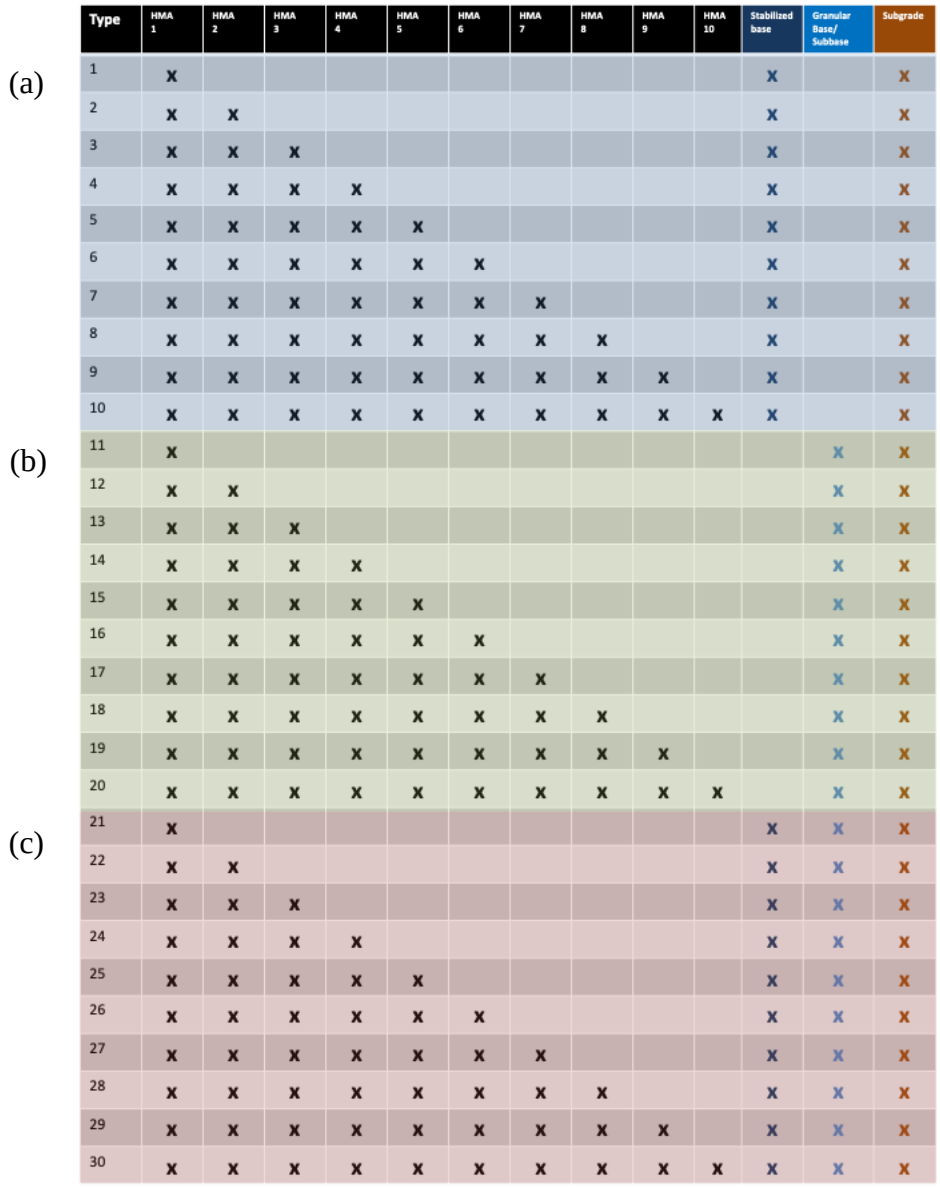

	Type	HMA 1	HMA 2	HMA 3	HMA 4	HMA 5	HMA 6	HMA 7	HMA 8	HMA 9	HMA 10	Stabilized base	Granular Base/ Subbase	Subgrade
(a)	1	X										X		X
	2	X	X									X		X
	3	X	X	X								X		X
	4	X	X	X	X							X		X
	5	X	X	X	X	X						X		X
	6	X	X	X	X	X	X					X		X
	7	X	X	X	X	X	X	X				X		X
	8	X	X	X	X	X	X	X	X			X		X
	9	X	X	X	X	X	X	X	X	X		X		X
	10	X	X	X	X	X	X	X	X	X	X	X		X
(b)	11	X											X	X
	12	X	X										X	X
	13	X	X	X									X	X
	14	X	X	X	X								X	X
	15	X	X	X	X	X							X	X
	16	X	X	X	X	X	X						X	X
	17	X	X	X	X	X	X	X					X	X
	18	X	X	X	X	X	X	X	X				X	X
	19	X	X	X	X	X	X	X	X	X			X	X
	20	X	X	X	X	X	X	X	X	X	X		X	X
(c)	21	X										X	X	X
	22	X	X									X	X	X
	23	X	X	X								X	X	X
	24	X	X	X	X							X	X	X
	25	X	X	X	X	X						X	X	X
	26	X	X	X	X	X	X					X	X	X
	27	X	X	X	X	X	X	X				X	X	X
	28	X	X	X	X	X	X	X	X			X	X	X
	29	X	X	X	X	X	X	X	X	X		X	X	X
	30	X	X	X	X	X	X	X	X	X	X	X	X	X

Figure 17. Synthetic database structure including 1 to 10 HMA layers, subgrade layer, and (a) stabilized base, (b) granular base, and (c) stabilized base + granular base/subbase

Each group, comprised of 10 different pavement types with 1 to 10 HMA layers, contained 50,000 different pavement cases. Figure 18 shows an example of a synthetic database worksheet that included a granular base.

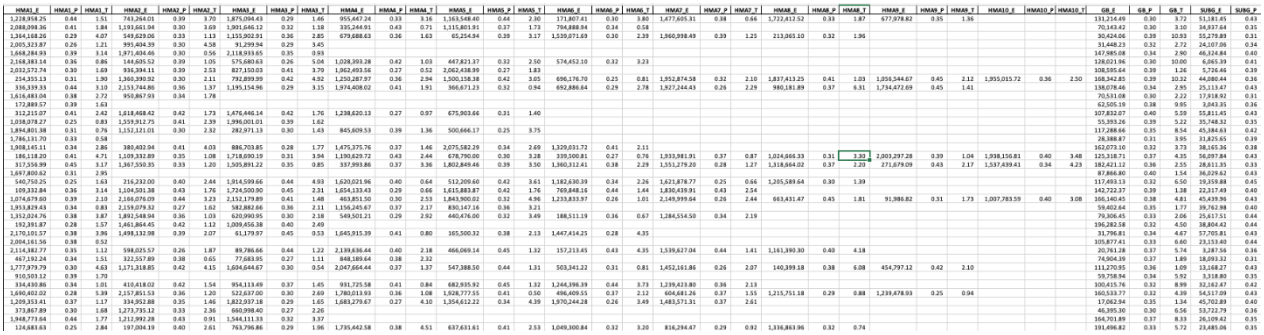

Figure 18. An example of synthetic database worksheet

In the synthetic database, each column indicates each input variable, while each pavement system case is represented by each row. The elastic modulus per each HMA layer (from 1 to 10), granular base layer, and subgrade layer are shown as "HMA1_E, HMA2_E, …, HMA10_E, GB_E, and SUBG_E," respectively. The thickness per each HMA layer (from 1 to 10) and granular base layer is shown as "HMA1_T, HMA2_T, …, HMA10_T, and GB_T," respectively. The Poisson's ratio per each HMA layer (from 1 to 10), granular base layer, and subgrade layer is shown as "HMA1_P, HMA2_P, …, HMA10_P, GB_P, and SUBG_P," respectively.

The database was randomly generated within the pavement characteristic ranges defined previously in Table 5. Each input variable (i.e., each column in Figure 18) except for thickness was uniformly distributed throughout all pavement cases over the interval [0, 1] and then incorporated into the above ranges, with equation 11 used to find the generated variable.

$$y_i = y_{min} + (y_{max} - y_{min}) \times x_i \qquad \textbf{(11)}$$

where:

y_i = Generated variable for the ith case
y_{min} = Minimum value of the variable within the range
y_{max} = Maximum value of the variable within the range
x_i = Uniformly distributed value of the variable for the ith case

However, since there are three boundary conditions for the thickness variable, it is more complex than the other variables given the following:

1. Each thickness variable within a pavement system had a minimum/maximum range—each thickness data point per row in Figure 18 (i.e., each HMA overlay thickness for each pavement case) (e.g., min 0.5 in. and max 10 in.).
2. Total HMA thickness within a pavement system had a minimum/maximum range—the sum of all HMA thickness data points per row in Figure 18 (i.e., total thickness of HMA layers for each pavement case) (e.g., maximum 25 in.).
3. The size of each thickness variable per column in Figure 18 is not the same as the size of other thickness variables—the quantity of pavement cases per column, in Figure 18, from the

1st HMA layer to the 10th HMA layer (e.g., the quantity of pavement cases from 1 layer of HMA [HMA_1_T] to 10 layers of HMA [HMA_10_T] is not equal for each one.). This means that pavement cases with 1 to 10 HMA layers always contain HMA_1_T, but for example, only pavement cases with 10 layers of HMA have HMA_10_T; the HMA pavement systems with 1 to 9 layers does not (Σ (HMA_1_T) $\neq$ Σ (HMA_2_T) $\neq$ Σ (HMA_3_T) .... $\neq$ Σ (HMA_10_T)). This, along with the distribution of each thickness variable, affects the data size.

There is therefore a dependency in the thickness variables generated using real distributions on historical data of Iowa county roads and highways. Using the historical pavement database, field investigations, and experience, the thickness variables were generated based on the specified population mean and standard deviation within the data ranges.

The next step was to check the quality of generated synthetic data. Since data quality is a fundamental point of assessment when beginning to develop any model, the generated synthetic database was evaluated during initial investigations to determine patterns, identify inconsistencies, test hypotheses, and check assumptions by means of summary statistics and graphical representations using EDA. For example, for the synthetic database developed for pavement systems including 1 to 10 HMA layers, a granular base, and a subgrade layer, the distributions of each variable (i.e., elastic modulus, Poisson's ratio, and thickness) were plotted as shown in Figure 19.

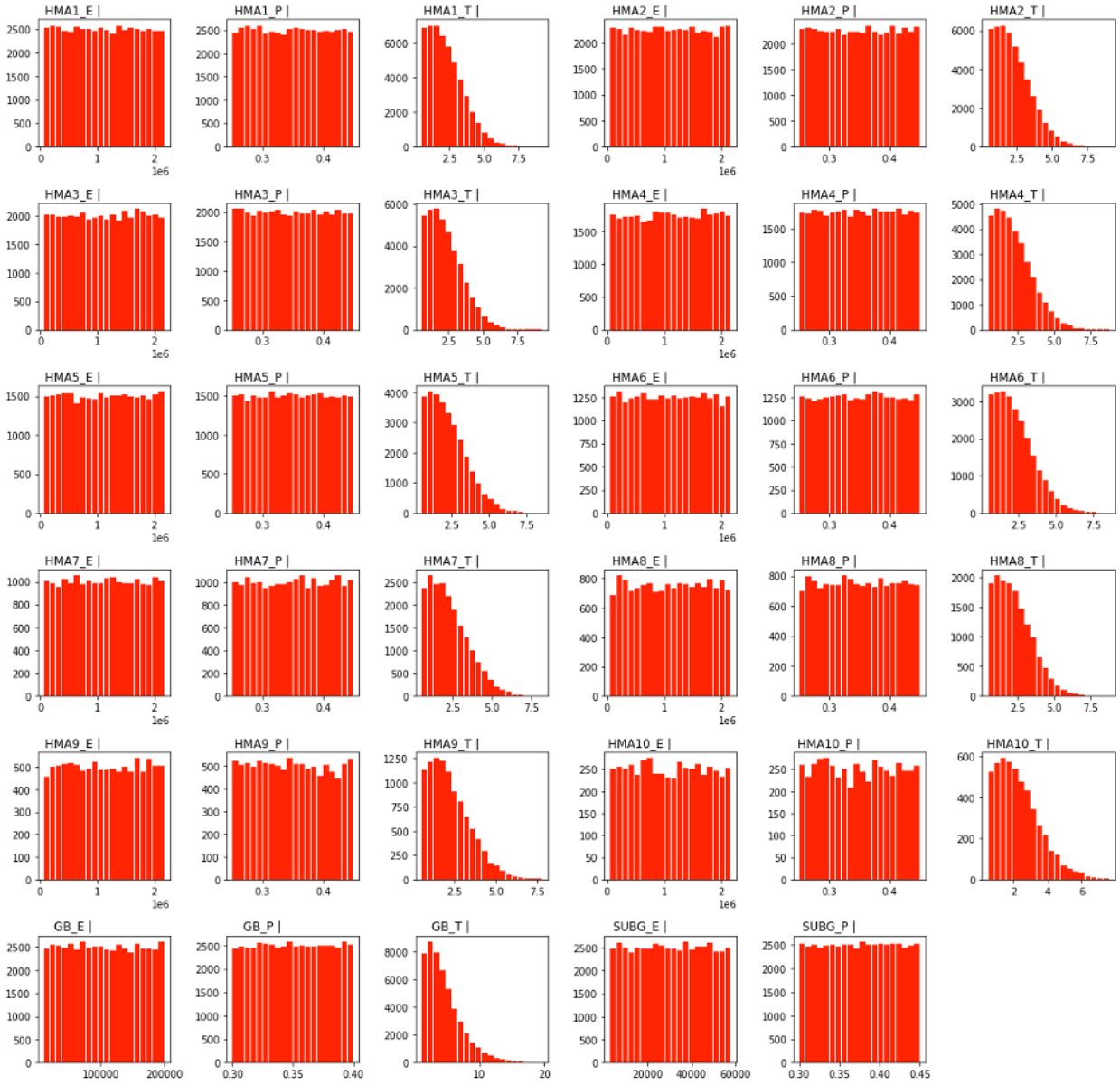

Figure 19. Sample distribution of each variable in the developed synthetic database for pavement systems with a granular base

Each variable except for thickness was tested to determine whether it satisfied the uniformity criterion using the kstest function from SciPy to perform a Kolmogorov-Smirnov test on each data set to calculate the probability value (p-value) under the following scenario:

- The null hypothesis proposes that there is no difference between a certain characteristic distribution and a uniform distribution.
- If the p-value is less than 0.05, the deviation from the null hypothesis is statistically significant, rejecting the null hypothesis. This means that the given data are not uniformly distributed.

- If the p-value is greater than 0.05, the deviation from the null hypothesis is not statistically significant, the null hypothesis is accepted, and the given data are uniformly distributed.

From the output, the p-value for each elastic modulus and Poisson's ratio variable was calculated, and it was confirmed that they were greater than 0.05, as indicated in Figure 18.

The thickness variables were tested to determine whether each satisfies the stated assumptions. For this purpose, the skew and statistics functions from SciPy were used to compute the moments of the probability density function (mean, variance, and skewness) on each thickness data set. Skewness is the measure of the asymmetry observed in a probability distribution; if the distribution has a long left tail, it is called a left-skewed or negative-skewed distribution. If the distribution has a long right tail, it is called a right-skewed or positive-skewed distribution.

- If -0.5 < skewness < 0.5, the distribution is approximately symmetric
- If 0.5 < skewness < 1.0, the distribution is moderately right-skewed
- If skewness < -1.0 or skewness > 1.0, the distribution is highly left- or right-skewed

From the output, skewness per each thickness variable was calculated and verified to be similar to the investigated values; based on the field data, the mean and standard deviation values also overlapped with the defined values, as shown in Figure 19 for pavement systems with a granular base.

Correlation analysis was performed to investigate input variable quality and their relationships, and the correlation matrices of the input variables for each type of pavement systems are presented in Figure 20.

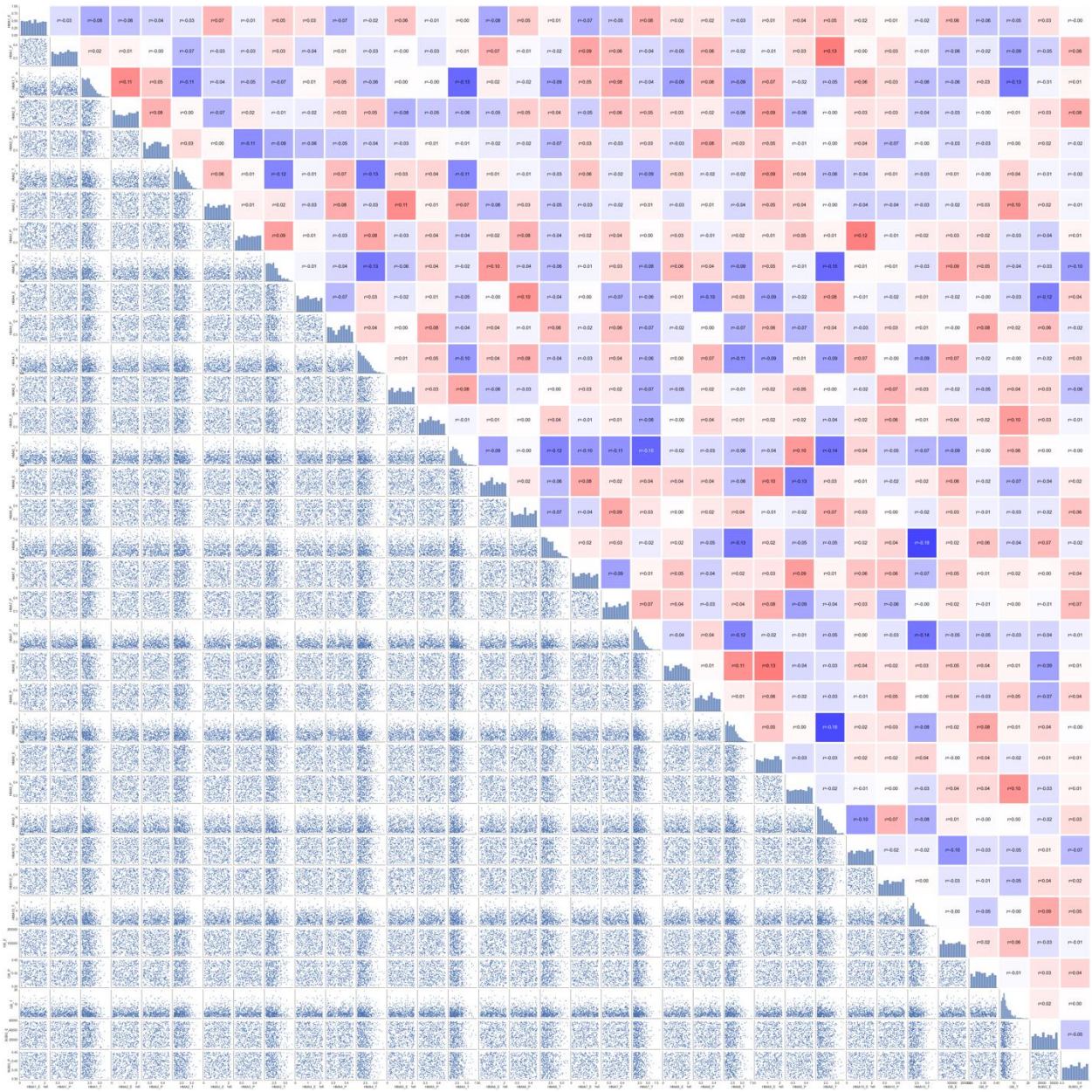

Figure 20. Sample correlation matrix of input variables of granular base pavement systems

The x- and y-axes of the correlation matrix represent each variable in the data set. The lower left part of Figure 20 reflects scatterplot correlation graphs comparing the two variables. The correlation graphs may either have positive correlation, negative correlation, or no correlation. Positive correlation means as one variable increases, the other variable also increases. Negative correlation means as one variable increases, the other variable decreases. No correlation means there is no connection between two variables, a desired condition for variables to be used in the development of ANN models, so variables exhibiting a strong correlation should be removed to improve model performance and reduce overfitting.

The upper right part of Figure 20 shows the correlation heatmap for visualizing the strength of relationships between the two variables using the correlation coefficient *r*. For this purpose, the pearsonr function from SciPy was used to perform correlation tests on each data set to calculate a Pearson correlation coefficient *r* that measures the linear relationship between two data sets. The *r* coefficients vary between -1 and +1, with 0 implying no correlation. In Figure 20, darker colors represent stronger relationships (e.g., dark blue shows positive correlation [between 0 and 1], while dark red indicates negative correlation [between -1 and 0]), and lighter colors visualize the absence of or weaker relationships (~0). Based on the outputs from the developed synthetic databases, it was confirmed that there was almost no correlation among the variables, with the highest *r* value of 0.18.

Table 6 through Table 8 provide information on the descriptive statistics of the synthetic databases used to develop the ANN models for pavement systems, including those with a stabilized base (Table 6), granular base (Table 7), and stabilized and granular base (Table 8).

Table 6. Statistics of synthetic databases for pavement systems with a stabilized base

SB CASE	***count***	***mean***	***std***	***min***	***25%***	***50%***	***75%***	***max***
HMA1_E	50,000	1,114,889.81	612,447.98	58,052.95	585,212.62	1,115,315.45	1,645,931.07	2,174,995.83
HMA1_P	50,000	0.35	0.06	0.25	0.30	0.35	0.40	0.45
HMA1_T	50,000	2.27	1.24	0.50	1.28	2.06	3.04	9.39
HMA2_E	45,000	1,114,257.28	612,953.73	58,007.62	582,490.52	1,110,293.69	1,648,372.38	2,174,944.00
HMA2_P	45,000	0.35	0.06	0.25	0.30	0.35	0.40	0.45
HMA2_T	45,000	2.26	1.23	0.50	1.28	2.05	3.03	9.50
HMA3_E	40,000	1,116,986.95	610,163.41	58,009.91	588,422.38	1,117,467.12	1,646,600.44	2,174,989.03
HMA3_P	40,000	0.35	0.06	0.25	0.30	0.35	0.40	0.45
HMA3_T	40,000	2.26	1.24	0.50	1.27	2.05	3.03	8.73
HMA4_E	35,000	1,117,415.68	613,353.22	58,037.73	583,769.13	1,118,966.67	1,649,354.30	2,174,866.40
HMA4_P	35,000	0.35	0.06	0.25	0.30	0.35	0.40	0.45
HMA4_T	35,000	2.28	1.24	0.50	1.29	2.09	3.04	8.72
HMA5_E	30,000	1,114,116.95	610,433.67	58,055.91	583,979.48	1,111,836.60	1,643,715.09	2,174,845.23
HMA5_P	30,000	0.35	0.06	0.25	0.30	0.35	0.40	0.45
HMA5_T	30,000	2.27	1.24	0.50	1.28	2.06	3.05	9.41
HMA6_E	25,000	1,122,386.83	611,228.29	58,002.42	592,265.99	1,121,852.28	1,655,927.43	2,174,959.54
HMA6_P	25,000	0.35	0.06	0.25	0.30	0.35	0.40	0.45
HMA6_T	25,000	2.26	1.24	0.50	1.27	2.05	3.01	9.31
HMA7_E	20,000	1,121,763.04	608,845.79	58,011.79	600,024.48	1,123,493.18	1,649,590.81	2,174,973.28
HMA7_P	20,000	0.35	0.06	0.25	0.30	0.35	0.40	0.45
HMA7_T	20,000	2.26	1.25	0.50	1.27	2.05	3.03	9.91
HMA8_E	15,000	1,115,352.60	607,822.56	58,185.91	593,154.73	1,113,409.69	1,640,362.87	2,174,561.05
HMA8_P	15,000	0.35	0.06	0.25	0.30	0.35	0.40	0.45
HMA8_T	15,000	2.28	1.24	0.50	1.29	2.07	3.03	8.53
HMA9_E	10,000	1,122,156.53	609,801.28	58,022.43	596,982.58	1,125,872.37	1,647,913.73	2,174,923.19
HMA9_P	10,000	0.35	0.06	0.25	0.30	0.35	0.40	0.45
HMA9_T	10,000	2.27	1.25	0.50	1.28	2.06	3.03	8.31
HMA10_E	5,000	1,101,951.96	610,233.28	58,430.62	577,576.77	1,090,702.66	1,621,480.68	2,174,861.76
HMA10_P	5,000	0.35	0.06	0.25	0.30	0.35	0.40	0.45
HMA10_T	5,000	2.27	1.24	0.50	1.28	2.06	3.02	8.43
SB_E	50,000	1,116,524.06	611,609.71	58,009.86	584,746.13	1,118,481.33	1,645,365.16	2,174,986.04
SB_P	50,000	0.35	0.06	0.25	0.30	0.35	0.40	0.45
SB_T	50,000	4.50	2.77	1.00	2.42	3.86	5.87	19.75
SUBG_E	50,000	30,399.08	15,833.54	3,001.60	16,546.20	30,531.15	43,939.19	57,998.36
SUBG_P	50,000	0.38	0.04	0.30	0.34	0.38	0.41	0.45

Table 7. Statistics of synthetic databases for pavement systems with a granular base

GB CASE	***count***	***mean***	***std***	***min***	***25%***	***50%***	***75%***	***max***
HMA1_E	50,000	1,112,752.87	611,751.99	58,026.67	583,748.24	1,110,991.44	1,641,808.38	2,174,997.09
HMA1_P	50,000	0.35	0.06	0.25	0.30	0.35	0.40	0.45
HMA1_T	50,000	2.28	1.25	0.50	1.28	2.07	3.06	9.17
HMA2_E	45,000	1,115,903.73	611,538.55	58,010.57	586,930.95	1,114,332.19	1,642,358.83	2,174,993.72
HMA2_P	45,000	0.35	0.06	0.25	0.30	0.35	0.40	0.45
HMA2_T	45,000	2.28	1.24	0.50	1.28	2.07	3.05	9.04
HMA3_E	40,000	1,118,761.77	612,236.05	58,137.70	587,753.12	1,120,044.37	1,654,987.77	2,174,943.34
HMA3_P	40,000	0.35	0.06	0.25	0.30	0.35	0.40	0.45
HMA3_T	40,000	2.28	1.24	0.50	1.29	2.06	3.06	9.27
HMA4_E	35,000	1,121,194.40	611,408.11	58,021.09	590,419.93	1,120,136.81	1,655,156.12	2,174,933.16
HMA4_P	35,000	0.35	0.06	0.25	0.30	0.35	0.40	0.45
HMA4_T	35,000	2.27	1.24	0.50	1.27	2.05	3.02	8.74
HMA5_E	30,000	1,118,026.69	612,640.22	58,033.37	581,453.56	1,119,777.88	1,647,926.90	2,174,766.93
HMA5_P	30,000	0.35	0.06	0.25	0.30	0.35	0.40	0.45
HMA5_T	30,000	2.27	1.25	0.50	1.27	2.06	3.04	8.56
HMA6_E	25,000	1,113,886.58	610,289.44	58,025.20	585,630.28	1,114,044.77	1,643,179.22	2,174,962.20
HMA6_P	25,000	0.35	0.06	0.25	0.30	0.35	0.40	0.45
HMA6_T	25,000	2.27	1.25	0.50	1.28	2.07	3.04	8.51
HMA7_E	20,000	1,118,041.12	610,470.90	58,124.17	593,262.01	1,121,198.70	1,646,723.09	2,174,934.04
HMA7_P	20,000	0.35	0.06	0.25	0.30	0.35	0.40	0.45
HMA7_T	20,000	2.27	1.24	0.50	1.27	2.05	3.04	8.19
HMA8_E	15,000	1,119,729.48	611,674.85	58,001.89	588,098.26	1,124,868.89	1,651,206.59	2,174,993.90
HMA8_P	15,000	0.35	0.06	0.25	0.30	0.35	0.40	0.45
HMA8_T	15,000	2.29	1.24	0.50	1.29	2.09	3.07	8.76
HMA9_E	10,000	1,121,015.31	611,460.67	58,262.78	588,360.13	1,117,369.91	1,656,409.66	2,174,699.51
HMA9_P	10,000	0.35	0.06	0.25	0.30	0.35	0.40	0.45
HMA9_T	10,000	2.24	1.22	0.50	1.27	2.02	2.99	7.82
HMA10_E	5,000	1,111,071.78	612,616.06	58,398.95	585,872.49	1,111,203.72	1,636,525.69	2,174,936.90
HMA10_P	5,000	0.35	0.06	0.25	0.30	0.35	0.40	0.45
HMA10_T	5,000	2.29	1.25	0.50	1.31	2.08	3.03	7.59
SB_E	50,000	104,795.56	54,953.02	10,001.99	57,064.16	104,279.62	152,698.86	199,997.71
SB_P	50,000	0.35	0.03	0.30	0.33	0.35	0.38	0.40
SB_T	50,000	4.52	2.78	1.00	2.43	3.86	5.89	19.65
SUBG_E	50,000	30,452.75	15,853.42	3,000.28	16,768.31	30,445.31	44,175.71	57,999.26
SUBG_P	50,000	0.38	0.04	0.30	0.34	0.38	0.41	0.45

Table 8. Statistics of synthetic databases for pavement systems with a stabilized base + granular base

SBGB CASE	***count***	***mean***	***std***	***min***	***25%***	***50%***	***75%***	***max***
HMA1_E	50,000	1,119,026.47	609,745.62	58,010.61	595,631.02	1,118,539.04	1,646,191.11	2,174,893.34
HMA1_P	50,000	0.35	0.06	0.25	0.30	0.35	0.40	0.45
HMA1_T	50,000	2.27	1.24	0.50	1.28	2.06	3.03	9.04
HMA2_E	45,000	1,115,625.53	612,156.03	58,053.44	580,996.68	1,114,197.24	1,645,830.72	2,174,985.67
HMA2_P	45,000	0.35	0.06	0.25	0.30	0.35	0.40	0.45
HMA2_T	45,000	2.27	1.24	0.50	1.28	2.07	3.05	8.91
HMA3_E	40,000	1,115,008.78	608,661.24	58,012.98	589,807.75	1,116,144.49	1,638,785.93	2,174,926.36
HMA3_P	40,000	0.35	0.06	0.25	0.30	0.35	0.40	0.45
HMA3_T	40,000	2.27	1.25	0.50	1.27	2.06	3.05	9.17
HMA4_E	35,000	1,115,375.68	607,919.79	58,161.38	594,592.52	1,113,850.17	1,640,660.24	2,174,910.10
HMA4_P	35,000	0.35	0.06	0.25	0.30	0.35	0.40	0.45
HMA4_T	35,000	2.27	1.24	0.50	1.28	2.06	3.04	10.07
HMA5_E	30,000	1,117,642.37	610,332.32	58,038.46	590,929.77	1,112,414.78	1,648,353.01	2,174,970.35
HMA5_P	30,000	0.35	0.06	0.25	0.30	0.35	0.40	0.45
HMA5_T	30,000	2.27	1.24	0.50	1.29	2.05	3.03	9.05
HMA6_E	25,000	1,114,991.26	610,661.16	58,163.43	582,809.49	1,116,506.85	1,640,483.36	2,174,994.37
HMA6_P	25,000	0.35	0.06	0.25	0.30	0.35	0.40	0.45
HMA6_T	25,000	2.27	1.25	0.50	1.28	2.05	3.06	9.91
HMA7_E	20,000	1,122,064.92	609,447.52	58,005.78	591,756.57	1,124,808.13	1,645,207.90	2,174,947.54
HMA7_P	20,000	0.35	0.06	0.25	0.30	0.35	0.40	0.45
HMA7_T	20,000	2.26	1.24	0.50	1.27	2.05	3.03	8.94
HMA8_E	15,000	1,124,476.64	612,038.59	58,032.98	599,603.24	1,128,569.04	1,653,749.19	2,174,709.76
HMA8_P	15,000	0.35	0.06	0.25	0.30	0.35	0.40	0.45
HMA8_T	15,000	2.27	1.24	0.50	1.27	2.07	3.02	8.22
HMA9_E	10,000	1,120,857.05	610,980.16	58,092.70	590,198.36	1,115,950.73	1,653,361.12	2,174,741.67
HMA9_P	10,000	0.35	0.06	0.25	0.30	0.35	0.40	0.45
HMA9_T	10,000	2.27	1.25	0.50	1.28	2.06	3.04	8.44
HMA10_E	5,000	1,113,609.01	610,535.08	58,538.81	583,915.10	1,105,777.75	1,639,948.47	2,174,743.48
HMA10_P	5,000	0.35	0.06	0.25	0.30	0.35	0.40	0.45
HMA10_T	5,000	2.25	1.22	0.50	1.27	2.04	2.99	7.61
SB_E	50,000	1,118,045.77	610,996.05	58,003.32	588,085.19	1,119,062.83	1,647,682.91	2,174,994.85
SB_P	50,000	0.35	0.06	0.25	0.30	0.35	0.40	0.45
SB_T	50,000	4.52	2.77	1.00	2.45	3.87	5.91	19.87
SUBG_E	50,000	105,174.80	54,828.92	10,002.39	57,854.66	104,965.86	152,836.49	199,998.92
SUBG_P	50,000	0.35	0.03	0.30	0.33	0.35	0.38	0.40

As indicated in the tables, a total of 50,000 different pavement cases were generated for pavement systems with a granular base representing 5,000 pavement cases per each type of pavement system (e.g., one layer of HMA + granular base + subgrade, two layers of HMA + granular base + subgrade, and so on).

Data Wrangling

After analyzing the data sets and summarizing their main characteristics, data wrangling—an important aspect of implementing ANN models—was the next main step used to convert the raw data into a format suitable for use by machine learning models. Decisions made at this stage of model development are critical to network performance. Feature transformation and scaling are two widely used preprocessing methods. During feature transformation, raw data inputs are manipulated to create a single input, while feature scaling involves evenly distributing the data and scaling it to an acceptable range for feeding the network.

One of the most commonly used feature transformation techniques is the log transform, primarily used to convert a skewed distribution into a normal or less-skewed distribution. A transformed data set is created by taking the log of the data points, after which any feature scaling method can be applied using the transformed data set. Although there are many feature scaling techniques, normalization or standardization methods are used in the majority of machine learning models.

If data are not scaled, one of the input features might completely dominate the others, resulting in loss of information. To prevent that, data normalization—a simple linear scaling of data that transforms the data to fall within the minimum and maximum boundaries, typically in the range of -1 to 1 or 0 to 1—is performed. Equation 12 was used for transforming each data value, x_{given}, to an input value, $x_{scaled,min-max}$, to be used in the models.

$$x_{scaled,min-max} = s_{min} + (s_{max} - s_{min}) \times \frac{x_{given} - x_{min}}{x_{max} - x_{min}} \quad \textbf{(12)}$$

where:

$x_{scaled,min-max}$ = Scaled value using min-max scaler
x_{given} = Given original value
x_{min} = Minimum value of the data set that is used to train a model
x_{max} = Maximum value of the data set that is used to train a model
s_{min} = Minimum value of the scaling range (e.g., 0)
s_{max} = Maximum value of the scaling range (e.g., 1)

Data standardization transforms the data to fall around a mean of 0, with a standard deviation of 1. It utilizes statistical measures (e.g., mean and variance) to help remove outliers and spread out the distribution of data, tending to increase uniformity. In this way, the mean and standard deviation of the input data sets are determined. Standardization makes the algorithm less sensitive to outliers compared to min-max scaling (normalization), since there is no predefined

scaling range. Equation 13 was used for transforming each data value, x_{given}, to an input value, $x_{scaled,std}$, for use in the models.

$$x_{scaled,std} = \frac{x_{given} - \bar{x}}{\sigma} \quad \textbf{(13)}$$

where:

$x_{scaled,std}$ = Scaled value using standard scaler
x_{given} = Given original value
$\bar{x}$ = Mean of the data set that is used to train a model
σ = Standard deviation of the data set that is used to train a model

In this study, the MinMaxScaler and StandardScaler modules from the sklearn.preprocessing library in Python were used to normalize and standardize each data set using the min-max scaling range and the mean and standard deviation, respectively. Log transformation was also used for highly skewed data sets.

Generation of Output Database for Models Using Process-Driven Methods

In this study, outputs for modeling were set up to address pavement responses as deflections and strains to compute fatigue and rutting failures and similar damages. It should be emphasized that since there was no available recorded pavement response data corresponding to field data inputs for the pavement systems, physics-based methods were utilized to compute those responses that were then considered as equivalent to field data for outputs.

MatLEA (Kutay and Lanotte 2020) was used to compute pavement responses. This software basically provides a default code for analyzing pavement responses for only one pavement case at a time, but it has been updated and improved by the Iowa State team (see Appendix A) to simultaneously analyze flexible pavement responses (i.e., strain, stress, and deflections) under a standard 9,000 lb traffic load for thousands of pavement cases. It was found that MatLEA accommodates more flexibility in modifying parameters such as defining multiple multilayered pavement systems and produces more accurate results compared to other elastic analysis programs without encountering technical issues during analysis of thousands of cases.

MatLEA inputs were individually prepared for 30 different pavement systems, providing a view of inputs similar to that previously shown in Figure 18. Outputs were calculated, numerically exported, and displayed in the 3D environment shown in Figure 21.

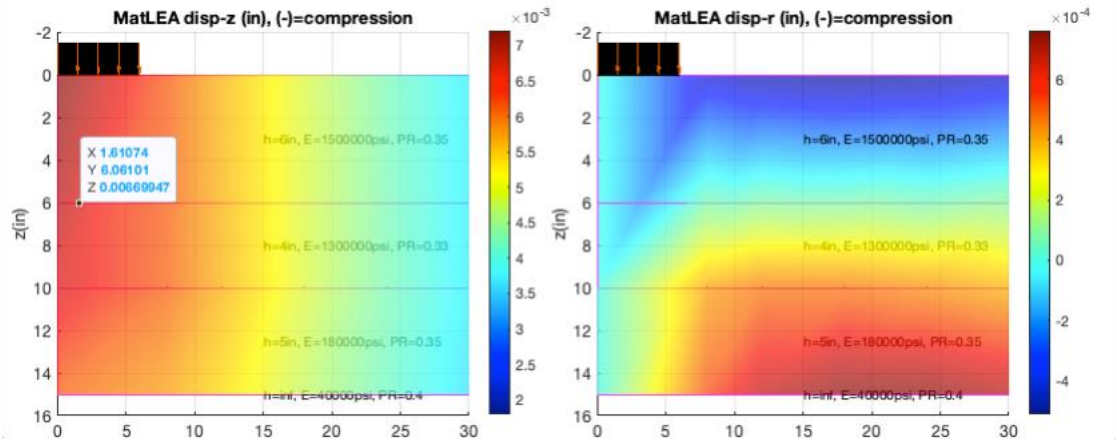

(a) Displacement graphs in vertical (*z*) and horizontal (*r*) directions

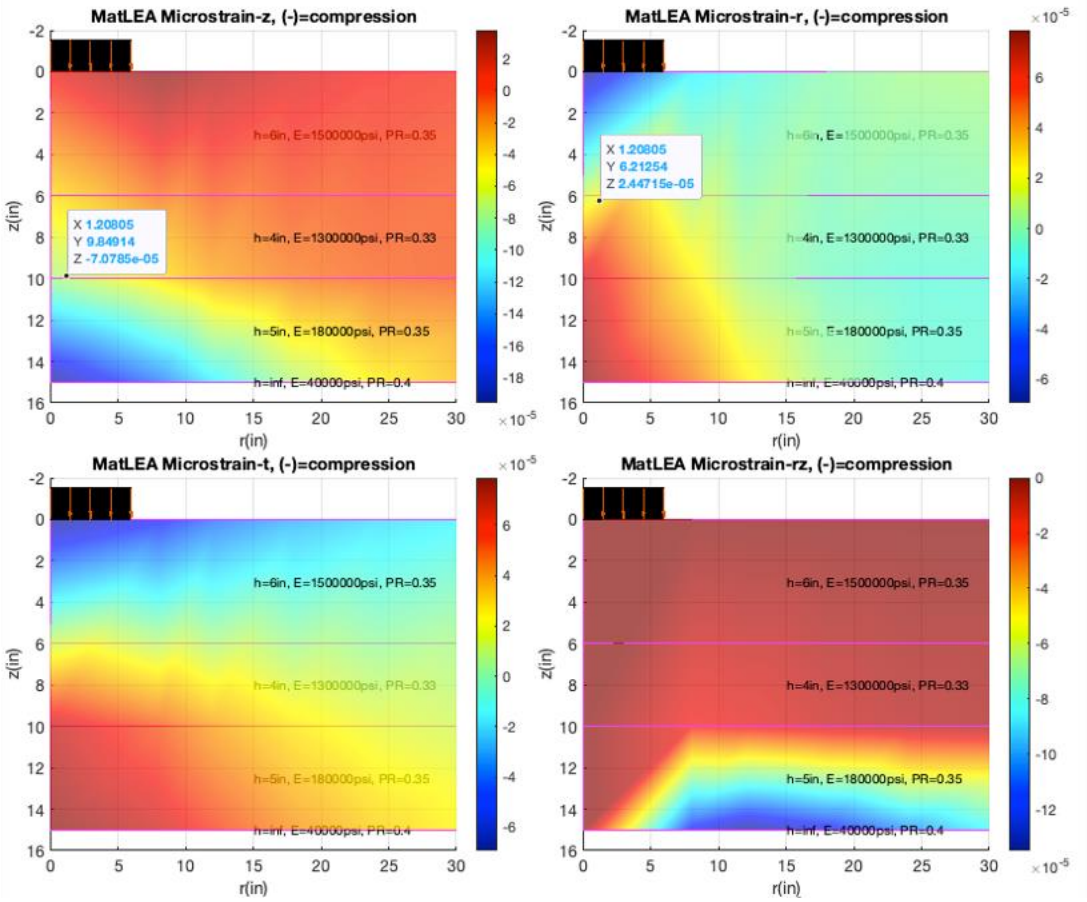

(b) Strain graphs in vertical (*z*), horizontal (*r* and *t*), and shear (*rz*) directions

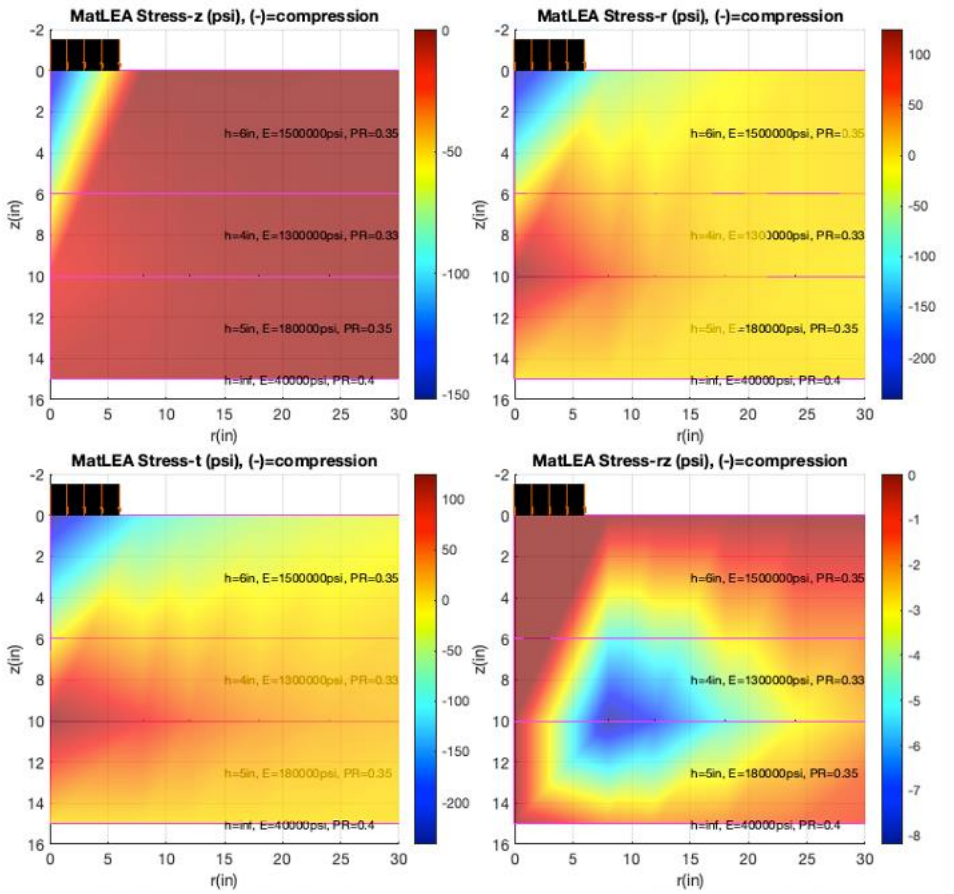

(c) Stress graphs in vertical (*z*), horizontal (*r* and *t*), and shear (*rz*) directions

Figure 21. Sample MatLEA 3D outputs

Clicking on any point on the figure causes outputs and locations of the analysis points (x- and y-axes) to be displayed on 3D graphs. Figures 21a–c show output graphs for displacement, strain, and stress for a sample three-layered pavement system. The material properties of this system assumed that every layer contained homogenous, linear elastic, and isotropic materials, and two adjacent layers of each type were assumed to be fully connected.

For further evaluation, analysis points were selected as the surface, bottom of the asphalt, and top of the subgrade under the applied load. The MatLEA analysis extracted vertical displacements at the surface, bottom of the asphalt layer, and on top of the subgrade, along with horizontal (tensile) strain at the bottom of the asphalt layer and vertical (compressive) strain at the top of the subgrade. These extracted results were used to train ANN models capable of predicting deflections and strain at critical points in pavement systems. Two ANN models were developed to predict deflection and strain for each group of pavement systems, representing a total of six ANN models for all three major groups of flexible pavement systems.

CHAPTER 4. DEVELOPMENT OF PAVEMENT RESPONSE PREDICTION MODELS

Description of ANNs Modeling Approach

The main objective of this study was to develop a pavement-oriented structural analysis tool to support Iowa county engineers' routine pavement analysis, design, and asset management practices for local roads with multiple cycles of construction and renewal. Based on a comprehensive literature review and experience with respect to surrogate pavement structural analysis and design model development using AI techniques, ANNs were selected as the first choice for developing this tool (Ceylan et al. 2014, Gopalakrishnan et al. 2009). The previous studies successfully demonstrated the concept of using surrogate pavement response modeling with ANNs in airport and highway concrete pavement analysis and design as a faster and more robust alternative to time-consuming and more complex FE-based structural modeling (Ceylan et al. 1999, Ceylan 2002, Ceylan and Guclu 2005). This concept of surrogate pavement response modeling, which provides rapid solutions to finding concrete pavement critical responses for various combinations of input parameters (similar to the ISLAB 2000 tool), was also adopted in the development of the MEPDG, now marketed as AASHTOWare Pavement ME Design (AASHTO 2008).

Neural networks are valuable computational tools increasingly being used as an alternative to more traditional techniques to solve complex resource-intensive problems. Over the past two decades there has been increased interest in the use of ANNs in civil engineering fields such as structural engineering, environmental and water resources engineering, traffic engineering, geotechnical engineering, and pavement engineering. Neural networks offer a number of advantages, including the capability to implicitly detect complex nonlinear relationships between dependent and independent variables and to detect all possible interactions between predictor variables, as well as the availability of multiple training algorithms.

ANN modeling has shown great promise as a useful and nontraditional computing tool for analyzing some of the excessively complex nonlinear problems inherent to pavement engineering. ANNs have the potential to investigate, properly model, and as a result provide better understanding of some of the complex pavement engineering mechanisms not previously well understood or even formulated. This is especially possible using the vastly powerful and nonlinear interconnections provided in a network architecture that enables an ANN to transform even very sophisticated FE-based numerical solutions into state-of-the-art pavement structural analysis results.

Among the various types of ANNs, the backpropagation ANN is the one most frequently used for modeling problems of this type and complexity. Backpropagation ANNs are very powerful and versatile networks that can be taught mapping from one data space to another using a representative set of patterns/examples to be learned. The term backpropagation network actually refers to a multilayered, feed-forward neural network trained using an error backpropagation algorithm (Figure 22).

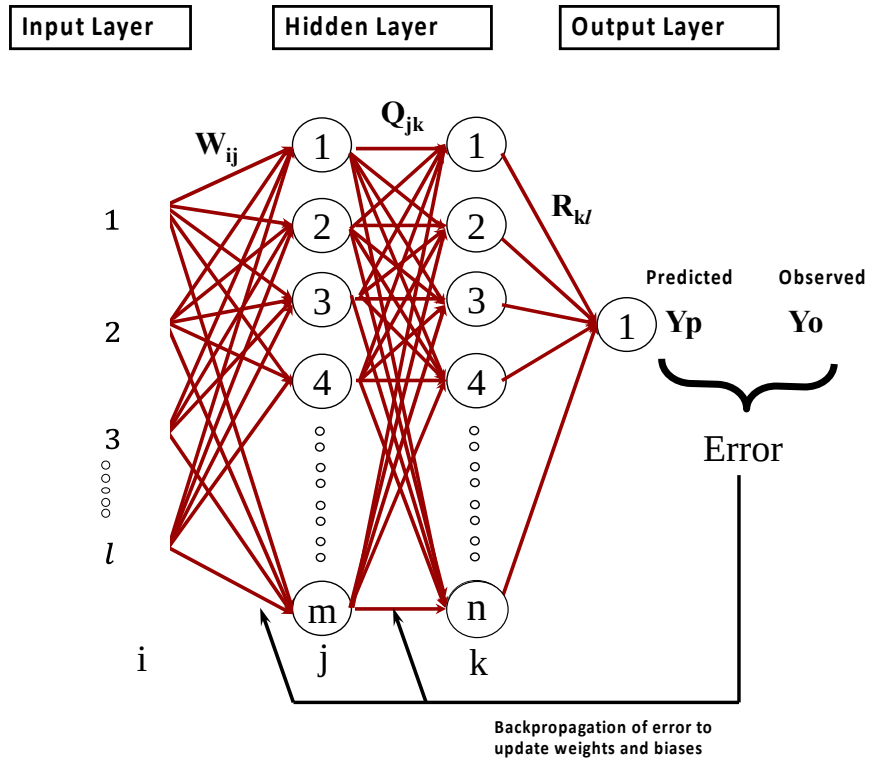

Figure 22. Typical backpropagation ANN architecture

The learning process performed by this algorithm is called backpropagation learning and is mainly an error minimization technique (Haykin 1999, Hecht-Nielsen 1990, Parker 1985, Rumelhart et al. 1986, Werbos 1974).

As with many ANNs, the connection weights in backpropagation ANNs are initially selected at random. Inputs from the mapping examples are propagated forward through each layer of the network and eventually emerge as outputs. The errors between the outputs and the correct answers are then propagated backward through the network and connection weights individually adjusted to reduce the error. After many iterations (training patterns) have been propagated through the network, the mapping function is eventually learned within some specified error tolerance. This is called supervised learning because the network must first be shown the correct answers in order for it to learn. Backpropagation networks with their superior function approximation capabilities excel at data modeling (Haykin 1999).

The overall approach to develop a computational pavement structural analysis model included the following steps:

- Step 1: Identify and finalize the explicit inputs to the ANN model and the desired output parameters, which were based on the findings discussed in previous chapters. The primary inputs to the ANN model included the thickness and modulus of each layer in multilayered pavement structures and the loading configuration in terms of an 18 kip equivalent single

axle load (ESAL). The primary outputs of the ANN model included critical pavement responses (like deflections, stresses, and strains).

- Step 2: Preprocess the synthetic database developed from previous tasks, split the training and independent testing data sets, and use a cross-validation technique that involves dividing data into two segments, one for learning or training a model and one for validating that model.

- Step 3: Start with a trial network architecture based on previous experience (i.e., set the number of hidden layers and other network parameters) to identify a range for parameters.

- Step 4: Conduct a sensitivity analysis (i.e., a grid search, a tuning technique that attempts to calculate the optimal values of hypermeters used to control the learning process) on network parameters to identify the best performing network architectures.

- Step 5: Assess network performance by studying the training and testing curves and statistical performance measures (absolute average error [AAE], standard error of the estimates [SEE], etc.)

The success of the pavement response prediction models in mimicking pavement critical responses computed by MatLEA was quantified using the R^2 (equation 14), the AAE (equation 15), and the SEE (equation 16). Higher R^2 and lower AAE and SEE values are indications of accurate model prediction.

$$R^2 = 1 - \frac{\sum_{j=1}^{n}\left(y_j^{measured} - y_j^{predicted}\right)^2}{\sum_{j=1}^{n}\left(y_j^{measured} - y_{mean}^{measured}\right)^2} \quad \textbf{(14)}$$

$$AAE = \frac{\sum_{j=1}^{n}\left|y_j^{measured} - y_j^{predicted}\right|}{n} \quad \textbf{(15)}$$

$$SEE = \sqrt{\frac{\sum_{j=1}^{n}\left(y_j^{measured} - y_j^{predicted}\right)^2}{n}} \quad \textbf{(16)}$$

where:

n = Data set size
j = Case number in the data set
$y_{measured}$ = Computed deflection or strain
$y_{prediction}$ = Predicted deflection or strain

ANN-Based Pavement Response Prediction Model Development for Pavement Systems with a Stabilized Base

ANN-Based Deflection Prediction Model Development for Pavements with a Stabilized Base

The nonlinear nature of the problem of predicting deflections of a multilayered pavement system leads to the use of ANNs. For training a neural network, 3 output parameters—deflections at the (1) surface, (2) bottom of the asphalt layer, and (3) top of the subgrade layer—were predicted using 35 input parameters, including 3 parameters per each layer: (a) modulus of elasticity, (b) Poisson's ratio, and (c) thickness, excluding the subgrade thickness. The data size of the developed synthetic database was 50,000 cases, 85% of which was used for training and the remainder for independent testing purposes, as shown in Figure 23.

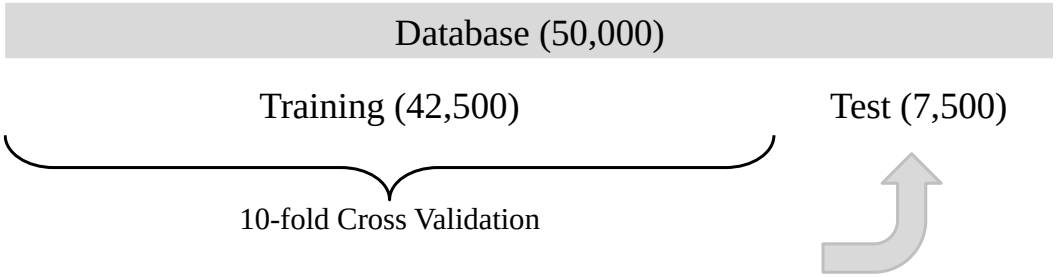

Figure 23. Sample of developed data sets

The 50,000 pavement cases considered included 10 different scenarios with 1 to 10 HMA layers with a stabilized base and subgrade layer. Each scenario reflects 5,000 pavement cases. For training and independent testing, the database was split using a stratified shuffle split technique, with each split maintaining the same percentage for each target class. The chosen target class included 10 different scenarios (i.e., a 3-layered pavement system, 4-layered pavement system, …, 13-layered pavement system). In this way, the independent testing data set had the same proportion of scenarios after the split to represent the entire training data set.

In the input data set used for training the ANN model, 0 represented no data for nonexistent layers, so the empty cells in the sample data set previously shown in Figure 18 were filled with 0s. For example, for a 7-layered pavement system (5 HMA layers, 1 base layer, and 1 subgrade layer), the data points for HMA layers 6 to 10 were set to 0 during training, thus enabling the model to learn to recognize layer existence.

After splitting the entire data set to avoid data leakage, transformation and scaling were applied only on the training data. To explain further, the training data was fitted and transformed using multiple preprocessing methods. Based on the preprocessing techniques and scaling parameters used in the training set, the testing set was then transformed and scaled. After trying various combinations of scaling and transformation techniques and evaluating their effects on model accuracy, the best data preprocessing techniques for each input and output parameter were selected as follows:

- Elastic modulus of layers: min-max scaler
- Poisson's ratio: min-max scaler
- Thickness: ln(x+1) transformation + min-max scaler
- Deflection: ln(x+1) transformation + standard scaler

Table 9 presents the values of the scaling parameters applied to the input and output parameters mentioned previously.

Table 9. Scaling parameters used to train deflection ANN model for pavements with a stabilized base

	Elastic modulus		**Poisson's ratio**		**Thickness**		**Deflection**	
	Scale	*Min*	*Scale*	*Min*	*Scale*	*Min*	*Std dev*	*Mean*
HMA1	4.72E-07	-2.74E-02	5.00	-1.25	0.517	-0.210	-	-
HMA2	4.60E-07	0.00E+00	2.22	0.00	0.425	0.000	-	-
HMA3	4.60E-07	0.00E+00	2.22	0.00	0.440	0.000	-	-
HMA4	4.60E-07	0.00E+00	2.22	0.00	0.445	0.000	-	-
HMA5	4.60E-07	0.00E+00	2.22	0.00	0.427	0.000	-	-
HMA6	4.60E-07	0.00E+00	2.22	0.00	0.429	0.000	-	-
HMA7	4.60E-07	0.00E+00	2.22	0.00	0.418	0.000	-	-
HMA8	4.60E-07	0.00E+00	2.22	0.00	0.446	0.000	-	-
HMA9	4.60E-07	0.00E+00	2.22	0.00	0.448	0.000	-	-
HMA10	4.60E-07	0.00E+00	2.22	0.00	0.446	0.000	-	-
SB	4.72E-07	-2.74E-02	5.00	-1.25	0.427	-0.296	-	-
SUBG	1.82E-05	-5.46E-02	6.67	-2.00	0.517	-0.210	-	-
Surface	-	-	-	-	-	-	9.97E-03	1.15E-02
Bottom of HMA	-	-	-	-	-	-	1.02E-02	1.03E-02
Top of SUBG	-	-	-	-	-	-	1.01E-02	1.00E-02

Since these parameters should be applied on the test input data before being tested in the ANN model, test input data were scaled based on the model training input data set properties. To obtain the output in the original unit, the output predicted by the ANN should be backprocessed based on the model training output data set properties.

A grid search with k-fold cross-validation was used to find the best neural network configuration for use as a surrogate in MatLEA. This validation technique divides the given training data into k-subsets/folds with each fold then used as a test set to produce an accuracy score at each iteration. The overall accuracy of the model is then determined by taking the mean of the accuracies of all the iterations. Using this technique, the capability of the model on new data can be measured. For the ANN-based deflection model, 10-fold cross-validation was used, as shown in Figure 24.

Model	Dataset split for each model (split)									
Split_1	Train	Train	Train	Train	Train	Train	Train	Train	Train	Val.
Split_2	Train	Train	Train	Train	Train	Train	Train	Train	Val.	Train
Split_3	Train	Train	Train	Train	Train	Train	Train	Val.	Train	Train
Split_4	Train	Train	Train	Train	Train	Train	Val.	Train	Train	Train
Split_5	Train	Train	Train	Train	Train	Val.	Train	Train	Train	Train
Split_6	Train	Train	Train	Train	Val.	Train	Train	Train	Train	Train
Split_7	Train	Train	Train	Val.	Train	Train	Train	Train	Train	Train
Split_8	Train	Train	Val.	Train	Train	Train	Train	Train	Train	Train
Split_9	Train	Val.	Train	Train	Train	Train	Train	Train	Train	Train
Split_10	Val.	Train	Train	Train	Train	Train	Train	Train	Train	Train

Figure 24. Sample 10-fold cross-validation

Training was performed 10 times in each new model to ensure that each fold appears as a test set exactly once.

In the grid search, the effects of activation functions (tanh, ReLU, and sigmoid), the number of hidden layers (1, 2, and 3), the number of neurons per hidden layer (8, 16, 32, 64, 96, 128, 160, and 196), solvers (stochastic gradient descent [SGD] and Adam), batch size (1, 10, and 100), and momentum (0.7, 0.8, and 0.9) were all investigated. Batch size determines the number of data points trained each time, and the momentum applied in the weight update speeds the learning and helps avoid getting stuck in local minima. The initial learning rate for the training was 1.0E-3, and it was adaptively changed. Since tolerance for loss was set as 1.0E-4, if the training loss did not decrease by at least the tolerance amount in 10 consecutive epochs, the learning rate was divided by 5. The minimum learning rate of training before termination was 3.2E-7 (i.e., the learning rate changed 5 times by dividing each time by 5, starting from 1.0E-3, then 2.0E-4, 4.0E-5, 8.0E-6, and 1.6E-6, and ending with 3.2E-7). This adaptive learning rate technique could accelerate training by calculating the step size in gradient-based optimization based on the loss gradient.

The optimum architecture for the ANN-based deflection model for pavement systems with a stabilized base was found to be 35-96-96-3, i.e., 35 input parameters with 2 hidden layers including 96 neurons in each hidden layer and 3 outputs, as visualized in Figure 25.

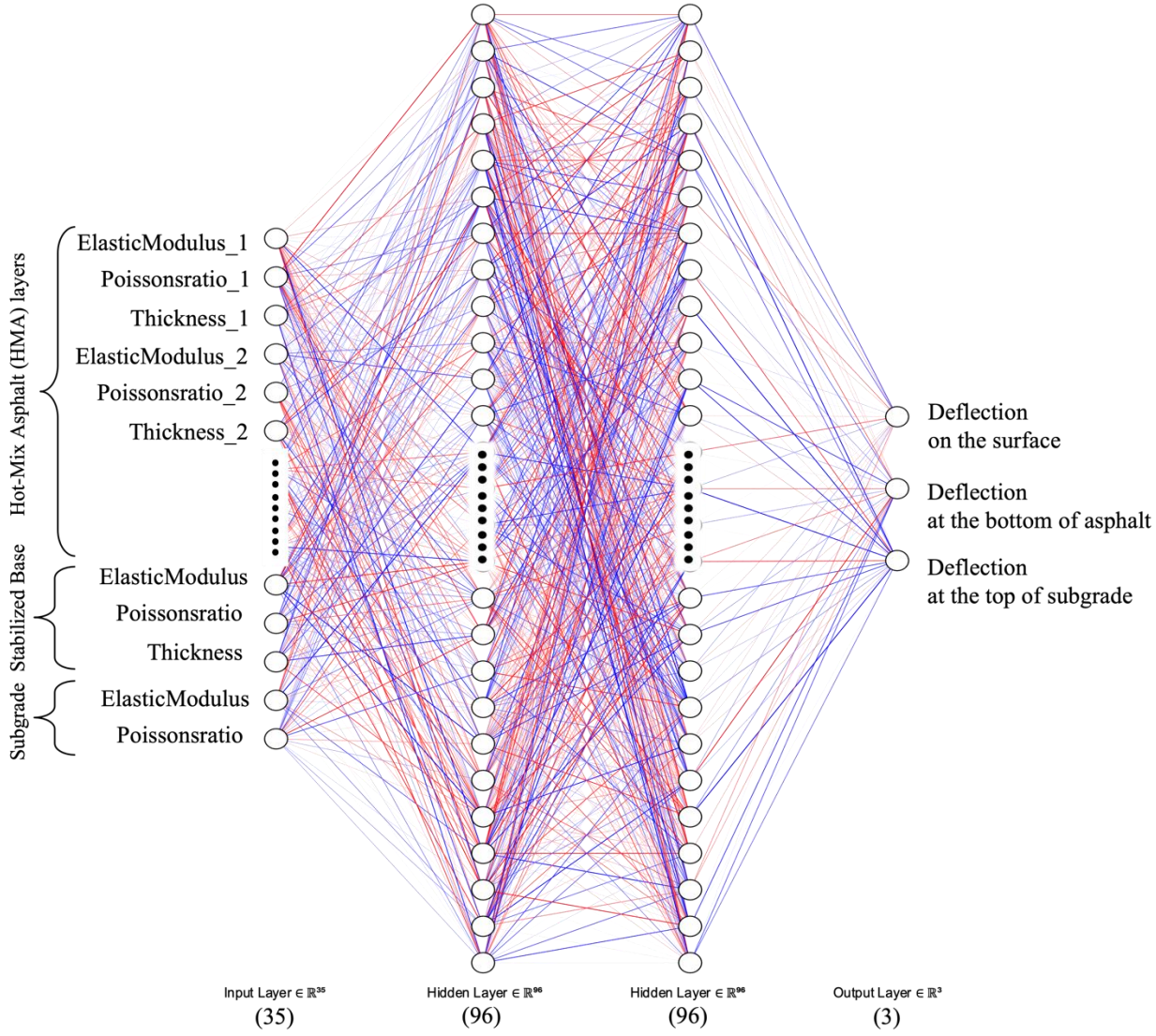

Figure 25. ANN-based deflection model for pavement systems with a stabilized base

This model was trained using a tanh activation function, an SGD optimization technique, a batch size of 1, and a momentum of 0.9. An evaluation to determine the best model was accomplished by comparing the accuracies of the training and validation data sets at each fold, and the mean accuracies of the 10-fold cross-validation represent the overall model training and validation accuracies, indicated by the rightmost bar in Figure 26.

Figure 26. Accuracies of deflection training and validation data sets for pavement systems with a stabilized base

As this comparative bar chart shows, the final scores (R^2) of the training and validation data sets in each of the 10 folds were very high (above 99%) and very similar to one another, with only a slight variation in the thousandths digit; this proves an absence of overfitting or underfitting.

Figures 27a–c and Figures 28a–c show the overall comparable accuracy results for training and independent testing, respectively, of the ANN-based deflection model (a) on the surface, (b) at the bottom of the asphalt layer, and (c) at the top of the subgrade for pavement systems with a stabilized base.

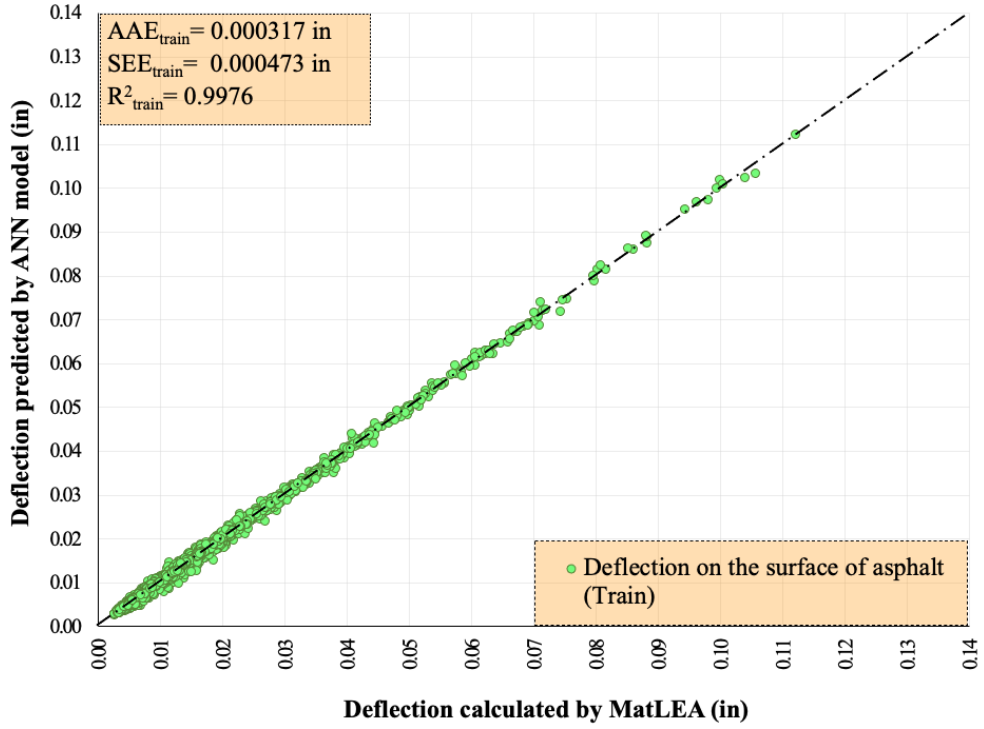

(a) Deflection on the surface

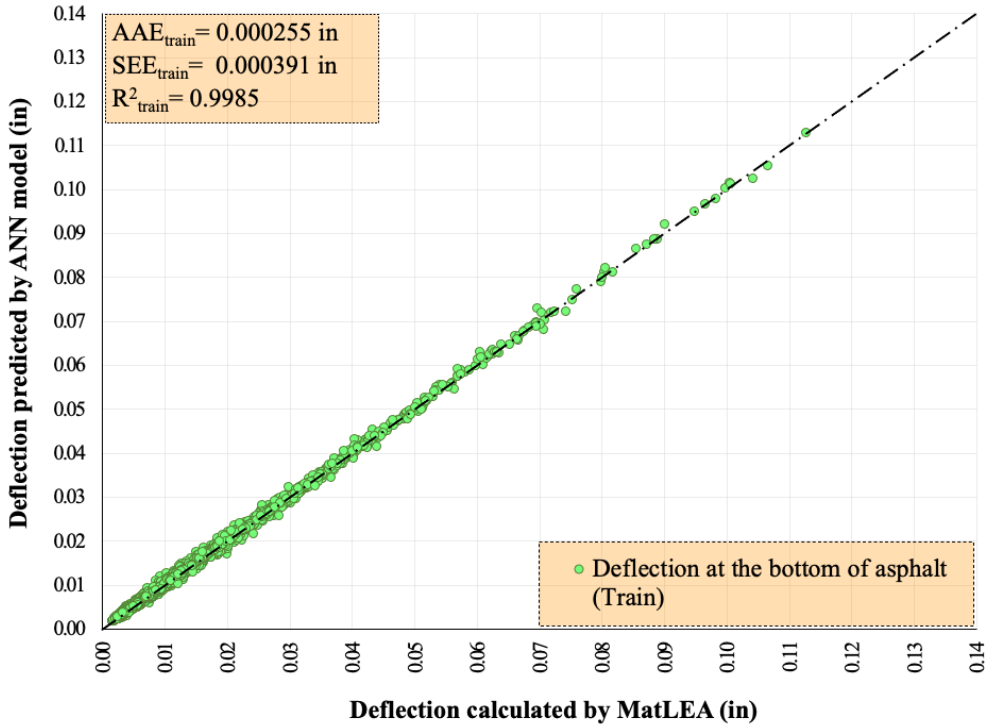

(b) Deflection at the bottom of the asphalt

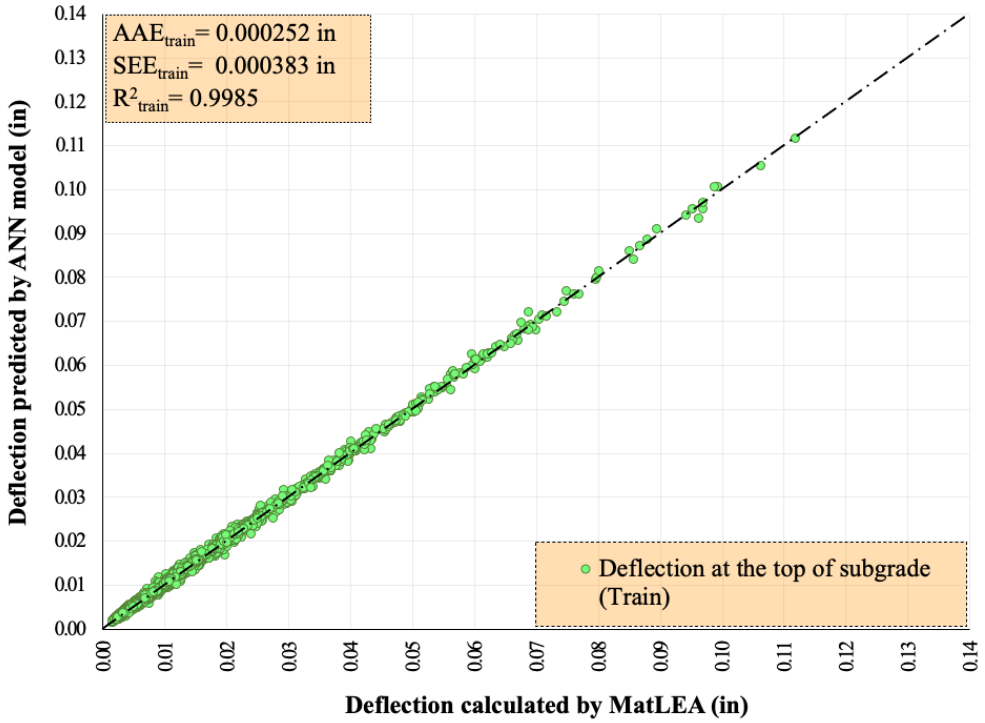

(c) Deflection at the top of the subgrade

Figure 27. Accuracies of training data set for each deflection for pavement systems with a stabilized base

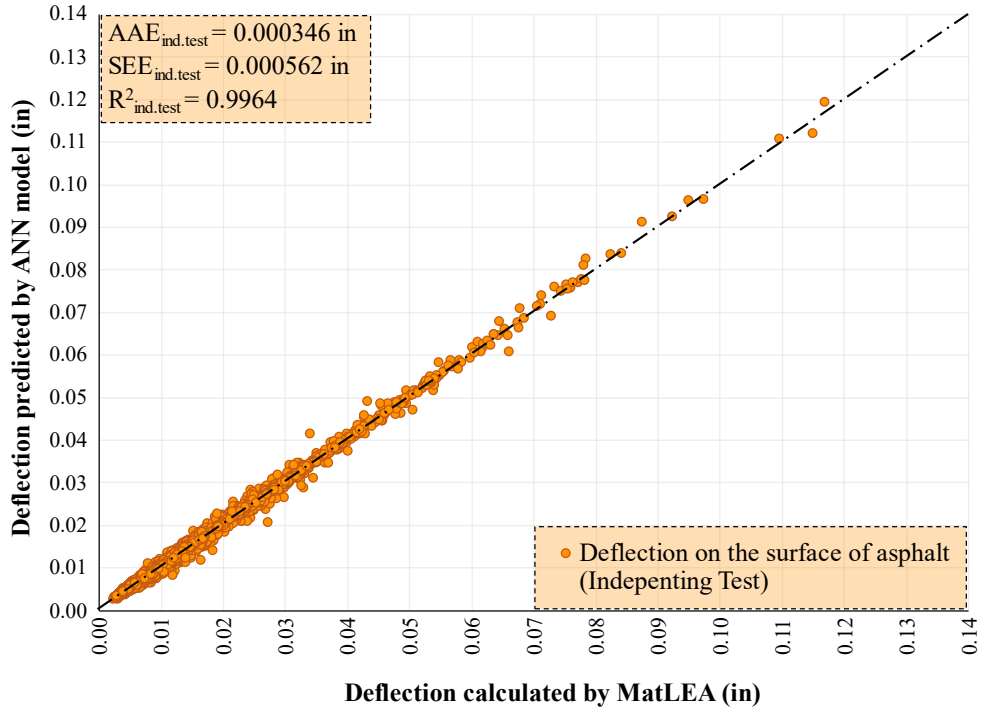

(a) Deflection on the surface

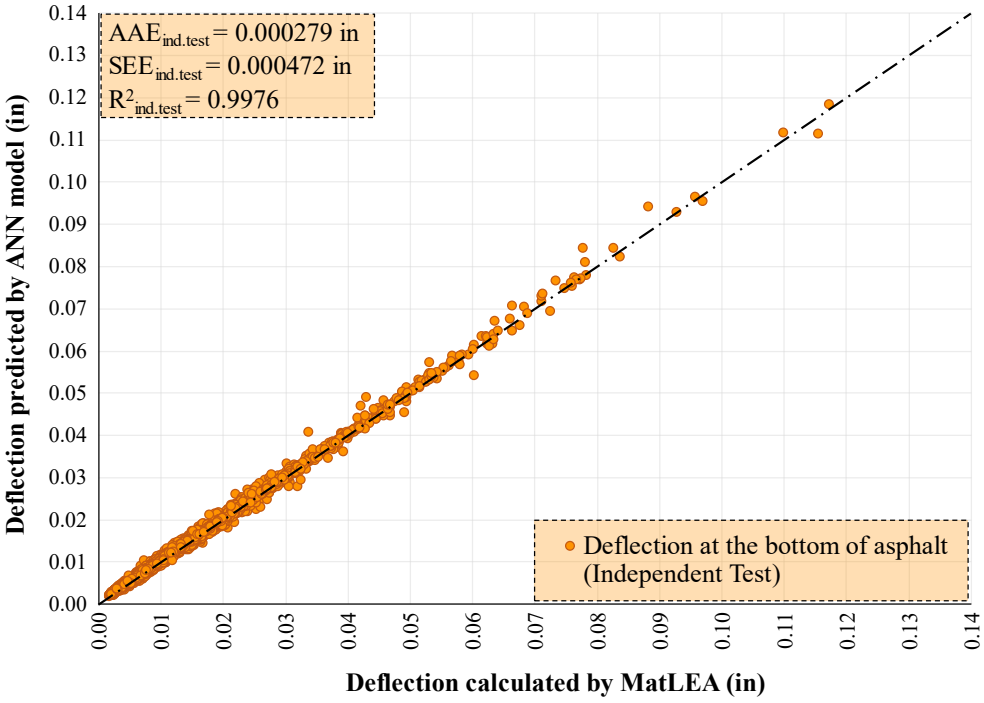

(b) Deflection at the bottom of the asphalt

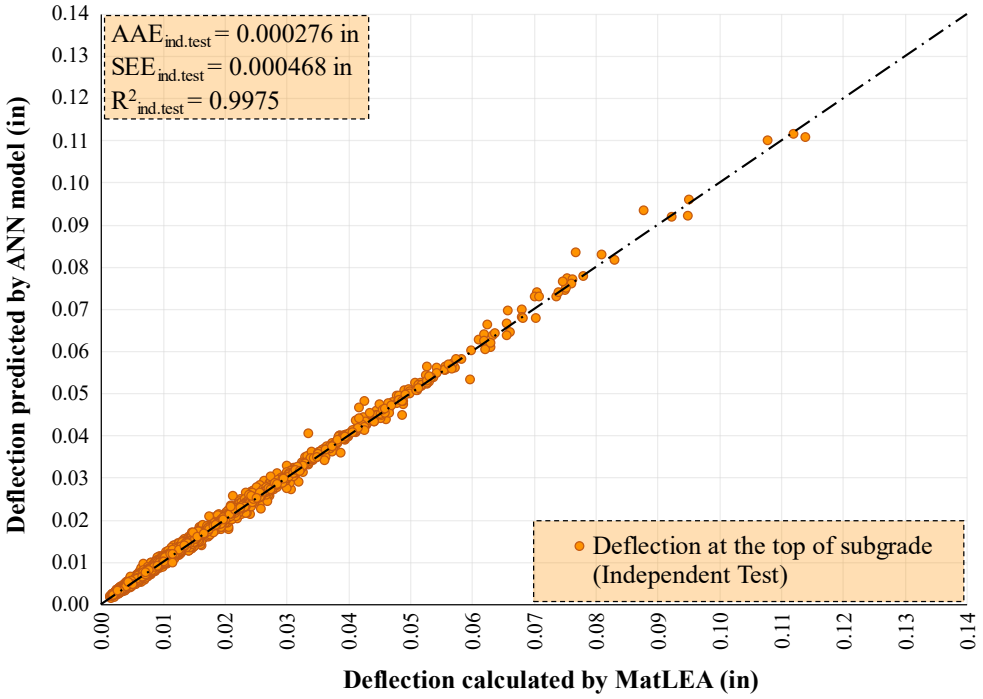

(c) Deflection at the top of the subgrade

Figure 28. Accuracies of independent testing data set for each deflection for pavement systems with a stabilized base

ANN-Based Strain Prediction Model Development for Pavements with a Stabilized Base

For training the neural network, 2 output parameters—strains at the (1) bottom of the asphalt layer and (2) top of the subgrade layer—were predicted using 35 input parameters, including 3 parameters per each layer: (a) modulus of elasticity, (b) Poisson's ratio, and (c) thickness, excluding subgrade thickness. The size of the developed synthetic database was 50,000 cases, of which 85% was used for training and the remainder for independent testing purposes, as shown in the previous Figure 23. The 50,000 pavement cases reflected 10 different scenarios, each with 1 to 10 HMA layers, a stabilized base, and a subgrade layer. Each scenario represents 5,000 pavement cases. For training and independent testing, since the database was split using a stratified shuffle split technique, each split could maintain the same percentage for each target class. Here, the chosen target class included 10 different scenarios (i.e., a 3-layered pavement system, 4-layered pavement system, …, 13-layered pavement system). In this way, the independent testing data set had the same proportion of scenarios after the split to represent the entire training data set.

In the input data set used for training the ANN model, 0 represented no data for nonexistent layers, so the empty cells in the sample data set previously shown in Figure 18 were filled with 0s. For example, for a 7-layered pavement system (5 HMA layers, 1 base layer, and 1 subgrade layer), the data points for HMA layers 6 to 10 were set to 0 during training, thus enabling the model to learn to recognize layer existence.

After splitting the entire data set to avoid data leakage, transformation and scaling were applied only to the training data. To explain further, the training data were fitted and transformed using multiple preprocessing methods. After trying various combinations of scaling and transformation techniques and evaluating their effects on model accuracy, the best data preprocessing techniques chosen for each input and output parameter were as follows:

- Elastic modulus of layers: min-max scaler
- Poisson's ratio: min-max scaler
- Thickness: ln(x+1) transformation + min-max scaler
- Strain: ln(x+1) transformation + standard scaler

The previously given Table 9 presents the values of the scaling parameters applied to the deflection input and output parameters mentioned previously, and Table 10 presents those applied to the input and output parameters for the strain model.

Table 10. Scaling parameters used to train strain ANN model for pavements with a stabilized base

	Strain	
	Std dev	*Mean*
Bottom of HMA	6.26E-05	2.49E-05
Top of SUBG	4.73E-04	-3.11E-04

Since these parameters should be applied on test input data before being tested in the ANN model, the test input data were scaled based on the model training input data set properties. To obtain the output in the original unit, the output predicted by the ANN should be backprocessed based on the model training output data set properties.

To find the best neural network configuration for used as a surrogate in MatLEA, a grid search with k-fold cross-validation was used. For the ANN-based strain model, the 10-fold cross-validation previously shown in Figure 24 was used. In the grid search, the effects of activation functions (tanh, ReLU, and sigmoid), the number of hidden layers (1, 2, and 3), the number of neurons per hidden layer (8, 16, 32, 64, 96, 128, 160, and 196), solvers (SGD and Adam), batch size (1, 10, and 100), and momentum (0.7, 0.8, and 0.9) were investigated. The initial learning rate for the training was 1.0E-3, and it was adaptively changed. The tolerance for loss was set as 1.0E-4. If the training loss did not decrease by at least the amount of the tolerance over 10 consecutive epochs, the learning rate was divided by 5. The minimum learning rate of training before termination was 6.4E-8 (i.e., the learning rate changed 6 times by dividing each time by 5, starting from 1.0E-3, then 2.0E-4, 4.0E-5, 8.0E-6, 1.6E-6, and 3.2E-7, and ending with 6.4E-8).

The optimum architecture for the ANN-based strain model for pavement systems with a stabilized base was found to be 35-128-128-3, i.e., 35 inputs parameters with 2 hidden layers including 128 neurons in each hidden layer and 3 outputs, as visualized in Figure 29.

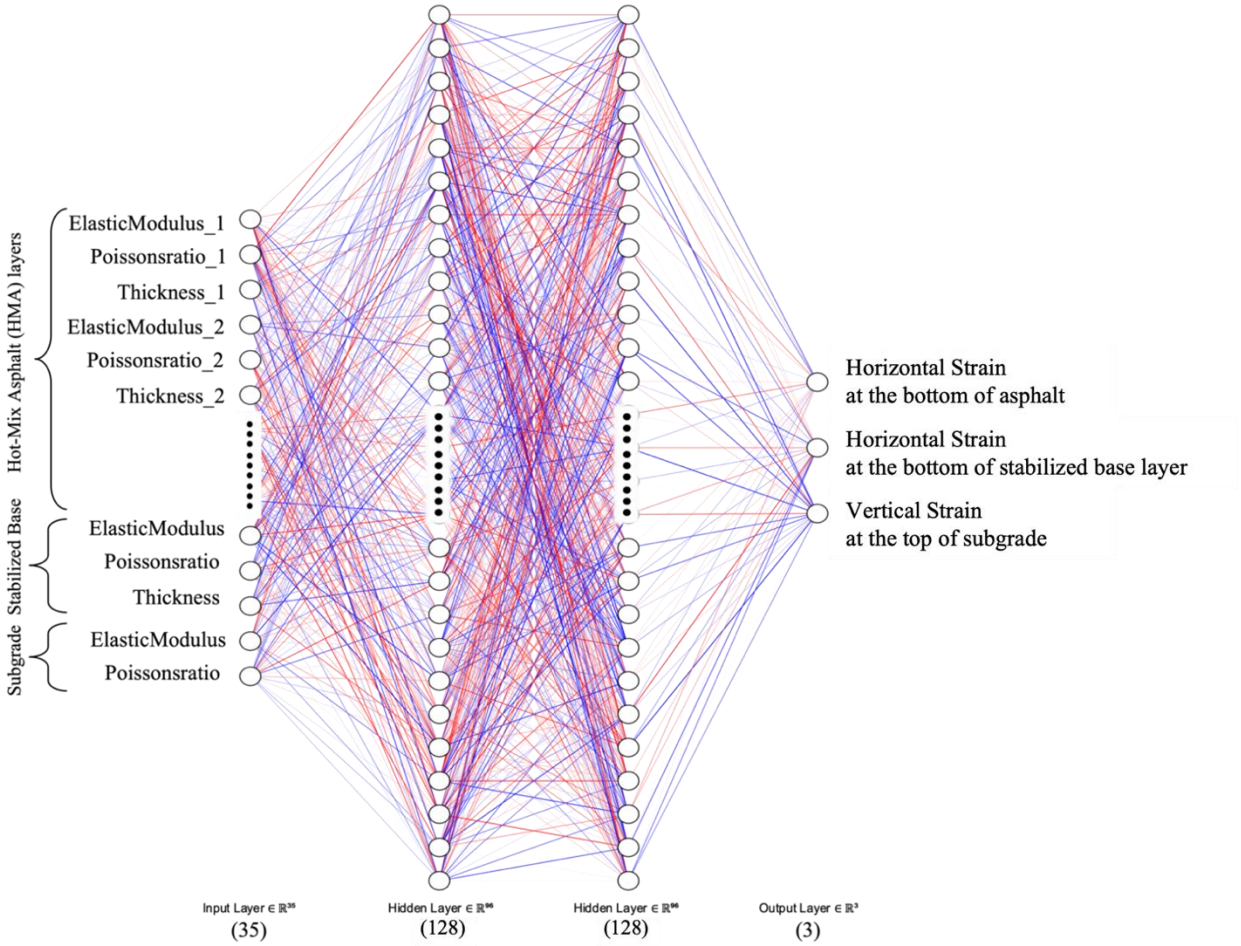

Figure 29. ANN-based strain model for pavement systems with a stabilized base

This model was trained using a tanh activation function, an SGD optimization technique, a batch size of 1, and a momentum of 0.9. An evaluation of the best model was performed by comparing the accuracies of the training and validation data sets at each fold, and the mean accuracies of the 10-fold cross-validation represent the overall model training and validation accuracies, indicated by the rightmost bar in Figure 30.

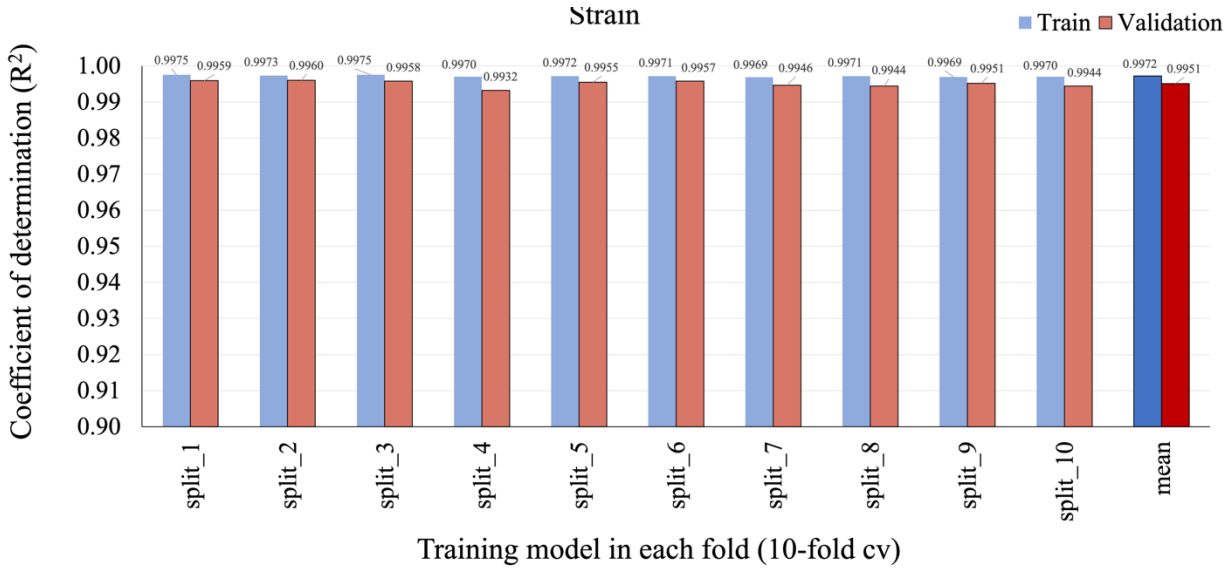

Figure 30. Accuracies of strain training and validation data sets for pavement systems with a stabilized base

As this comparative bar chart shows, the final scores (R^2) of the training and validation data sets in each of the 10 folds are very high (above 99%) and very similar to one another, with only a slight variation in the thousandths digit; this proves an absence of overfitting or underfitting.

Figures 31a–c and Figures 32a–c indicate the overall comparable accuracy results for training and independent testing, respectively, of the ANN-based strain model (a) on the surface, (b) at the bottom of the asphalt layer, and (c) at the top of the subgrade for pavement systems with a stabilized base.

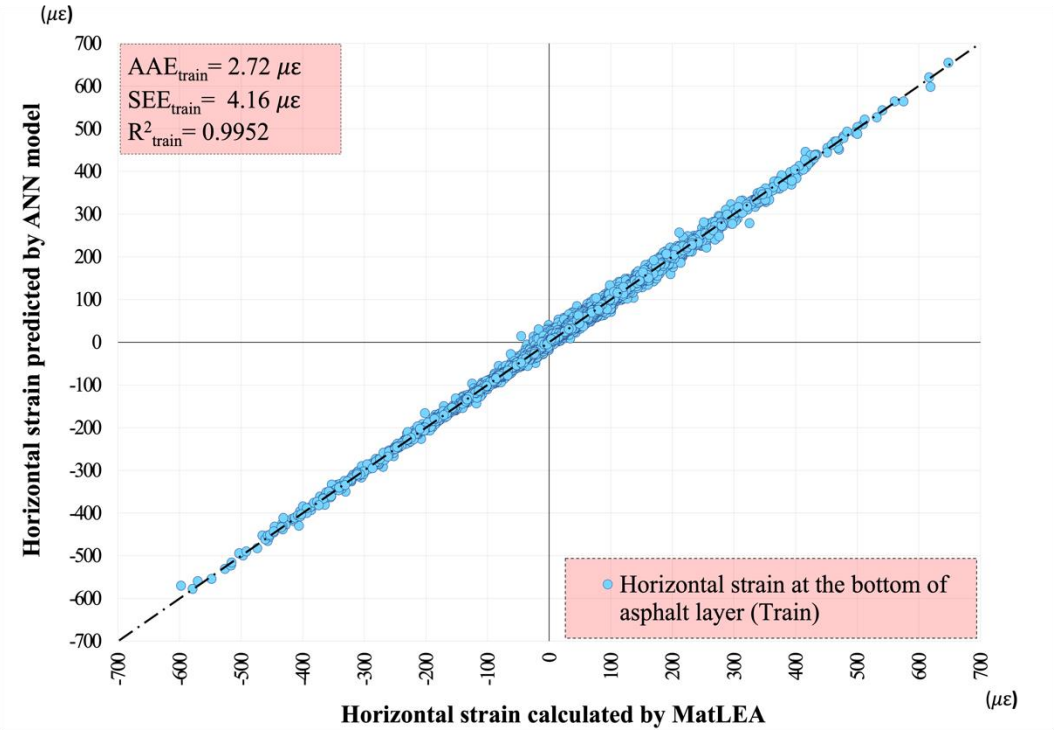

(a) Horizontal strain at the bottom of the asphalt layer

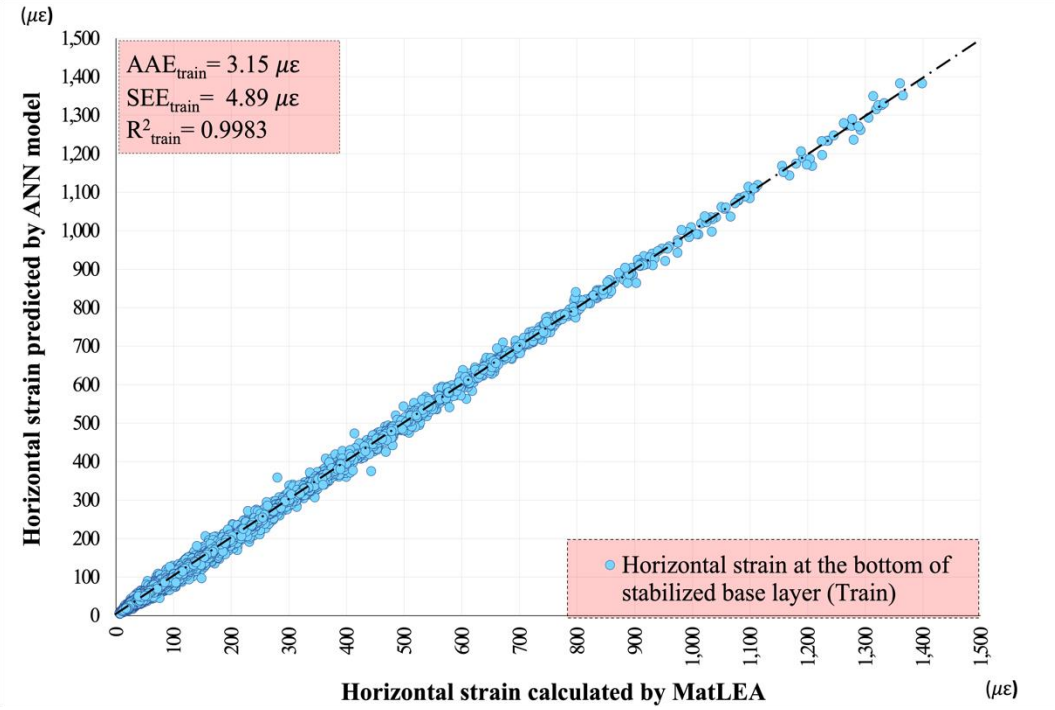

(b) Horizontal strain at the bottom of the stabilized base layer

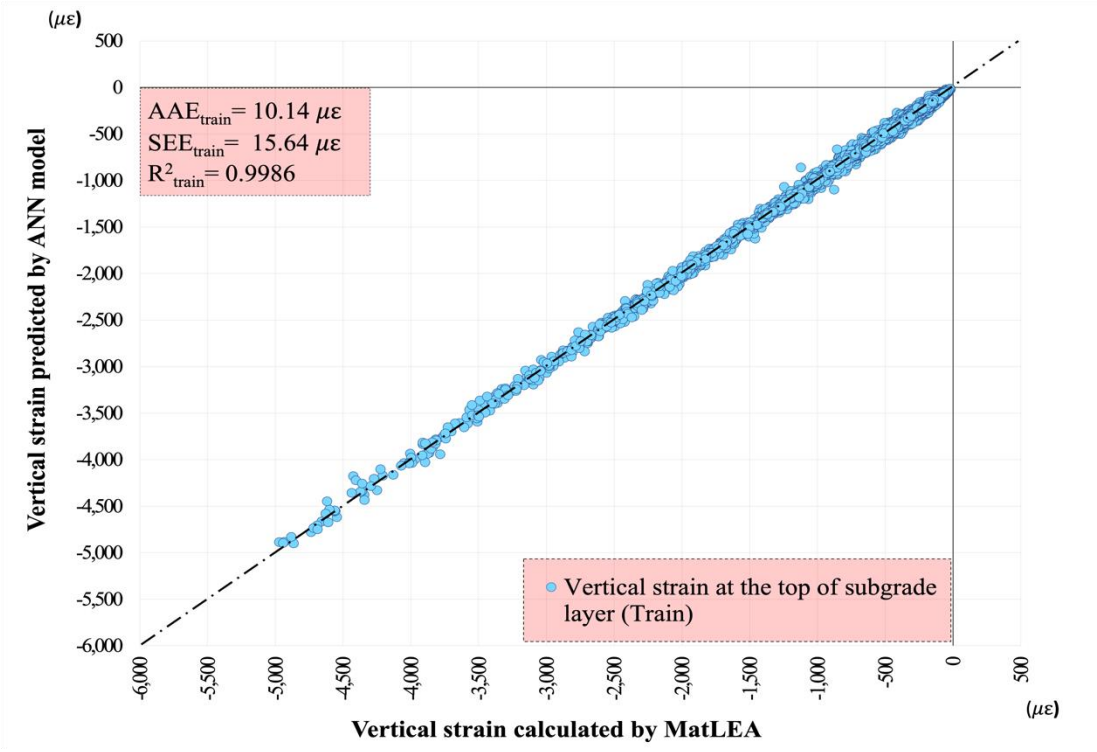

(c) Vertical strain at the top of subgrade

Figure 31. Accuracies of training data set for each strain for pavement systems with stabilized base

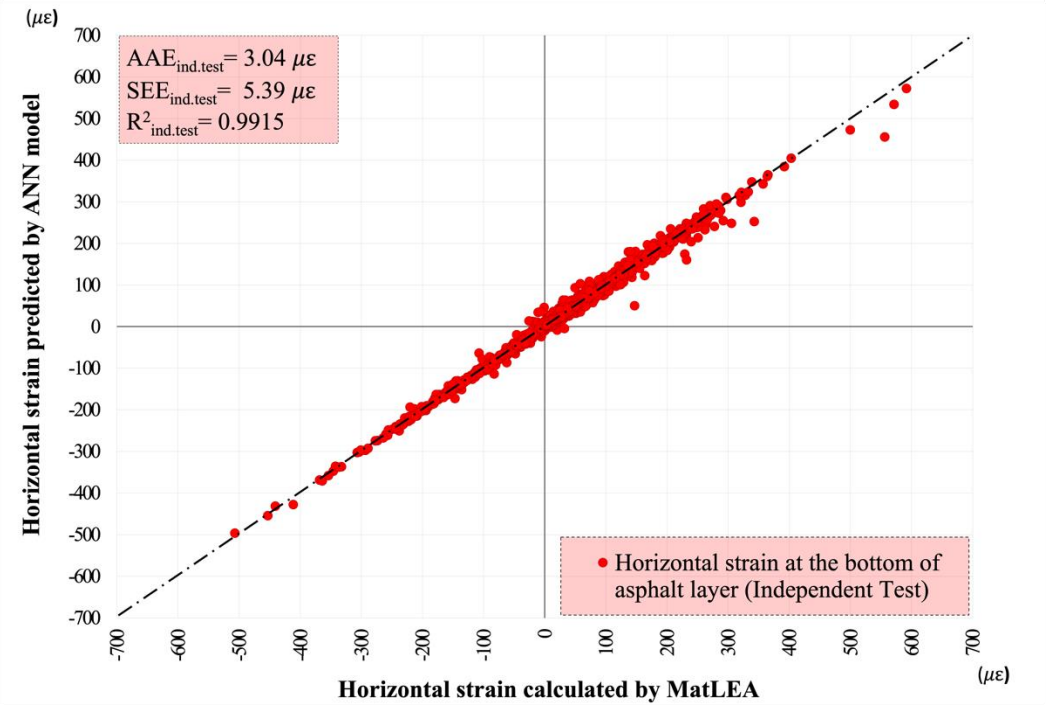

(a) Horizontal strain at the bottom of the asphalt layer

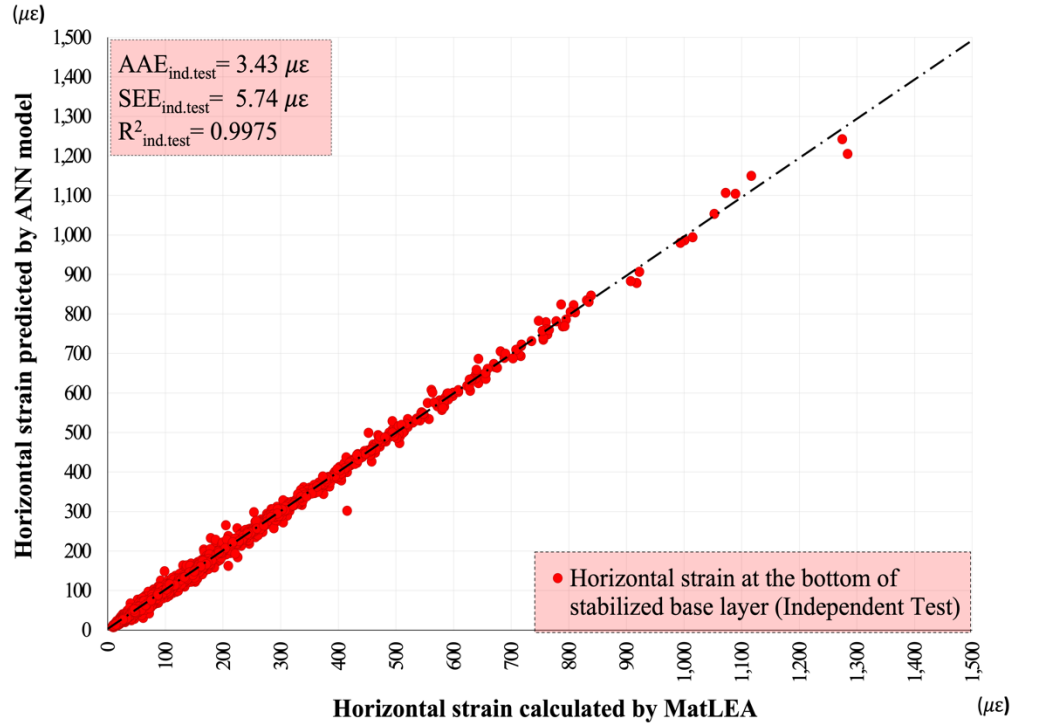

(b) Horizontal strain at the bottom of the stabilized base layer

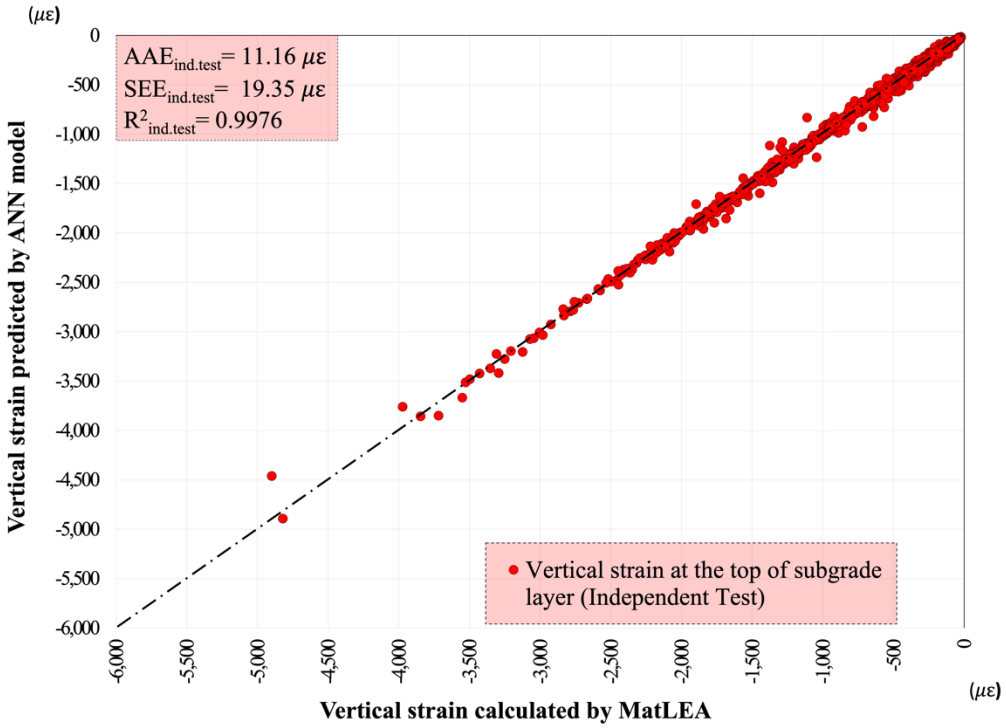

(c) Vertical strain at the top of the subgrade

Figure 32. Accuracies of independent testing data set for each strain for pavement systems with a stabilized base

ANN-Based Pavement Response Prediction Model Development for Pavement Systems with a Granular Base

ANN-Based Deflection Prediction Model Development for Pavements with a Granular Base

Due to the nonlinear nature of the problem, ANNs have been used in predicting deflections of a multilayered pavement system. For training a neural network, 3 output parameters—deflections at the (1) surface, (2) bottom of the asphalt layer, and (3) top of the subgrade layer—were predicted using 35 input parameters, including 3 parameters per each layer: (a) modulus of elasticity, (b) Poisson's ratio, and (c) thickness, excluding subgrade thickness. The size of the developed synthetic database was 50,000 cases, of which 85% was used for training and the remainder for independent testing purposes, as previously shown in Figure 23.

The 50,000 pavement cases included 10 different scenarios, each with 1 to 10 HMA layers, a granular base, and a subgrade layer. Each scenario reflected 5,000 pavement cases. For training and independent testing, the database was split using a stratified shuffle split technique, with each split maintaining the same percentage for each target class. Here, the chosen target class included 10 different scenarios (i.e., a 3-layered pavement system, 4-layered pavement system, …, 13-layered pavement system). In this way, the independent testing data set had the same proportion of scenarios after the split to represent the entire training data set.

In the input data set used for training the ANN model, 0 represented no data for nonexistent layers, so the empty cells in the sample data set previously shown in Figure 18 were filled with 0s. For example, for a 7-layered pavement system (5 HMA layers, 1 base layer, and 1 subgrade layer), the data points for HMA layers 6 to 10 were set to 0 during training, thus enabling the model to learn to recognize layer existence.

After splitting the entire data set to avoid data leakage, transformation and scaling were applied only to the training data. The training data was fitted and transformed using multiple preprocessing methods. To explain further, the testing set was then transformed and scaled based on the preprocessing technique and scaling parameters used in the training set. After trying various combinations of scaling and transformation techniques and evaluating their effects on model accuracy, the best data preprocessing techniques selected for each input and output parameter were as follows:

- Elastic modulus of layers: standard scaler
- Poisson's ratio: standard scaler
- Thickness: ln(x+1) transformation + standard scaler
- Deflection: ln(x) transformation + standard scaler

Table 11 presents the values of the scaling parameters applied to the input and output parameters mentioned previously.

Table 11. Scaling parameters used to train deflection ANN model for pavements with a granular base

	Elastic modulus		**Poisson's ratio**		**Thickness**		**Deflection**	
	Std dev	Mean	Std dev	Mean	Std dev	Mean	Std dev	Mean
HMA1	6.12E+05	1.12E+06	0.058	0.350	0.374	1.118	-	-
HMA2	6.70E+05	1.01E+06	0.119	0.315	0.487	1.005	-	-
HMA3	7.07E+05	8.95E+05	0.149	0.280	0.557	0.893	-	-
HMA4	7.26E+05	7.87E+05	0.168	0.245	0.599	0.781	-	-
HMA5	7.24E+05	6.70E+05	0.177	0.210	0.618	0.668	-	-
HMA6	7.05E+05	5.58E+05	0.180	0.175	0.617	0.558	-	-
HMA7	6.70E+05	4.47E+05	0.175	0.140	0.594	0.445	-	-
HMA8	6.14E+05	3.36E+05	0.164	0.105	0.553	0.336	-	-
HMA9	5.25E+05	2.24E+05	0.142	0.070	0.472	0.221	-	-
HMA10	3.84E+05	1.11E+05	0.106	0.035	0.357	0.112	-	-
SB	5.50E+04	1.05E+05	0.029	0.350	0.473	1.594	-	-
SUBG	1.59E+04	3.04E+04	0.043	0.375	0.374	1.118	-	-
Surface	-	-	-	-	-	-	0.678	-4.439
Bottom of HMA	-	-	-	-	-	-	0.771	-4.589
Top of SUBG	-	-	-	-	-	-	0.762	-4.691

Since these parameters should be applied on the test input data before being tested in the ANN model, the test input data were scaled based on the model training input data set properties. To

obtain the output in the original unit, the output predicted by the ANN should be backprocessed based on the model training output data set properties.

To find the best neural network configuration for use as a surrogate in MatLEA, a grid search with k-fold cross-validation was used. For the ANN-based deflection model, the 10-fold cross-validation previously shown in Figure 24 was used. Training was performed 10 times as a new model to ensure that each fold appeared as a test set exactly once.

In the grid search, the effects of activation functions (tanh, ReLU, and sigmoid), the number of hidden layers (1, 2, and 3), the number of neurons per hidden layer (8, 16, 32, 64, 96, 128, 160, and 196), solvers (SGD and Adam), batch size (1, 10, and 100), and momentum (0.7, 0.8, and 0.9) were investigated. Batch size determines the number of data points trained each time. Momentum applied in the weight update speeds the learning and helps avoid getting stuck in the local minima. The initial learning rate for the training was 1.0E-3 and changed adaptively, and tolerance for loss was set as 1.0E-4. If the training loss did not decrease by at least the amount of the tolerance in 10 consecutive epochs, the learning rate was divided by 5. The minimum learning rate of training before termination was 6.4E-8 (i.e., the learning rate changed 6 times by dividing each time by 5, starting from 1.0E-3, then 2.0E-4, 4.0E-5, 8.0E-6, 1.6E-6, and 3.2E-7, and ending with 6.4E-8). This adaptive learning rate technique could accelerate training by calculating the step size in gradient-based optimization based on the loss gradient.

The optimum architecture for the ANN-based deflection model for pavement systems with a granular base was found to be 35-96-96-3, i.e., 35 input parameters with 2 hidden layers including 96 neurons in each hidden layer and 3 outputs, as visualized in Figure 33.

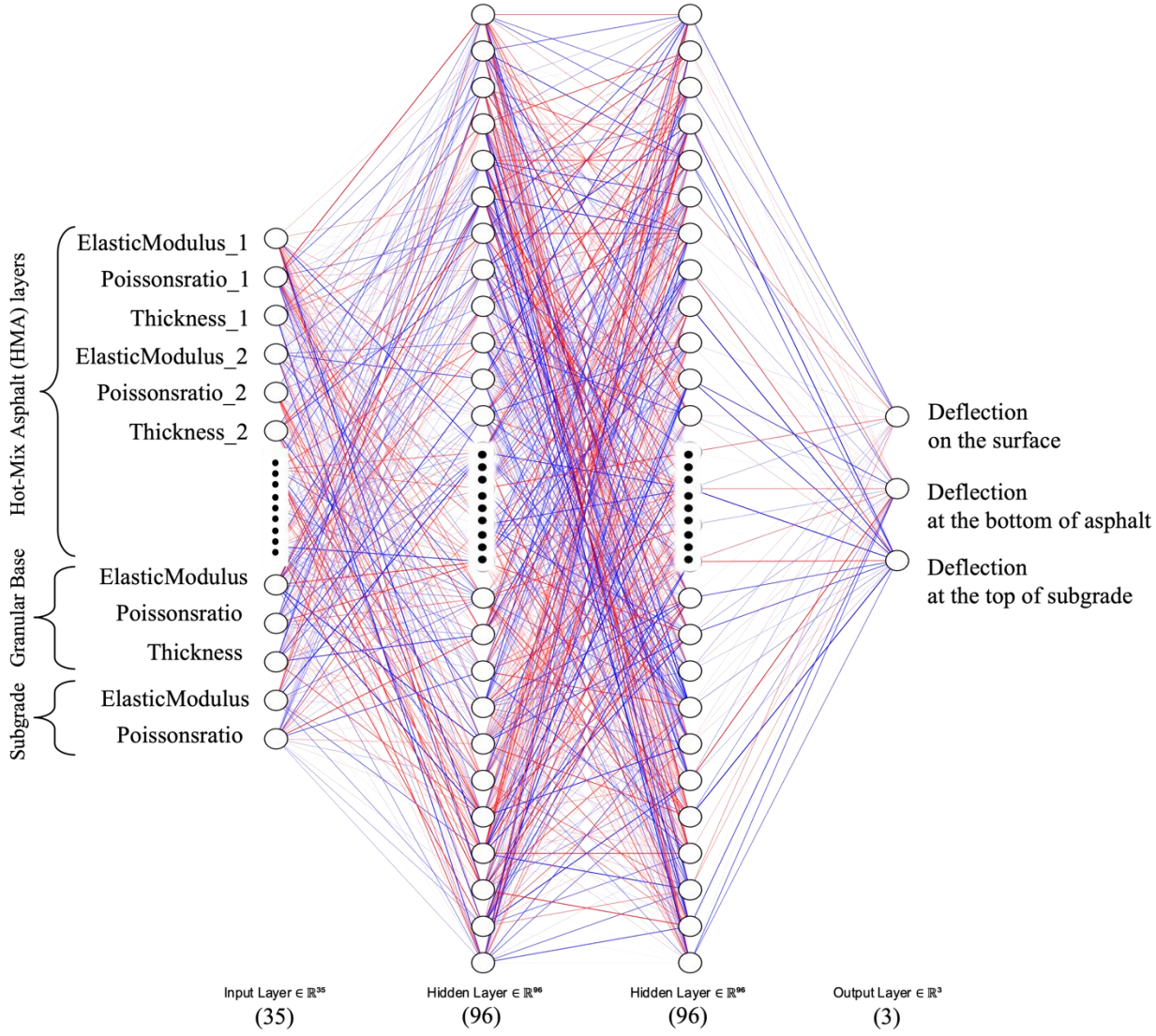

Figure 33. ANN-based deflection model for pavement systems with a granular base

This model was trained using a tanh activation function, an SGD optimization technique, a batch size of 1, and a momentum of 0.9. An evaluation to determine the best model was accomplished by comparing the accuracies of the training and validation data sets at each fold, and the mean accuracies of the 10-fold cross-validation represent the overall model training and validation accuracies, indicated by the rightmost bar in Figure 34.

Figure 34. Accuracies of training and validation data sets for pavement systems with a granular base

As this comparative bar chart shows, the final scores (R^2) of the training and validation data sets in each of the 10 folds were very high (above 99%) and very similar to one another other, with only a slight variation in the ten-thousandths digit; this proves an absence of overfitting or underfitting.

Figures 35a–c and Figures 36a–c indicate the overall comparable accuracy results for training and independent testing, respectively, of the ANN-based deflection model (a) on the surface, (b) at the bottom of the asphalt layer, and (c) at the top of the subgrade for pavement systems with a granular base.

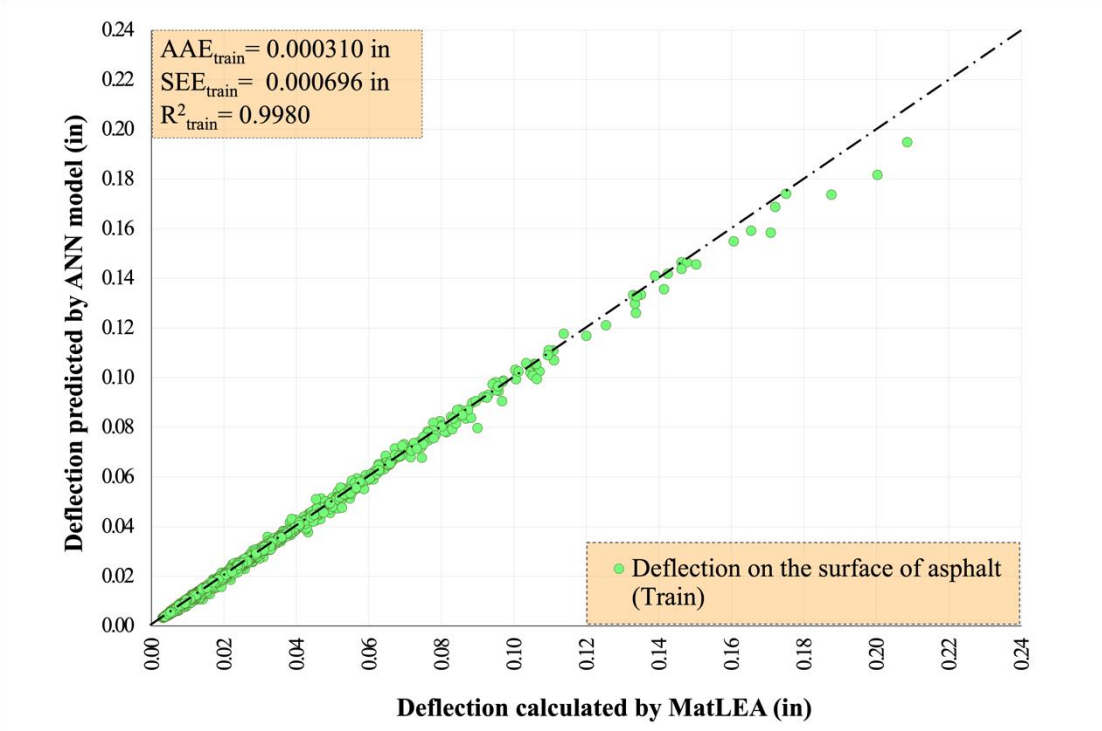

(a) Deflection on the surface

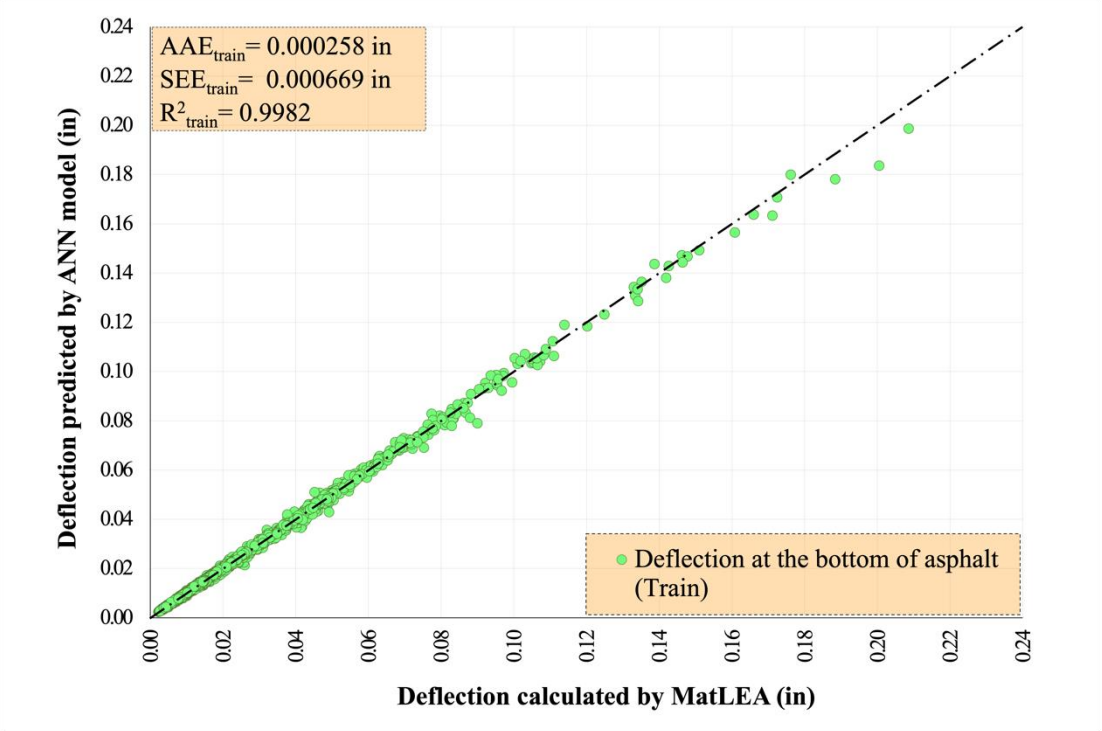

(b) Deflection at the bottom of the asphalt layer

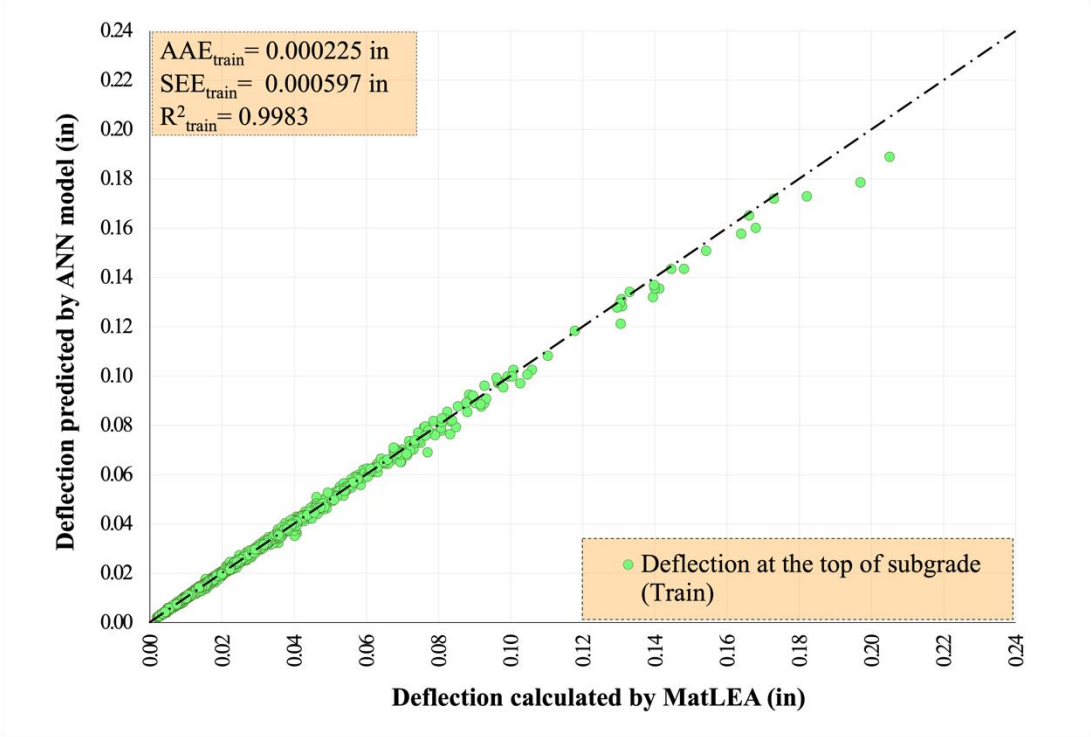

(c) Deflection at the top of the subgrade

Figure 35. Accuracies of training data set for each deflection for pavement systems with a granular base

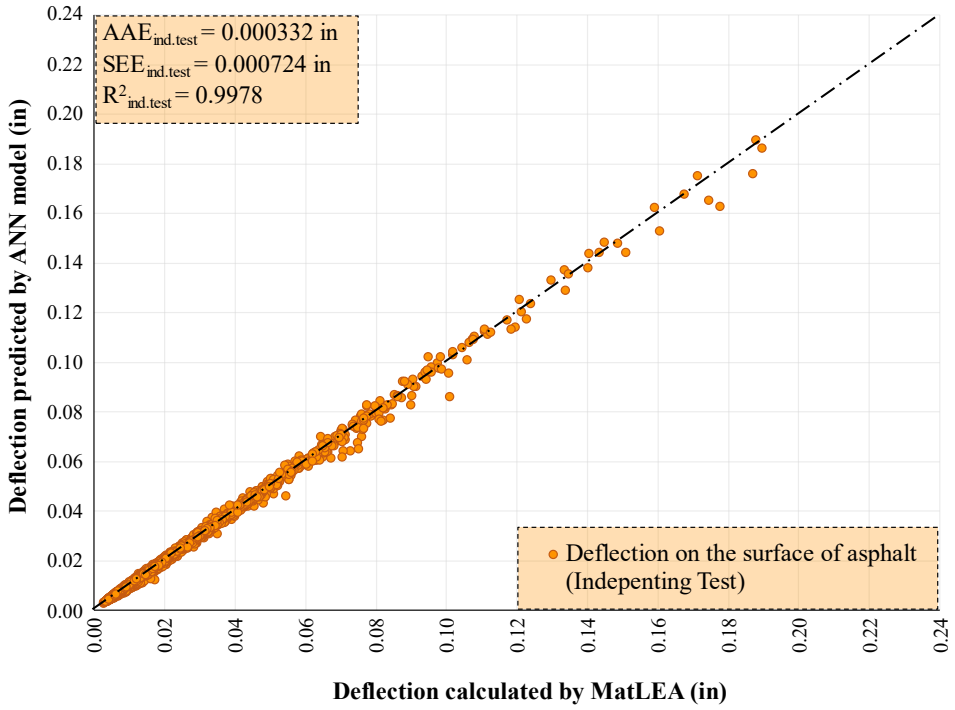

(a) Deflection on the surface

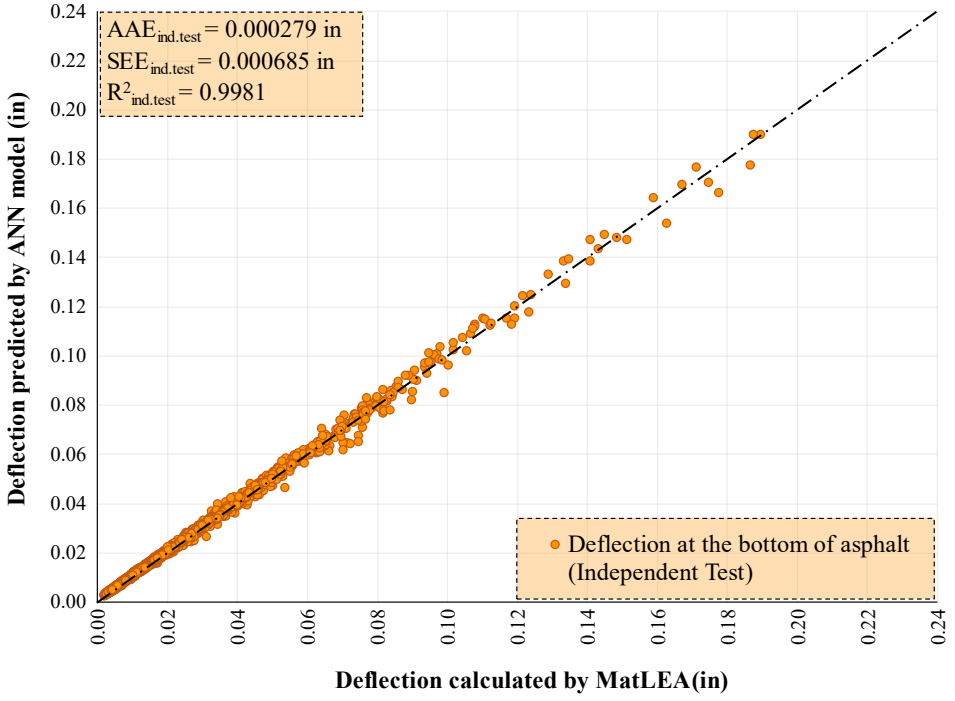

(b) Deflection at the bottom of the asphalt layer

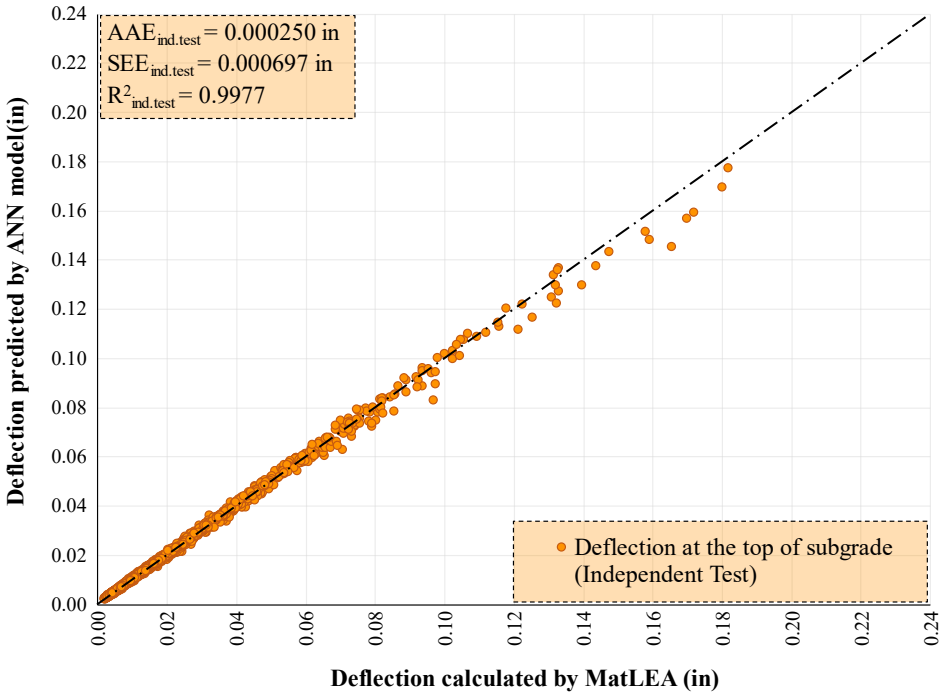

(c) Deflection at the top of the subgrade

Figure 36. Accuracies of independent testing data set for each deflection for pavement systems with a granular base

ANN-Based Strain Prediction Model Development for Pavements with a Granular Base

For training a neural network, 2 output parameters—strains at the (1) bottom of the asphalt layer and (2) top of the subgrade layer—were predicted using 35 input parameters including 3 parameters per each layer: (a) modulus of elasticity, (b) Poisson's ratio, and (c) thickness, excluding subgrade thickness. The size of the developed synthetic database was 50,000 cases, of which 85% was used for training and the remainder for independent testing purposes, as shown in the previous Figure 23. The 50,000 pavement cases included 10 different scenarios with 1 to 10 HMA layers, a granular base, and a subgrade layer. Each scenario reflected 5,000 pavement cases. For training and independent testing, the database was split using a stratified shuffle split technique in which each split can maintain the same percentage for each target class, chosen here for 10 different scenarios (i.e., a 3-layered pavement system, 4-layered pavement system, …, 13-layered pavement system). In this way, the independent testing data set had the same proportion of scenarios after the split to represent the entire training data set.

In the input data set used for training the ANN model, 0 represented no data for nonexistent layers, so the empty cells in the sample data set previously shown in Figure 18 were filled with 0s. For example, for a 7-layered pavement system (5 HMA layers, 1 base layer, and 1 subgrade layer), the data points for HMA layers 6 to 10 were set to 0 during training, thus enabling the model to learn to recognize layer existence.

After splitting the entire data set to avoid data leakage, transformation and scaling were applied only to the training data, and the training data was fitted and transformed using multiple preprocessing methods. After trying various combinations of scaling and transformation techniques and evaluating their effects on model accuracy, the best data preprocessing techniques selected for each input and output parameter were as follows:

- Elastic modulus of layers: min-max scaler
- Poisson's ratio: min-max scaler
- Thickness: ln(x+1) transformation + min-max scaler
- Strain: ln(x+1) transformation + standard scaler

Table 12 presents the values of the scaling parameters applied to the input and output parameters mentioned previously.

Table 12. Scaling parameters used to train strain ANN model for pavements with a granular base

	Elastic modulus		**Poisson's ratio**		**Thickness**		**Strain**	
	Scale	*Min*	*Scale*	*Min*	*Scale*	*Min*	*Std dev*	*Mean*
HMA1	4.72E-07	-2.74E-02	5.00	-1.25	0.522	-0.212	-	-
HMA2	4.6E-07	0.00E+00	2.22	0.00	0.434	0.000	-	-
HMA3	4.6E-07	0.00E+00	2.22	0.00	0.429	0.000	-	-
HMA4	4.6E-07	0.00E+00	2.22	0.00	0.439	0.000	-	-
HMA5	4.6E-07	0.00E+00	2.22	0.00	0.443	0.000	-	-
HMA6	4.6E-07	0.00E+00	2.22	0.00	0.456	0.000	-	-
HMA7	4.6E-07	0.00E+00	2.22	0.00	0.451	0.000	-	-
HMA8	4.6E-07	0.00E+00	2.22	0.00	0.439	0.000	-	-
HMA9	4.6E-07	0.00E+00	2.22	0.00	0.459	0.000	-	-
HMA10	4.6E-07	0.00E+00	2.22	0.00	0.473	0.000	-	-
SB	5.26E-06	-5.26E-02	10.00	-3.00	0.428	-0.297	-	-
SUBG	1.82E-05	-5.46E-02	6.67	-2.00	0.522	-0.212	-	-
Bottom of HMA	-	-	-	-	-	-	1.36E-04	1.16E-04
Top of SUBG	-	-	-	-	-	-	9.14E-04	-5.30E-04

Since these parameters should be applied on the test input data before being tested in the ANN model, the test input data were scaled based on the model training input data set properties. The output predicted by the ANN should be backprocessed based on the model training output data set properties to obtain the original unit output.

To find the best neural network configuration for use as a surrogate in MatLEA, a grid search with k-fold cross-validation was used. For the ANN-based strain model, the 10-fold cross-validation was used, as previously shown in Figure 24. In the grid search, the effects of activation functions (tanh, ReLU, and sigmoid), the number of hidden layers (1, 2, and 3), the number of neurons per hidden layer (8, 16, 32, 64, 96, 128, 160, and 196), solvers (SGD and Adam), batch size (1, 10, and 100), and momentum (0.7, 0.8, and 0.9) were investigated. The

initial learning rate for the training was 1.0E-3 and adaptively changed. Tolerance for loss was set as 1.0E-4. If the training loss did not decrease by at least the amount of this tolerance over 10 consecutive epochs, the learning rate was divided by 5. The minimum learning rate of training before termination was 3.2E-7 (i.e., the learning rate changed 5 times by dividing each time by 5, starting from 1.0E-3, then 2.0E-4, 4.0E-5, 8.0E-6, and 1.6E-6, and ending with 3.2E-7).

The optimum architecture for the ANN-based strain model for pavement systems with a stabilized base was found to be 35-128-128-2, i.e., 35 inputs parameters with 2 hidden layers including 128 neurons in each hidden layer and 2 outputs, as visualized in Figure 37.

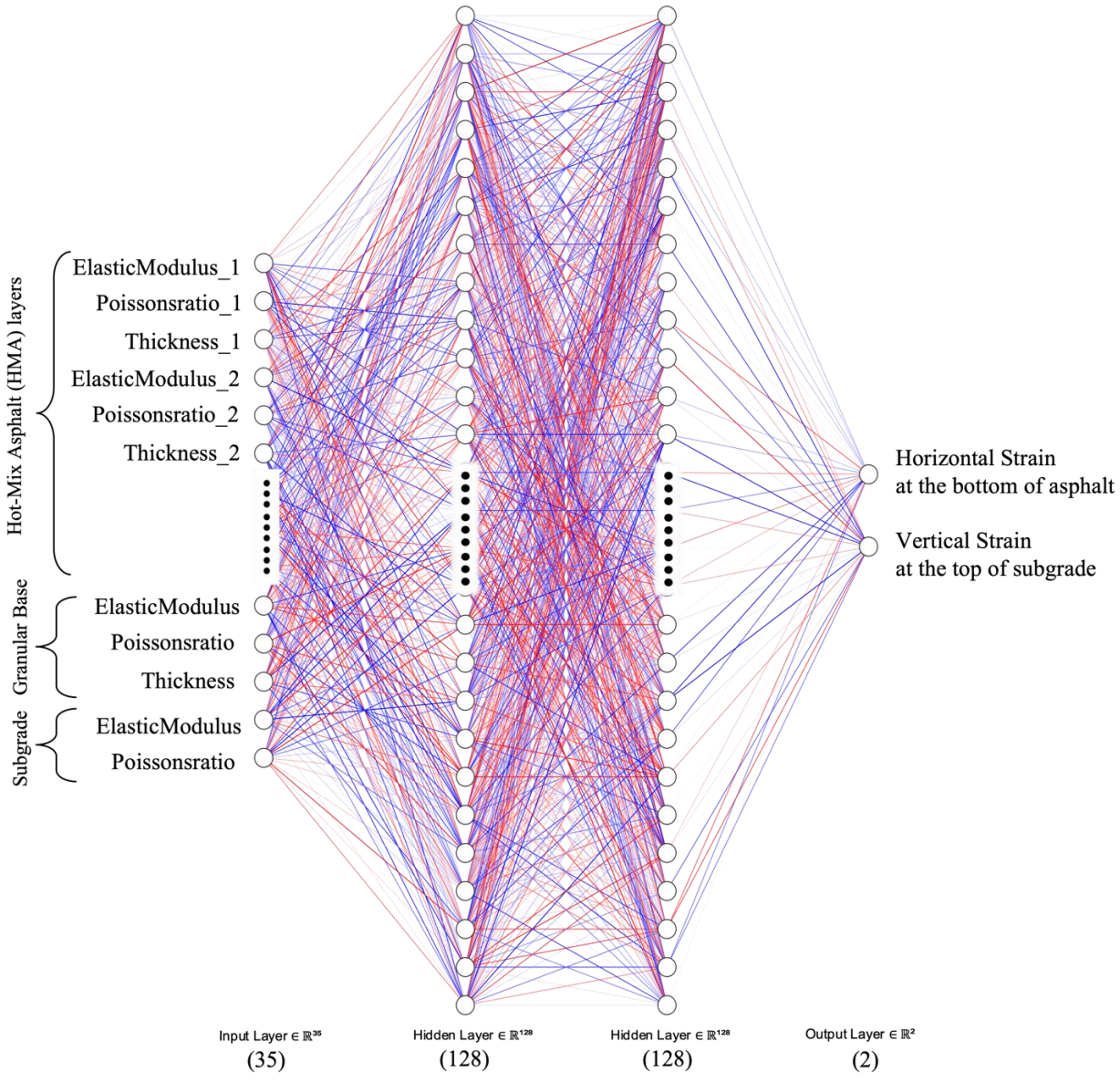

Figure 37. ANN-based strain model for pavement systems with a granular base

This model was trained using a tanh activation function, an SGD optimization technique, a batch size of 1, and a momentum of 0.9. An evaluation of the best model was performed by comparing the accuracies of the training and validation data sets at each fold, and the mean accuracies of the 10-fold cross-validation represent the overall model training and validation accuracies, indicated by the rightmost bar in Figure 38.

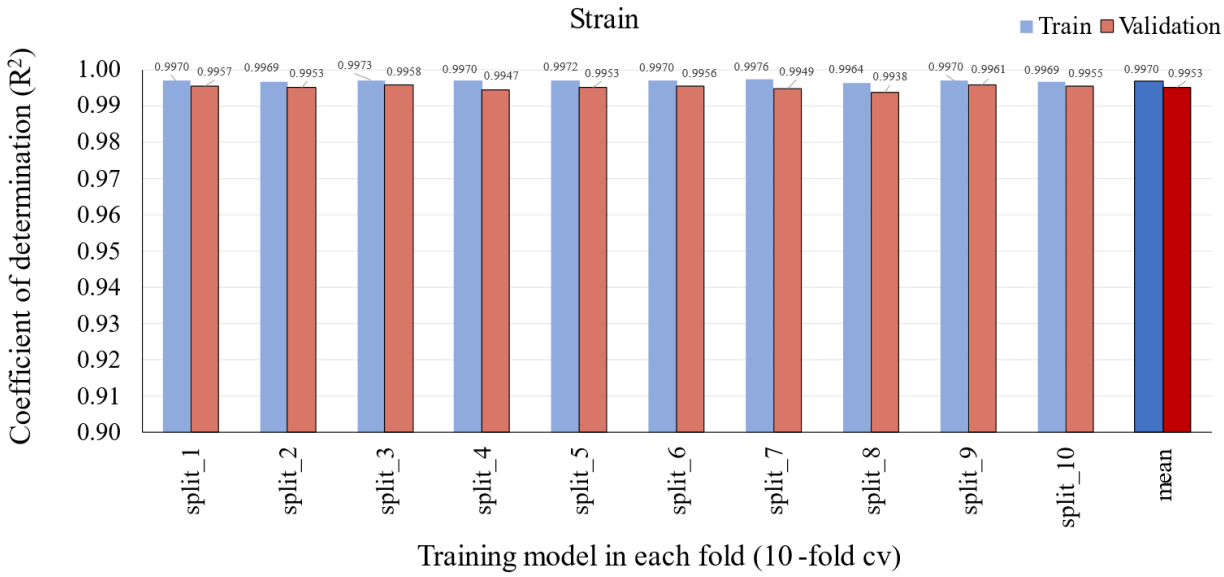

Figure 38. Accuracies of strain training and validation data sets for pavement systems with a granular base

As this comparative bar chart shows, the final scores (R^2) of the training and validation data sets in each of the 10 folds are very high (above 99%) and very similar to one other, with only a slight variation in the thousandths digit; this proves an absence of overfitting or underfitting.

Figures 39a–c and Figures 40a–c show the overall comparable accuracy results for training and independent testing, respectively, of the ANN-based strain model (a) on the surface, (b) at the bottom of the asphalt layer, and (c) at the top of the subgrade.

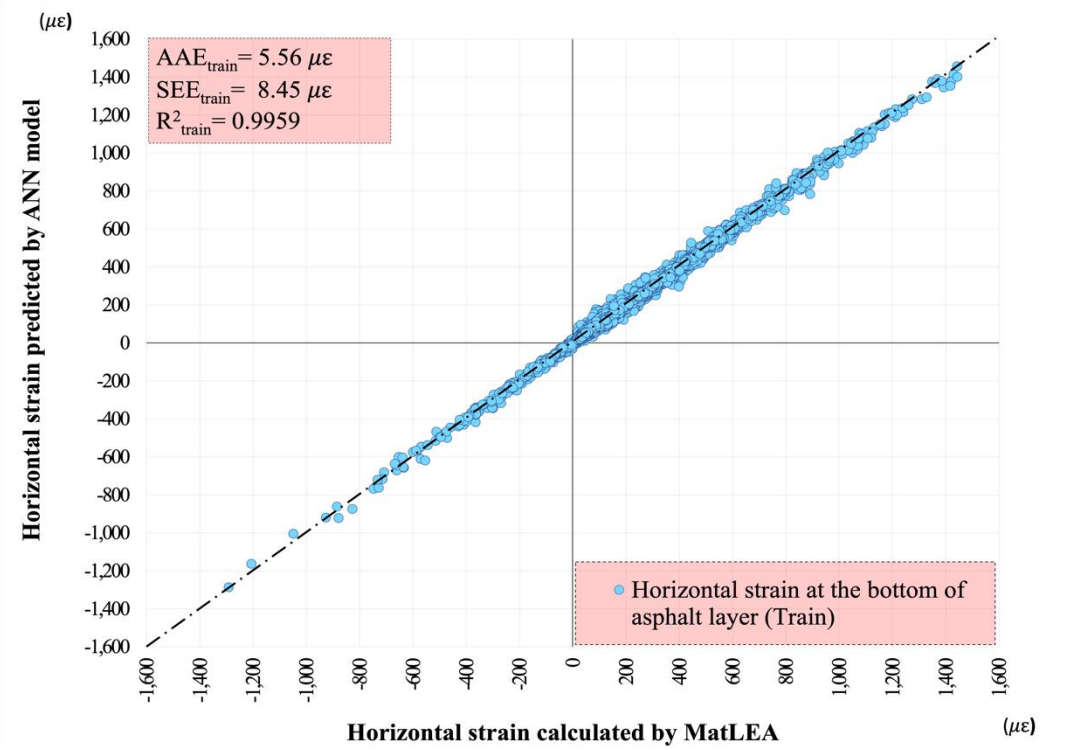

(a) Horizontal strain at the bottom of the asphalt layer

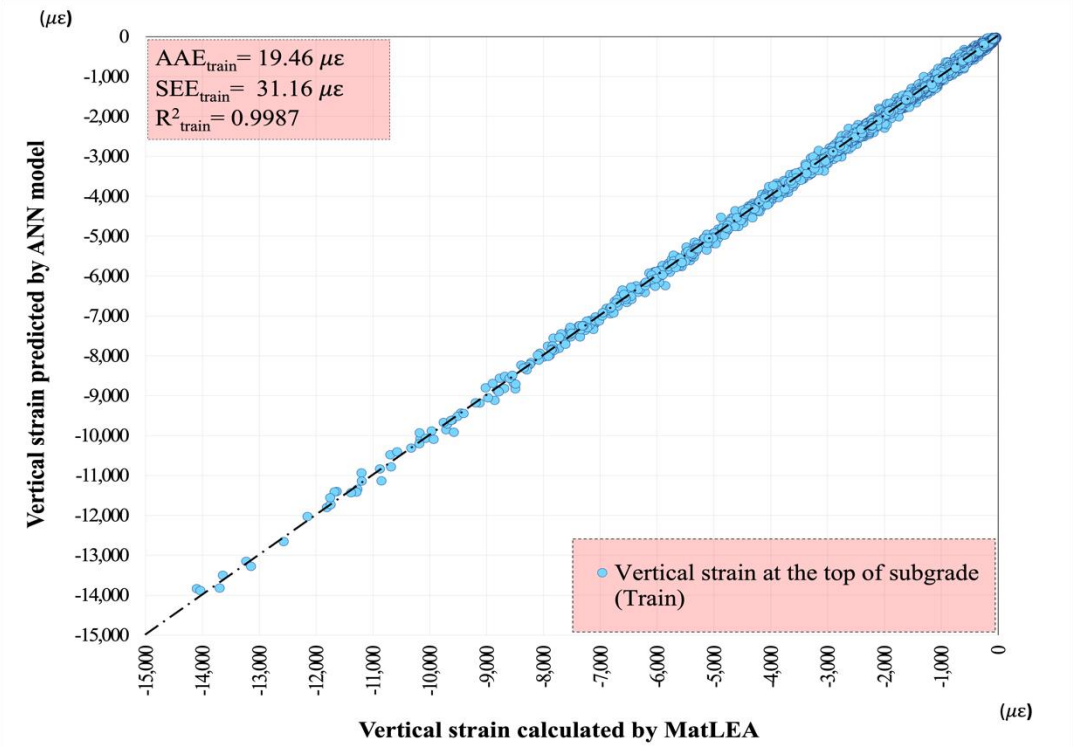

(b) Vertical strain at the top of the subgrade

Figure 39. Accuracies of training data set for each strain for pavement systems with a granular base

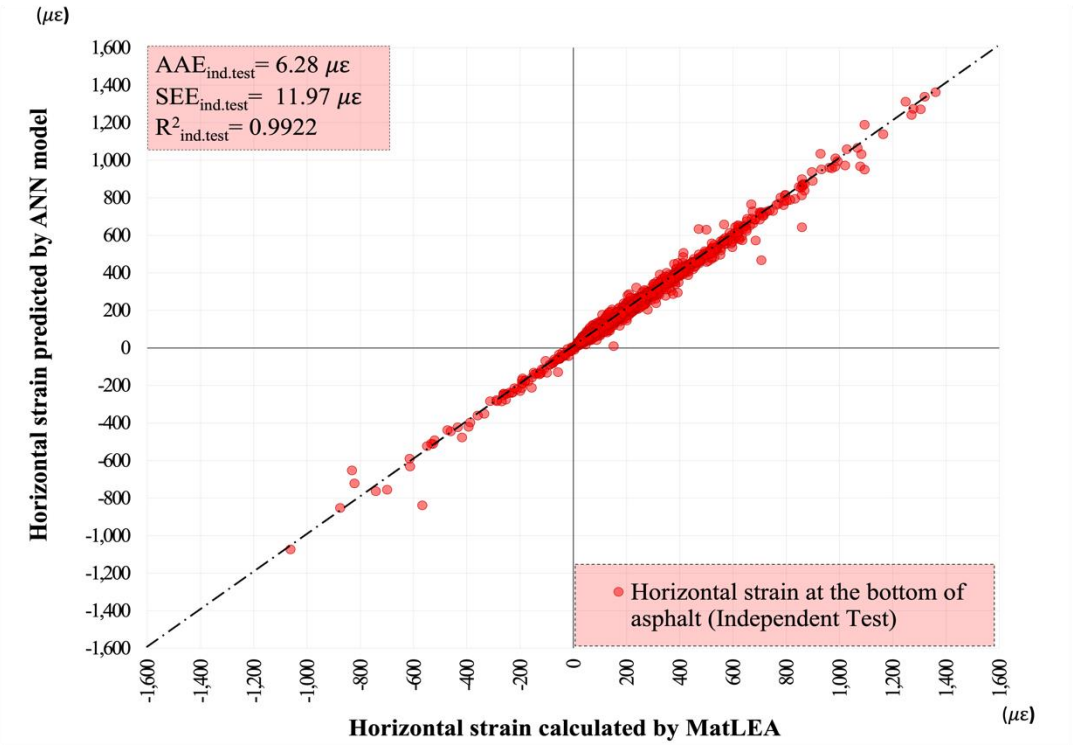

(a) Horizontal strain at the bottom of the asphalt layer

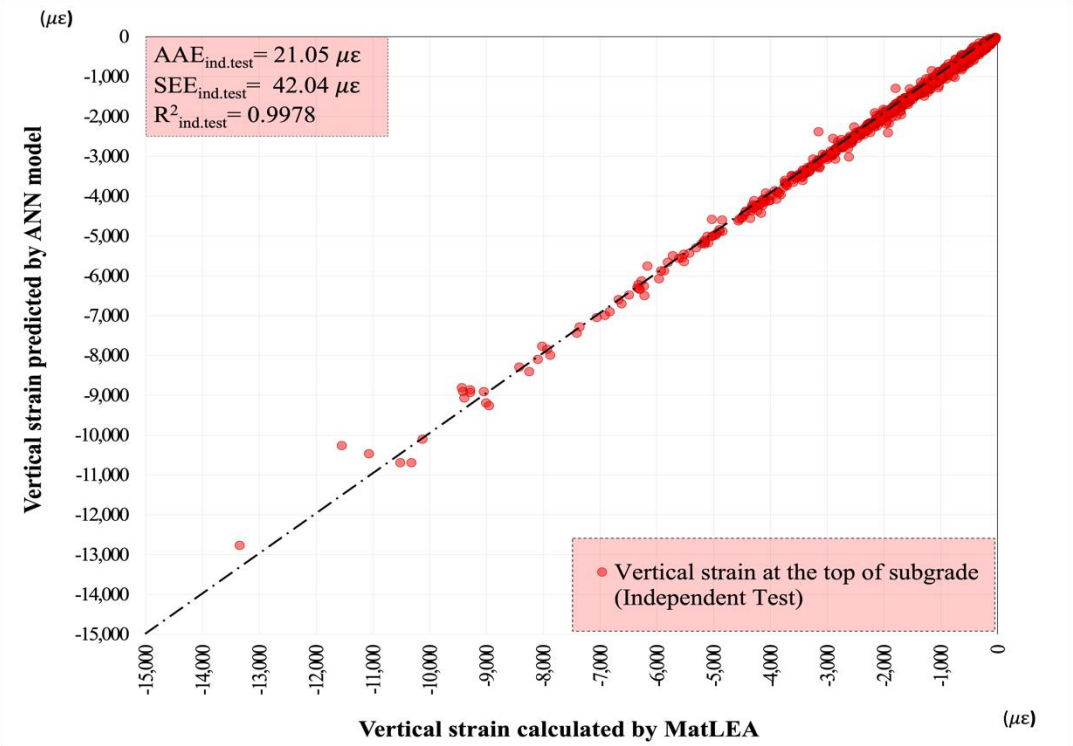

(b) Vertical strain at the top of the subgrade

Figure 40. Accuracies of independent testing data set for each strain for pavement systems with a granular base

ANN-Based Pavement Response Prediction Model Development for Pavement Systems with a Stabilized Base and Granular Base/Subbase

ANN-Based Deflection Prediction Model Development for Pavements with Stabilized and Granular Bases

Due to the nonlinear nature of the problem, ANNs have been used for predicting the deflections of a multilayered pavement system. For training a neural network, 3 output parameters—deflections at the (1) surface, (2) bottom of the asphalt layer, and (3) top of the subgrade layer—were predicted using 38 input parameters, including 3 parameters per each layer: (a) modulus of elasticity, (b) Poisson's ratio, and (c) thickness, excluding subgrade thickness. The size of the developed synthetic database is 50,000 cases, of which 85% was used for training and the remainder for independent testing purposes, as shown in the previous Figure 23.

The 50,000 pavement cases included 10 different scenarios with 1 to 10 HMA layers, a stabilized base, a granular base/subbase, and a subgrade layer. Each scenario represents 5,000 pavement cases. For training and independent testing, the database was split using a stratified shuffle split technique, so that each split can maintain the same percentage for each target class, here chosen for 10 different scenarios (i.e., a 4-layered pavement system, 5-layered pavement system, …, 14-layered pavement system). In this way, the independent testing data set had the same proportion of scenarios after the split to represent the entire training data set.

In the input data set used for training the ANN model, 0 represented no data for nonexistent layers. Empty cells in the sample data set previously shown in Figure 18 were filled with 0s. For example, for a 7-layered pavement system (4 HMA layers, 2 base layers, and 1 subgrade layer), the data points for HMA layers 5 to 10 were set to 0 during training. Thus, the model will be able to learn to recognize layer existence.

Transformation and scaling were applied on only to the training data after splitting the entire data set to avoid data leakage. To explain further, the training data were fitted and transformed using multiple preprocessing methods. The testing set was then transformed and scaled based on the preprocessing techniques and scaling parameters used in the training set. After trying various combinations of scaling and transformation techniques and evaluating their effects on model accuracy, the best data preprocessing techniques for each input and output parameter were selected as follows:

- Elastic modulus of layers: min-max scaler
- Poisson's ratio: min-max scaler
- Thickness: ln(x+1) transformation + min-max scaler
- Deflection: ln(x+1) transformation + standard scaler

Table 13 presents the values of the scaling parameters applied to the input and output parameters mentioned previously.

Table 13. Scaling parameters used to train deflection ANN model for pavements with stabilized and granular bases

	Elastic modulus		Poisson's ratio		Thickness		Deflection	
	Scale	*Min*	*Scale*	*Min*	*Scale*	*Min*	*Std dev*	*Mean*
HMA1	4.7E-07	-2.7E-02	5.00	-1.25	0.526	-0.213	-	-
HMA2	4.6E-07	0.0E+00	2.22	0.00	0.436	0.000	-	-
HMA3	4.6E-07	0.0E+00	2.22	0.00	0.441	0.000	-	-
HMA4	4.6E-07	0.0E+00	2.22	0.00	0.416	0.000	-	-
HMA5	4.6E-07	0.0E+00	2.22	0.00	0.433	0.000	-	-
HMA6	4.6E-07	0.0E+00	2.22	0.00	0.418	0.000	-	-
HMA7	4.6E-07	0.0E+00	2.22	0.00	0.435	0.000	-	-
HMA8	4.6E-07	0.0E+00	2.22	0.00	0.451	0.000	-	-
HMA9	4.6E-07	0.0E+00	2.22	0.00	0.445	0.000	-	-
HMA10	4.6E-07	0.0E+00	2.22	0.00	0.464	0.000	-	-
SB	4.7E-07	-2.7E-02	5.00	-1.25	0.426	-0.296	-	-
SUBG	5.3E-06	-5.3E-02	10.00	-3.00	0.426	-0.295	-	-
Surface	-	-	-	-	-	-	8.10E-03	1.06E-02
Bottom of HMA	-	-	-	-	-	-	8.35E-03	9.44E-03
Top of SUBG	-	-	-	-	-	-	7.74E-03	8.47E-03

Since these parameters should be applied on the test input data before being tested in the ANN model, test input data were scaled based on the model training input data set properties. The output predicted by the ANN should be backprocessed based on the model training output data set properties to obtain the output from the original unit.

A grid search with k-fold cross-validation was used to find the best neural network configuration for use as a surrogate in MatLEA. For the ANN-based deflection model, the 10-fold cross-validation shown in the previous Figure 24 was used. Training was performed 10 times as a new model to ensure that each fold appears as a test set exactly once.

In the grid search, the effects of activation functions (tanh, ReLU, and sigmoid), the number of hidden layers (1, 2, and 3), the number of neurons per hidden layer (8, 16, 32, 64, 96, 128, 160, and 196), solvers (SGD and Adam), batch size (1, 10, and 100), and momentum (0.7, 0.8, and 0.9) were investigated, with batch size determining the number of data points trained each time. Momentum applied in the weight update speeds the learning and helps avoid getting stuck in local minima. The initial learning rate for the training was 1.0E-3 and changed adaptively. Tolerance for loss was set as 1.0E-4. If the training loss did not decrease by at least the amount of the tolerance over 10 consecutive epochs, the learning rate was divided by 5. The minimum learning rate of training before termination was 6.4E-8 (i.e., the learning rate changed 6 times by dividing each time by 5, starting from 1.0E-3, then 2.0E-4, 4.0E-5, 8.0E-6, 1.6E-6, and 3.2E-7, and ending with 6.4E-8). This adaptive learning rate technique could accelerate training by calculating the step size in gradient-based optimization based on the loss gradient.

The optimum architecture for the ANN-based deflection model for pavement systems with a stabilized base and granular base was found to be 38-128-128-3, i.e., 38 input parameters with 2

hidden layers including 128 neurons in each hidden layer and 3 outputs, as visualized in Figure 41.

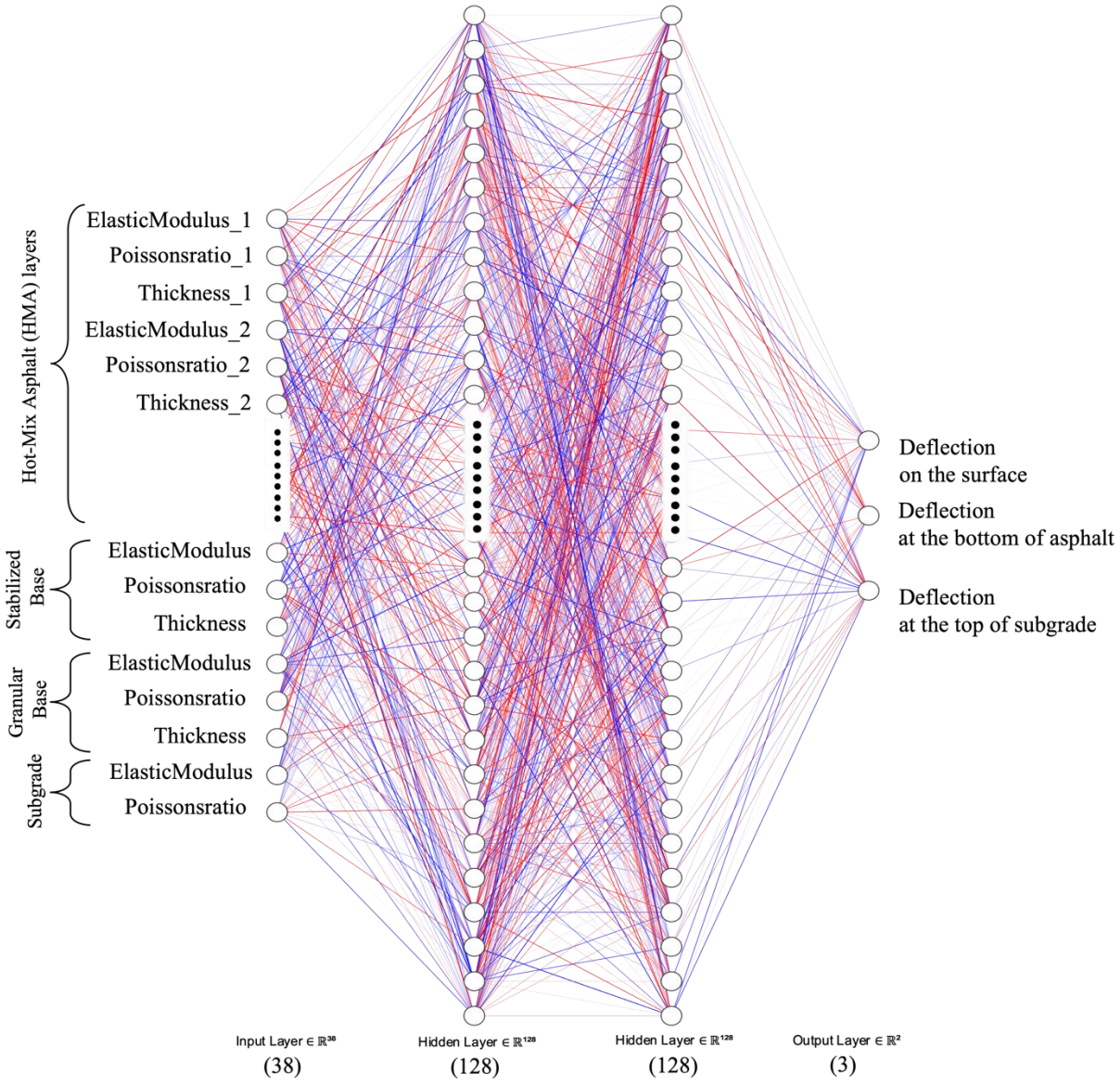

Figure 41. ANN-based deflection model for pavement systems with stabilized and granular bases

This model was trained using a tanh activation function, an SGD optimization technique, a batch size of 1, and a momentum of 0.9. An evaluation of the best model was performed by comparing the accuracies of the training and validation data sets at each fold, and the mean accuracies of the 10-fold cross-validation represent the overall model training and validation accuracies, indicated by the rightmost bar in Figure 42.

Figure 42. Accuracies of training and validation data sets for pavement systems with stabilized and granular bases

As this comparative bar chart shows, the final scores (R^2) of the training and validation data sets in each of the 10 folds were very high (above 99%) and very similar to one another, with only a slight variation in the thousandths digit; this proves an absence of overfitting or underfitting.

Figures 43a–c and Figures 44a–c indicate the overall comparable accuracy results for training and independent testing, respectively, of the ANN-based deflection model (a) on the surface, (b) at the bottom of the asphalt layer, and (c) at the top of the subgrade for pavement systems with a stabilized base and granular base.

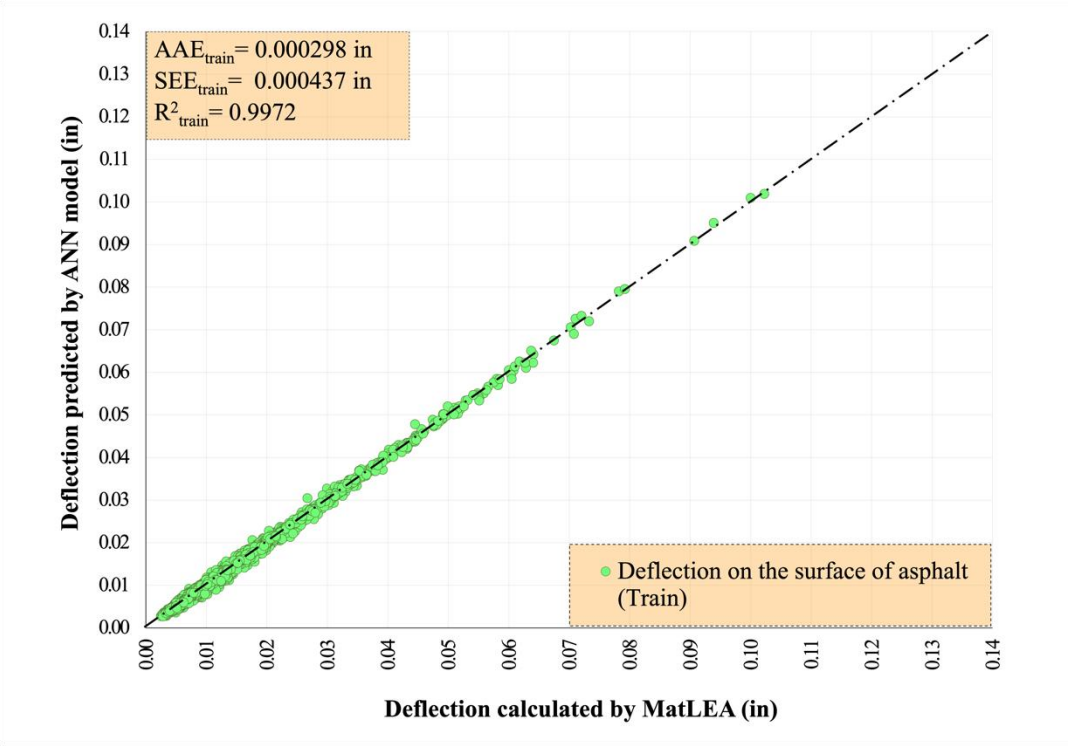

(a) Deflection on the surface

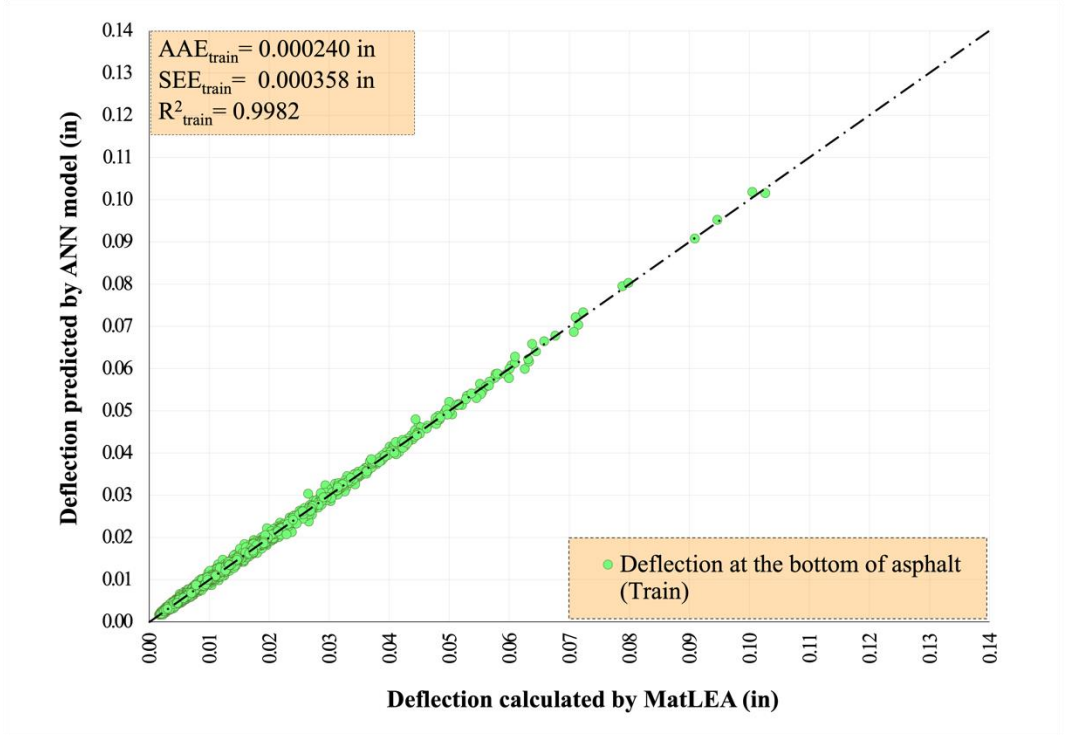

(b) Deflection at the bottom of the asphalt layer

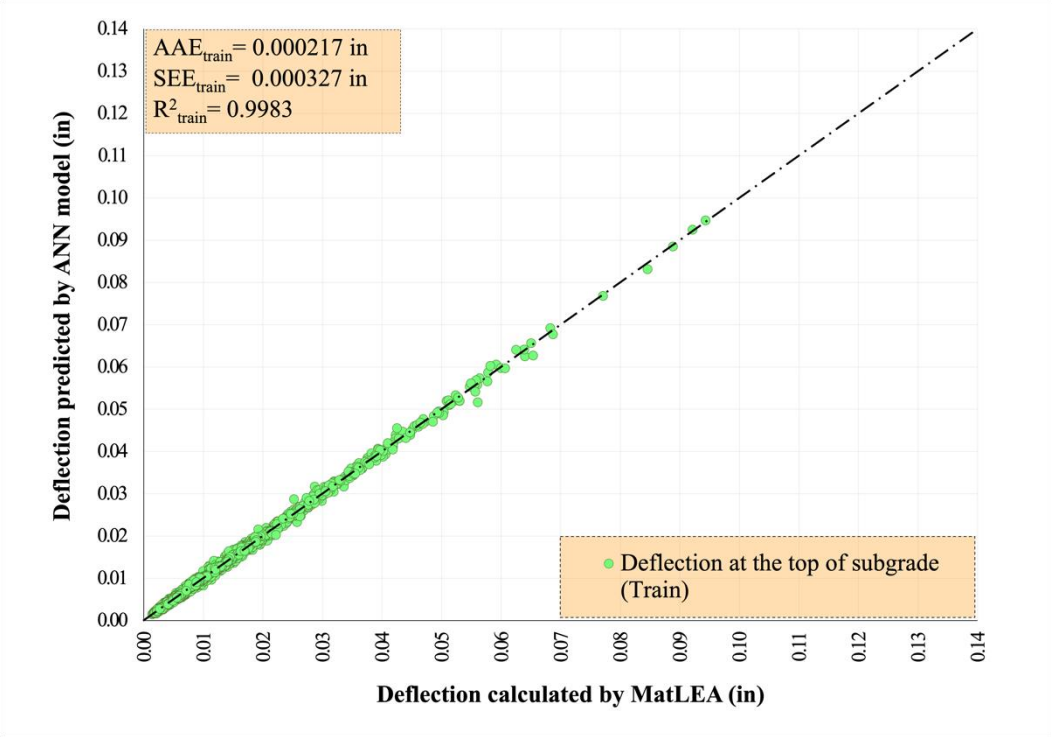

(c) Deflection at the top of the subgrade

Figure 43. Accuracies of training data set for each deflection for pavement systems with stabilized and granular bases

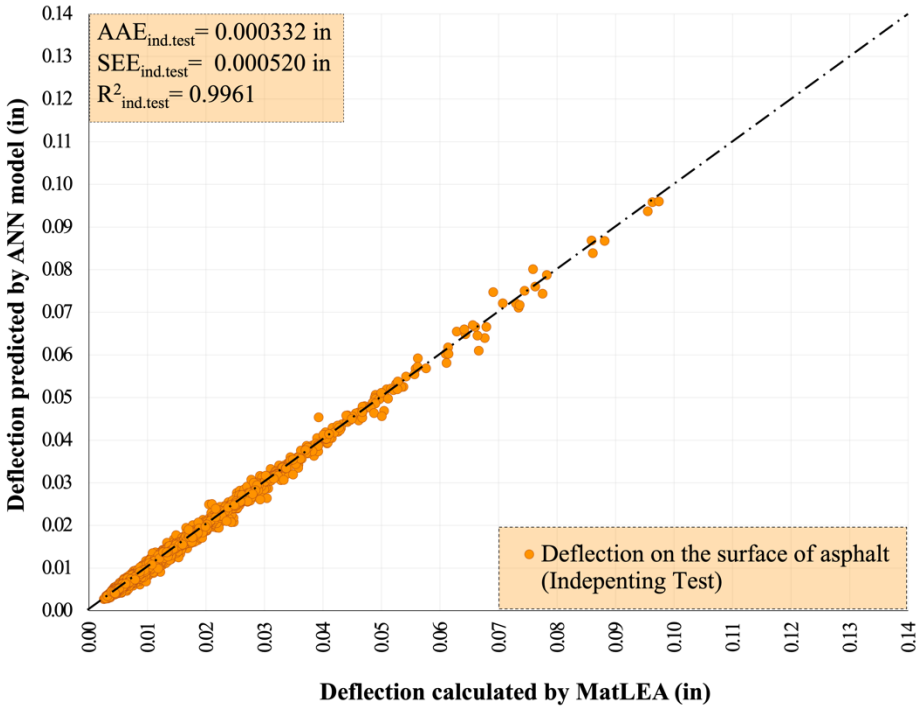

(a) Deflection on the surface

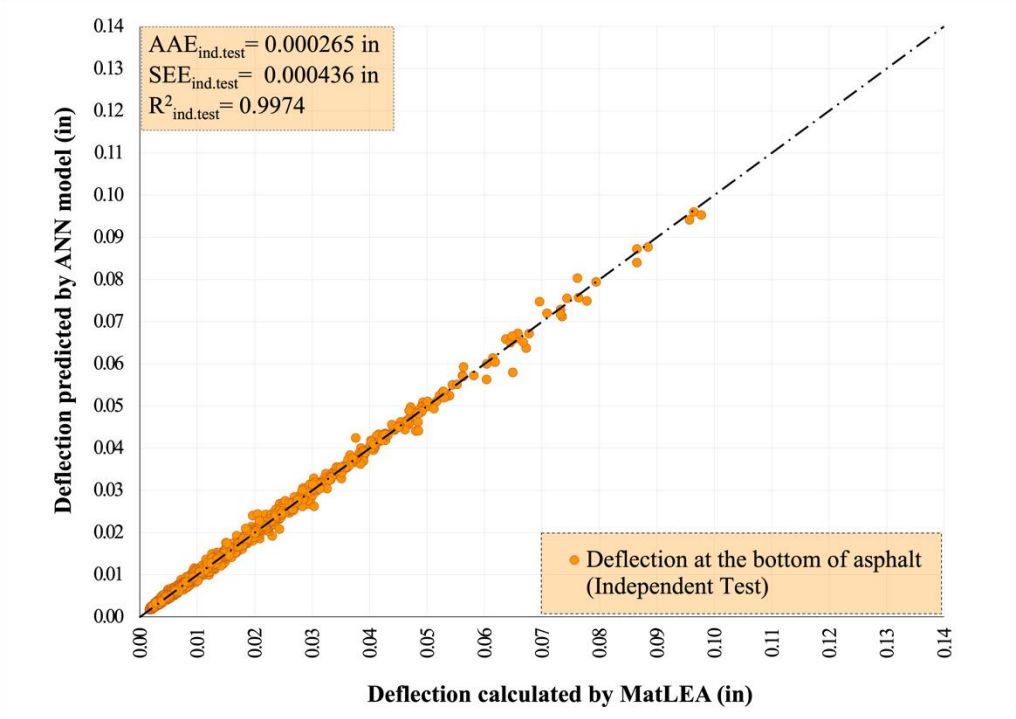

(b) Deflection at the bottom of the asphalt layer

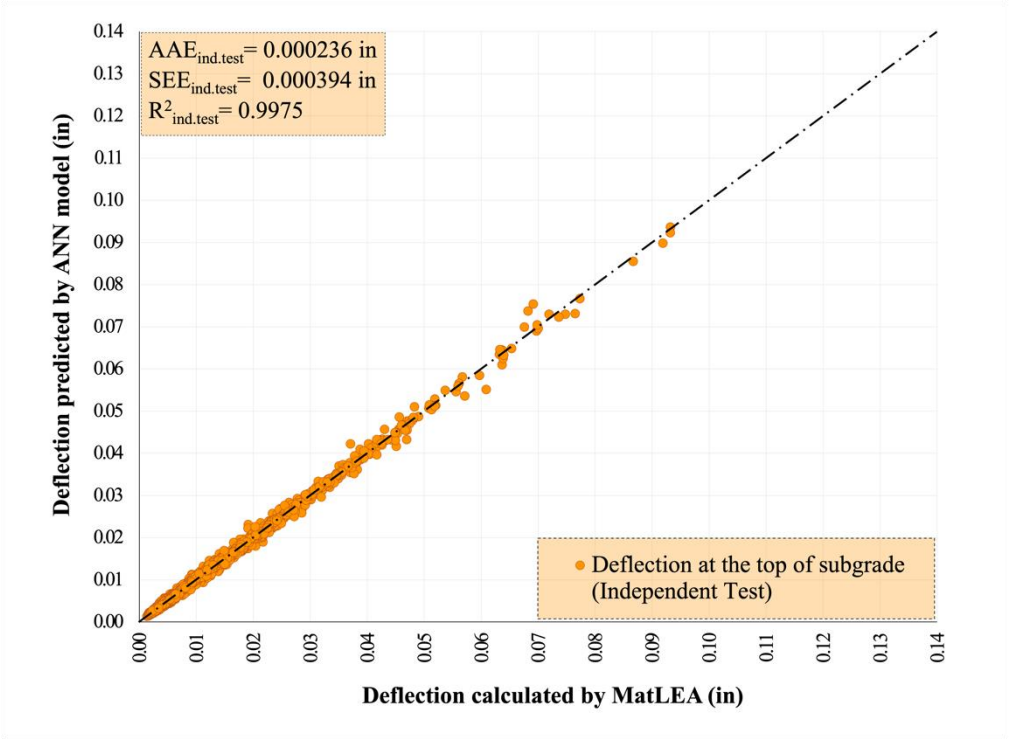

(c) Deflection at the top of the subgrade

Figure 44. Accuracies of independent testing data set for each deflection for pavement systems with stabilized and granular bases

ANN-Based Strain Prediction Model Development for Pavements with Stabilized and Granular Bases

For training the neural network, 2 output parameters—strains at the (1) bottom of the asphalt layer and (2) top of the subgrade layer—were predicted using 38 input parameters, including 3 parameters per each layer: (a) modulus of elasticity, (b) Poisson's ratio, and (c) thickness, excluding subgrade thickness. The size of the developed synthetic database was 50,000 cases, of which 85% was used for training and the remainder for independent testing purposes, as shown in the previous Figure 23. The 50,000 pavement cases included 10 different scenarios with 1 to 10 HMA layers, a stabilized base, a granular base, and a subgrade layer. Each scenario represents 5,000 pavement cases. For training and independent testing, the database was split using a stratified shuffle split technique so that each split can maintain the same percentage for each target class. Here, the chosen target class included 10 different scenarios (i.e., a 4-layered pavement system, 5-layered pavement system, …, 14-layered pavement system). In this way, the independent testing data set had the same proportion of scenarios after the split to represent the entire training data set.

In the input data set used for training the ANN model, 0 represented no data for nonexistent layers, so the empty cells in the sample data set previously shown in Figure 18 were filled with 0s. For example, for a 7-layered pavement system (4 HMA layers, 2 base layers, and 1 subgrade

layer), the data points for HMA layers 5 to 10 were set to 0 during training, thus making the model capable of learning to recognize layer existence.

After splitting the entire data set to avoid data leakage, transformation and scaling were applied only to the training data, and the training data were fitted and transformed using multiple preprocessing methods. After trying various combinations of scaling and transformation techniques and evaluating their effects on model accuracy, the best data preprocessing techniques for each input and output parameter were selected as follows:

- Elastic modulus of layers: standard scaler
- Poisson's ratio: standard scaler
- Thickness: ln(x+1) transformation + standard scaler
- Strain: standard scaler

Table 14 presents the values of the scaling parameters applied to the input and output parameters mentioned previously.

Table 14. Scaling parameters used to train strain ANN model for pavements with stabilized and granular bases

	Elastic modulus		**Poisson's ratio**		**Thickness**		**Strain**	
	Std dev	*Mean*	*Std dev*	*Mean*	*Std dev*	*Mean*	*Std dev*	*Mean*
HMA1	6.10E+05	1.12E+06	0.058	0.350	0.374	1.115	-	-
HMA2	6.70E+05	1.00E+06	0.119	0.316	0.487	1.004	-	-
HMA3	7.03E+05	8.90E+05	0.149	0.280	0.558	0.893	-	-
HMA4	7.22E+05	7.82E+05	0.167	0.245	0.598	0.780	-	-
HMA5	7.24E+05	6.72E+05	0.177	0.210	0.618	0.670	-	-
HMA6	7.05E+05	5.58E+05	0.180	0.175	0.618	0.558	-	-
HMA7	6.72E+05	4.49E+05	0.175	0.140	0.594	0.445	-	-
HMA8	6.15E+05	3.37E+05	0.163	0.105	0.551	0.335	-	-
HMA9	5.25E+05	2.24E+05	0.142	0.070	0.476	0.223	-	-
HMA10	3.87E+05	1.12E+05	0.107	0.035	0.352	0.111	-	-
SB	6.10E+05	1.12E+06	0.058	0.350	0.470	1.596	-	-
SUBG	5.48E+04	1.05E+05	0.029	0.350	0.471	1.597	-	-
Bottom of HMA	-	-	-	-	-	-	5.17E-05	2.18E-05
Top of SUBG	-	-	-	-	-	-	3.25E-04	-2.42E-04

Since these parameters should be applied on the test input data before being tested in the ANN model, test input data were scaled based on the model training input data set properties. The output predicted by the ANN should be backprocessed based on the model training output data set properties to obtain the output from the original unit.

A grid search with k-fold cross-validation was used to find the best neural network configuration to be used as a surrogate in MatLEA. For the ANN-based strain model, the 10-fold cross-validation previously shown in Figure 24 was used. In the grid search, the effects of activation

functions (tanh, ReLU, and sigmoid), the number of hidden layers (1, 2, and 3), the number of neurons per hidden layer (8, 16, 32, 64, 96, 128, 160, and 196), solvers (SGD and Adam), batch size (1, 10, and 100), and momentum (0.7, 0.8, and 0.9) were investigated. The initial learning rate for the training was 1.0E-3 and then adaptively changed. Tolerance for loss was set as 1.0E-4, and if the training loss did not decrease by at least the amount of the tolerance in 10 consecutive epochs, the learning rate was divided by 5. The minimum learning rate of training before termination was 6.4E-8 (i.e., the learning rate changed 6 times by dividing each time by 5, starting from 1.0E-3, then 2.0E-4, 4.0E-5, 8.0E-6, 1.6E-6, and 3.2E-7, and ending with 6.4E-8).

The optimum architecture for the ANN-based strain model for pavement systems with a stabilized base and granular base was found to be 38-128-128-3, i.e., 38 inputs parameters with 2 hidden layers including 128 neurons in each hidden layer and 3 outputs, as visualized in Figure 45.

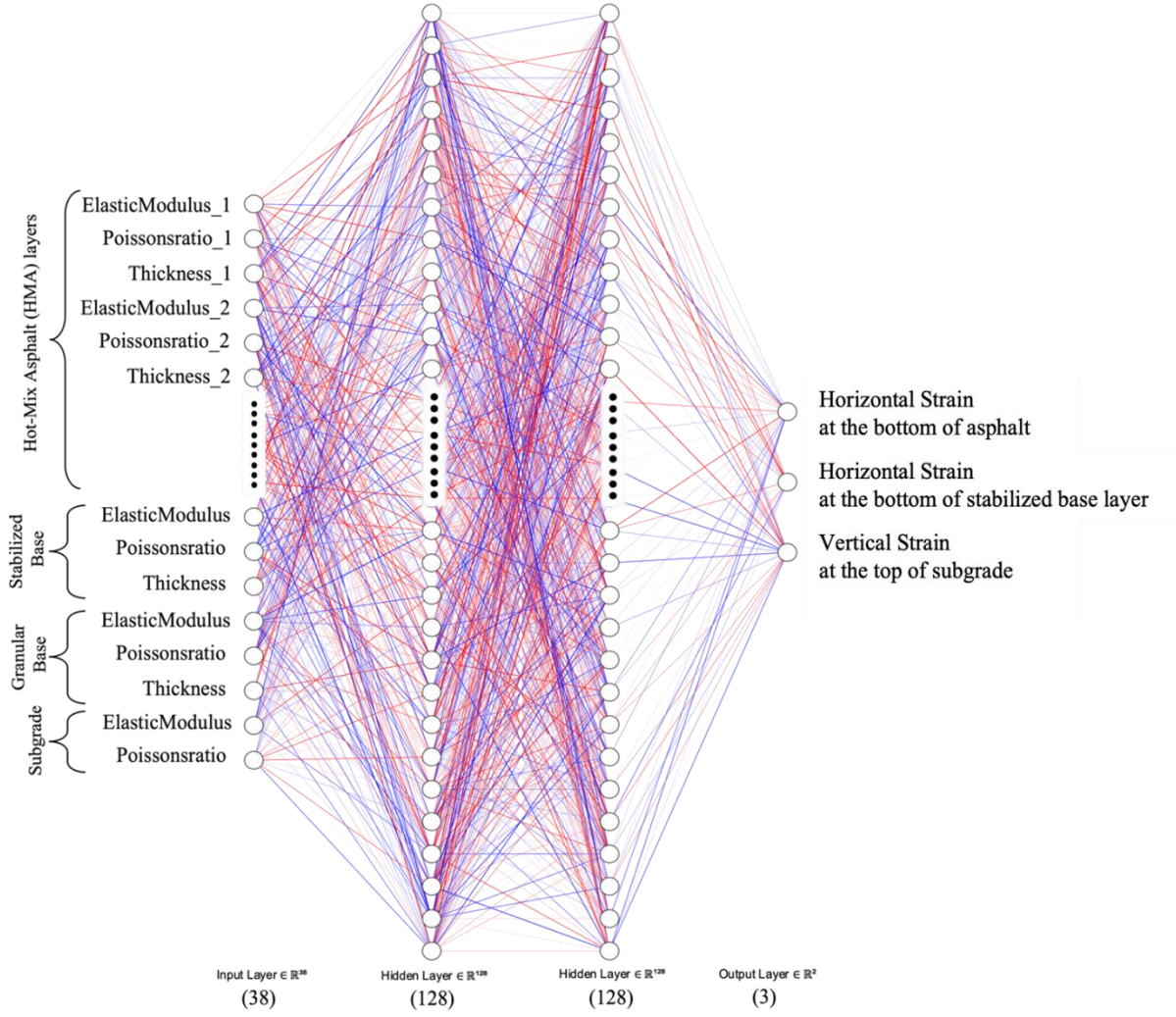

Figure 45. ANN-based strain model for pavement systems with stabilized and granular bases

This model was trained using a tanh activation function, an SGD optimization technique, a batch size of 1, and a momentum of 0.9. The evaluation of the best model was made by comparing the accuracies of the training and validation data sets at each fold, and the mean accuracies of the 10-fold cross-validation represent the overall model training and validation accuracies, indicated by the rightmost bar in Figure 46.

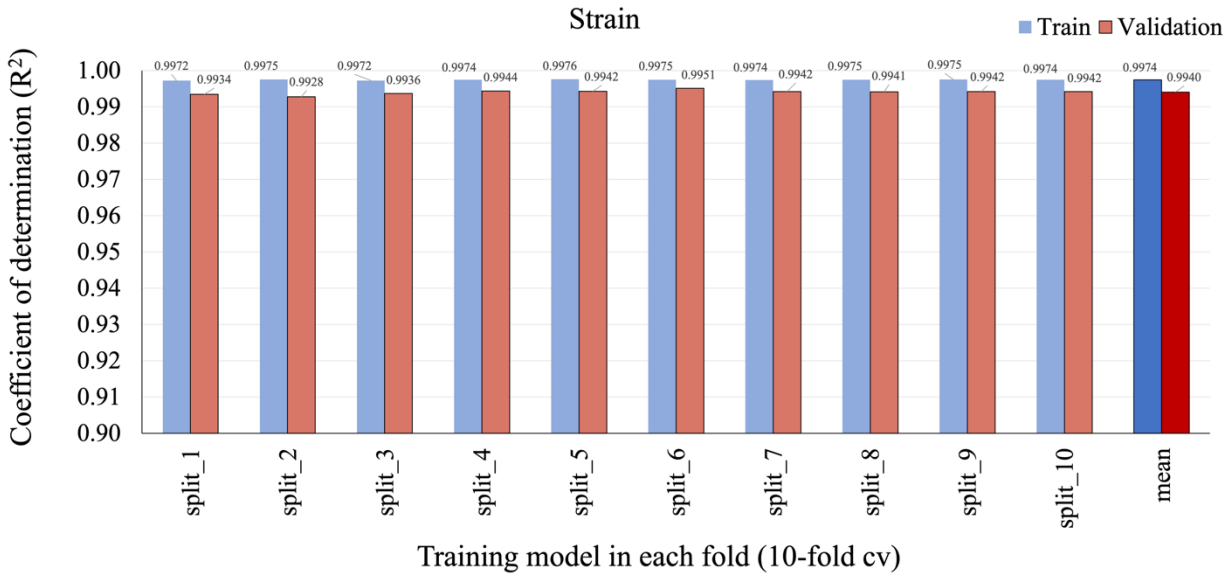

Figure 46. Accuracies of training and validation data sets for pavement systems with stabilized and granular bases

As this comparative bar chart shows, the final scores (R^2) of the training and validation data sets in each of the 10 folds were very high (above 99%) and very similar to one another, with only a slight variation in the thousandths digit; this proves an absence of overfitting or underfitting.

Figures 47a–c and Figures 48a–c indicate the overall comparable accuracy results for training and independent testing, respectively, of the ANN-based strain model (a) on the surface, (b) at the bottom of the asphalt layer, (c) at the top of the subgrade for pavement systems with a stabilized base and granular base.

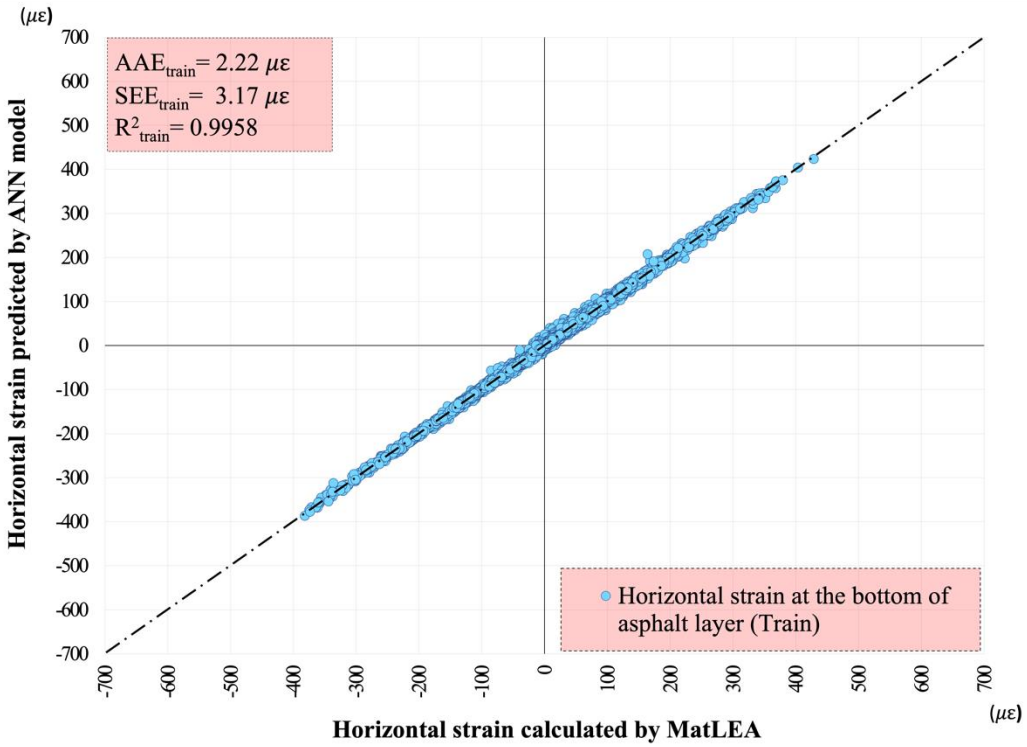

(a) Horizontal strain at the bottom of the asphalt layer

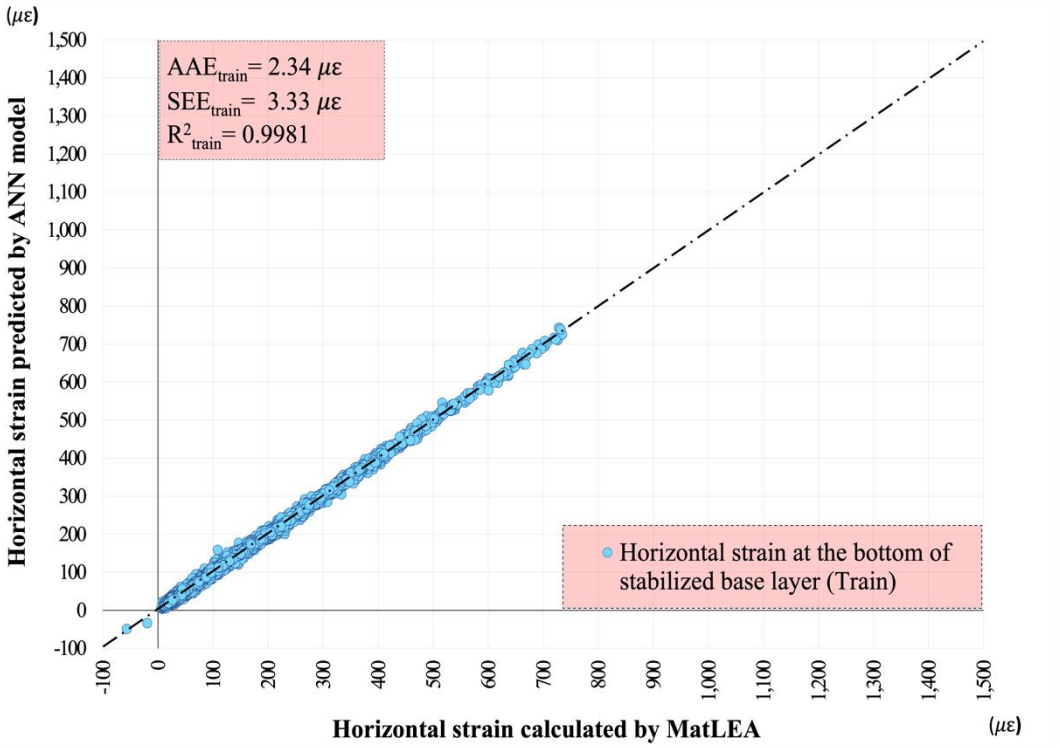

(b) Horizontal strain at the bottom of the stabilized base layer

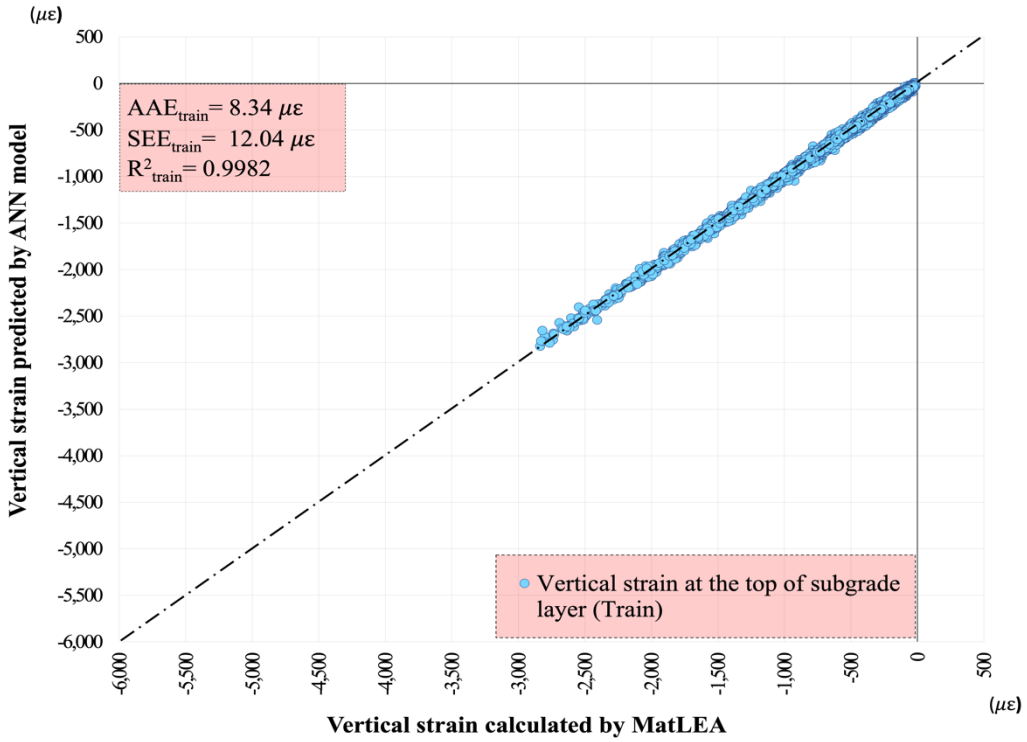

(c) Vertical strain at the top of subgrade

Figure 47. Accuracies of training data set for each strain for pavement systems with stabilized and granular bases

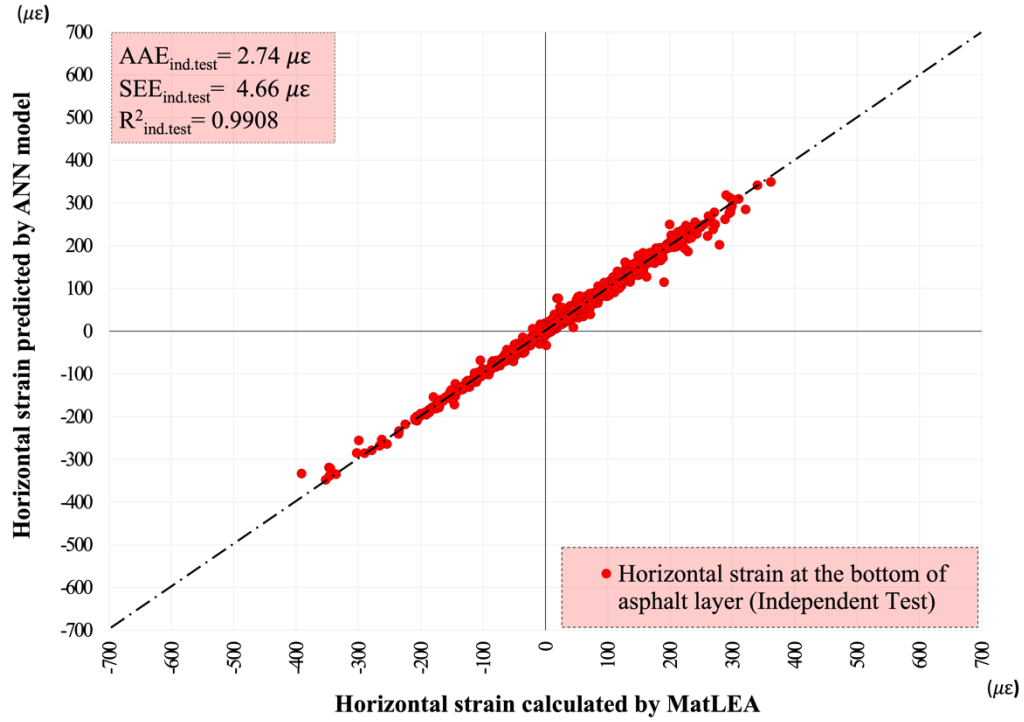

(a) Horizontal strain at the bottom of the asphalt layer

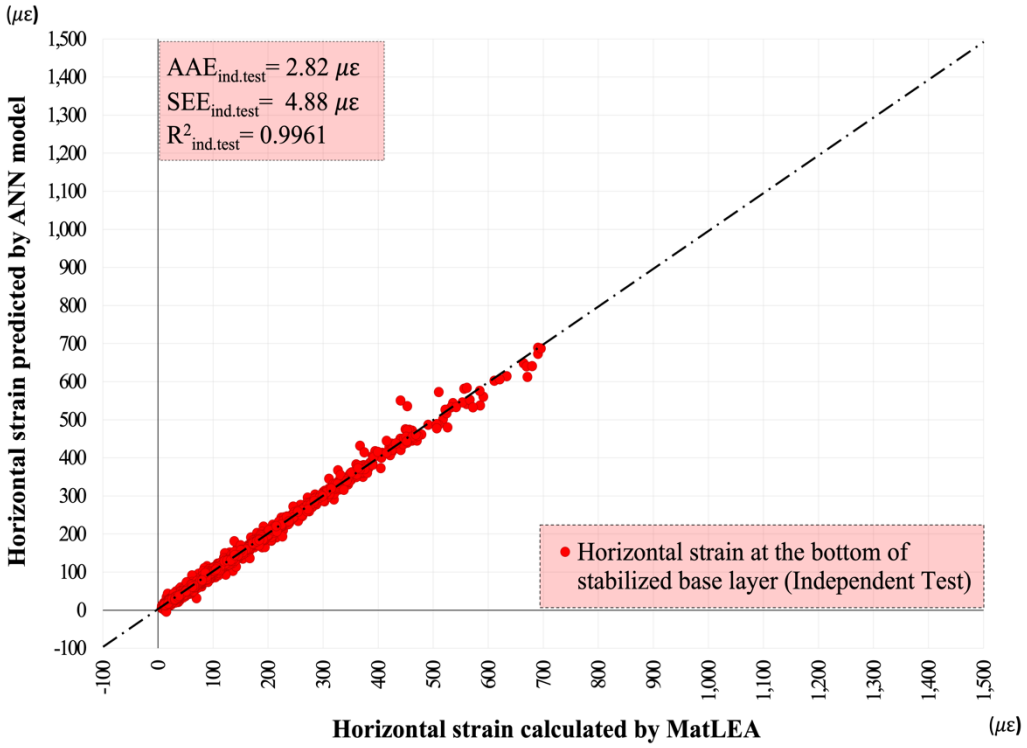

(b) Horizontal strain at the bottom of the stabilized base layer

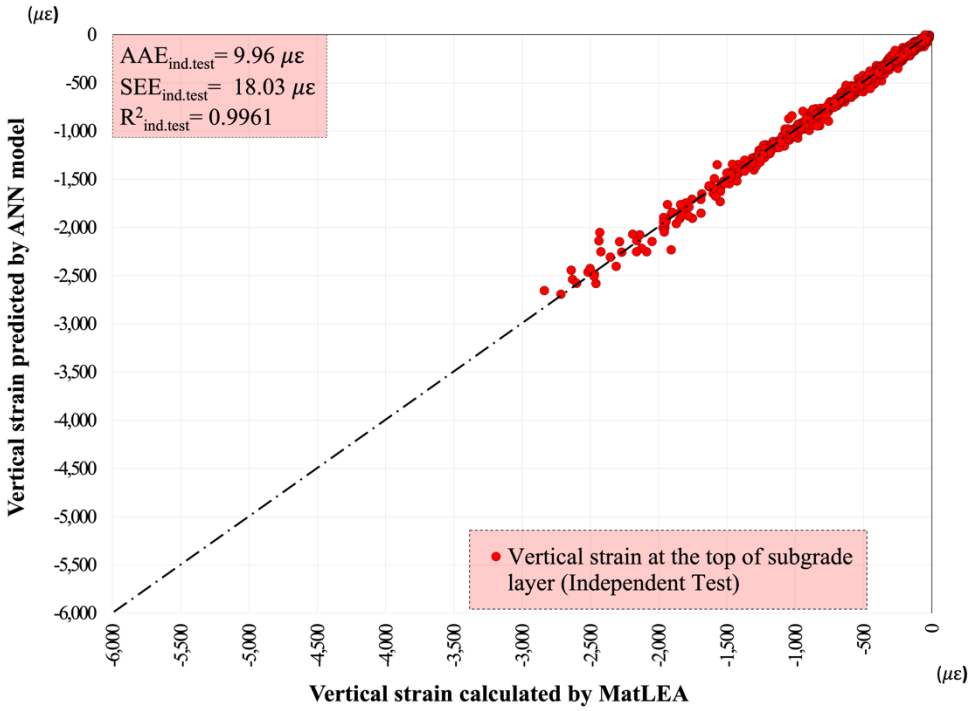

(c) Vertical strain at the top of the subgrade

Figure 48. Accuracies of independent testing data set for each strain for pavement systems with stabilized and granular bases

CHAPTER 5. DEVELOPMENT OF AN ALGORITHM FOR ESTIMATING CURRENT STRUCTURAL CAPACITIES

Description of Techniques for Calculating Structural Capacities of Pavements

The structural capacities of in-service pavements are often characterized in a mechanistic-based pavement design approach in terms of an allowable number of load repetitions (N_f) (AASHTO 2008, Asphalt Institute 1982, Claessen et al. 1977, Thompson 1987) and SN for an American Association of State Highway and Transportation Officials (AASHTO) empirical design approach (AASHTO 1993).

In a mechanistic-based pavement design approach, critical pavement responses calculated from mechanistic models are related to various types of distresses (e.g., fatigue cracking and rutting for flexible pavements) through transfer functions. While transfer function properties differ from one design method to other, they can be commonly expressed as a damage ratio (*DR*, calculated using Miner's law, equation 17) between actual or predicted accumulated load repetitions (n) and the allowable number of load repetitions ($N_{f,r}$). Miner's law states that structural fatigue damage is cumulative, and each load application consumes a small amount of fatigue life. When the actual number of load applications equals the number of allowable load repetitions, critical damage occurs, and the *DR* reaches a value of 1.0, i.e., since the pavement system has no remaining service life (RSL) left, it will fail when the critical damage, *DR* of 1, is reached.

$$\text{DR}= \sum_{i=1}^{m} \left(\frac{n}{N_{f,r}}\right)_i \quad \textbf{(17)}$$

where:

DR = Damage ratio
m = Number of load groups
i = ith load group (or truck classification group)
n = Number of load repetitions for the ith load group (specific cumulative traffic)
$N_{f,r}$ = Maximum allowable number of load repetitions required to cause fatigue/rutting failure

In flexible pavement analysis, traffic loads applied to a pavement surface create two strains that are critical for pavement design purposes. These are the horizontal tensile strain at the bottom of the asphalt layer and the vertical compressive strain at the top of the subgrade, and both have frequently been used as design criteria. The N_f and N_r in the *DR* equation can be related to these strains (e.g., the horizontal tensile strain at the bottom the asphalt layer for fatigue cracking and the vertical compressive strain at the top of the subgrade for rutting) in mechanistic-based flexible pavement design methods, including those from the Asphalt Institute (1982), Shell (Claessen et al. 1977), and the Illinois DOT (Thompson 1987).

Fatigue cracking on a pavement surface occurs if there is excessive horizontal tensile strain in a pavement system. Fatigue cracking is manifested as a series of interconnecting cracks that result

from fatigue failure of an asphalt surface or a stabilized base under repeated traffic loads. Such cracking is initiated below the asphalt surface or stabilized base where the tensile stress or strain is greatest under wheel load. The cracks initially propagate to the surface as one or more longitudinal parallel cracks; then, after repeated traffic loading, they usually connect to form many-sided pieces, resulting in a pattern resembling alligator skin (Huang 2004). For commonly used pavement structures, when the interface between the asphalt layer and the asphaltic base layer (i.e., stabilized base) is fully bonded, the maximum tensile strain at the bottom of the asphalt layer is small, while it is largest at the bottom of an asphaltic base layer. However, when the pavement structure has a granular base layer (i.e., untreated base), the maximum tensile strain is located at the bottom of the asphalt layer (Highway Research Board 1973, Huang 2004, Sun 2016).

If there is excessive vertical compressive strain in the pavement system, permanent deformation (rutting) can occur due to overloading of the subgrade, and significant rutting can lead to major structural failures. The vertical stress at the subgrade top is an important factor in preventing detrimental pavement deterioration on the subgrade. Vertical strain, used as a failure criterion by combining the effects of the stress on and the strength of the pavement system, is mainly caused by such vertical stress (Huang 2004). While Qiu et al. (2000) showed that the great majority of rutting occurs within the granular and subgrade layers for low-volume roads with thin bituminous layers, another study (Majidzadeh et al. 1978) revealed that the subgrade layer contributes to a significant proportion of total pavement rutting (i.e., approximately 40%).

Huang (2004) offered the best-known deterministic models for determining the RSL of flexible pavement. He proposed equation 18 and equation 19 based on the fatigue and rutting criteria, respectively, for calculating the RSL of pavement systems. It is important to note that a layer that has lost its elastic stiffness will no longer be able to resist the stresses induced by traffic, resulting in excessive strain within the pavement.

$$N_f = f_1 \times {\varepsilon_t}^{-f_2} \times {E_1}^{-f_3} \quad \textbf{(18)}$$

$$N_r = f_4 \times {\varepsilon_c}^{-f_5} \quad \textbf{(19)}$$

where:

N_f = Maximum allowable number of load repetitions required to cause fatigue failure
N_r = Maximum allowable number of load repetitions required to cause rutting failure
ε_t = Tensile (horizontal) strain at the bottom of the asphalt layer
ε_c = Compressive (vertical) strain on the top of the subgrade
E_1 = Elastic modulus of asphalt layer
$f_{1,2,3}$ = Regression coefficients obtained from fatigue tests in the road location or the laboratory
$f_{4,5}$ = Regression coefficients obtained from rutting tests in the road location or the laboratory

Various institutions have computed different regression coefficient values based on failure limits, material type, traffic, and environment conditions specified by these institutions, as presented in Table 15.

Table 15. Fatigue and rutting model coefficients by various institutions

Institution	Reference	Fatigue failure model ($N_f = f_1 \times \varepsilon_t^{-f_2} \times E_1^{-f_3}$)			Rutting failure model ($N_r = f_4 \times \varepsilon_c^{-f_5}$)	
		f_1	f_2	f_3	f_4	f_5
Shell	Claessen et al. (1977)	0.0685	5.671	2.363	0	0
Shell (50% reliability)		-	-	-	6.15×10^{-7}	4
Shell (85% reliability)		-	-	-	1.94×10^{-7}	4
Shell (90% reliability)		-	-	-	1.05×10^{-7}	4
Asphalt Institute	Asphalt Institute (1982)	0.0796	3.291	0.854	1.365×10^{-9}	4.477
Belgian Road Research Center	Verstraeten et al. (1982)	4.92×10^{-14}	4.76	0	3.05×10^{-9}	4.35
Transport and Road Research Laboratory	Powell et al. (1984)	1.66×10^{-10}	4.32	0	6.18×10^{-8}	3.95
UC-Berkeley	Craus et al. (1984)	0.0636	3.291	0.854	-	-
Illinois DOT	Thompson (1987)	5×10^{-6}	3.0	0	3	0
University of Nottingham	Brunton et al. 1987	-	-	-	1.13×10^{-6}	3.571
U.S. Army Corps of Engineers	Chou (1987)	478.63	5.0	2.66	1.81×10^{-15}	6.527
Mn/ROAD	Timm et al. (1998)	2.83×10^{-6}	3.21	0	-	-
Indian Federal Highway Administration	Das and Pandey (1999)	0.1001	3.565	1.474	-	-
Alabama DOT	Priest (2005)					
Thin Model		0.4875	3.0312	0.06529	-	-
Thick Model		0.4801	3.143	0.4834	-	-

The Shell asphalt fatigue model (Claessen et al. 1977), which uses the mean performance obtained from the test results from 12 mixes from the US and Europe, was developed as a laboratory model in which mean laboratory performance is converted into predicted pavement field performance using a reliability factor. The regression coefficients used in the Shell model are presented in Table 15. The Asphalt Institute (1982) also established a fatigue-cracking model

for asphalt pavements that used equation 20, based on the results of laboratory beam-type testing and correlations with field observations. Assuming the percentage volume of air voids (V_v) to be 5% and the percentage volume of asphalt (V_b) to be 11%, the *M* coefficient in equation 20 is calculated as zero, reducing to the N_f model with regression coefficients presented in Table 15.

$$N_f = 18.4 \times 10^{\mathrm{M}} \times 0.004325 \times {\varepsilon_t}^{-3.291} \times {\mathrm{E}_1}^{-0.854} \quad \textbf{(20)}$$

where:

$$\mathrm{M} = 4.84 \times \left(\frac{V_b}{V_v + V_b} - 0.69\right)$$

For rutting failure, the Asphalt Institute (1982) proposed a model for determining the relationship between rutting failure of asphalt pavement and compressive strain at the top of subgrade using equation 21.

$$N_r = 1.365 \times 10^{-9} \times \left(\frac{1}{\varepsilon}\right)^{4.477} \quad \textbf{(21)}$$

Owende et al. (2001) represented an algorithm similar to the Asphalt Institute's model but using the different mathematical form shown in equation 22 to determine a relationship between fatigue failure and tensile strain.

$$\log(N_f) = 16.664 - 3.291 \times \log(\varepsilon_t \times 10^6) - 0.854 \times \log(E_1) \quad \textbf{(22)}$$

By removing the effect of the asphalt layer's elastic modulus from the Asphalt Institute's model, Park and Kim (2003) proposed another model, shown in equation 23, in which *K* and *C* are regression coefficients, based on evaluation of FWD data.

$$N_f = K \times {\varepsilon_t}^{C} \quad \textbf{(23)}$$

Das and Pandey (1999) developed a mechanistic design model that, by correlating performance data with critical responses, leads to pavement failure. The model was developed by axle-loading in equation 24, where M_R is the resilient modulus. Its difference from Huang's model is its use of M_R instead of E_1.

$$N_f = 1.001 \times 10^{-1} \times {\varepsilon_t}^{-3.565} \times {M_R}^{-1.4747} \quad \textbf{(24)}$$

Likewise, Hossain and Wu (2002) used a different mathematical form shown in equation 25, in which *a*, *b*, and *c* are regression coefficients, using the same model inputs to relate pavement responses to asphalt pavement life.

$$\ln(N_f) = a - b \times \ln(\varepsilon_t) - c \times \ln(E_1) \quad \textbf{(25)}$$

Some researchers also have developed different approaches using different parameters in their model. A study used experimental parameters, i.e., pavement surface curvature (δ) and area under pavement profile (AUPP) to compute N_f using α and β regression coefficients as material constants, as shown in equations 26 and 27 (Saleh 2016). The δ coefficient was obtained from FWD deflections (D_0-D_{200}).

$$N_f = \alpha \left(\frac{1}{2.3\times10^{-3}\times\delta+2\times10^{-5}}\right)^{\beta} \quad \textbf{(26)}$$

$$N_f = \alpha \left(\frac{1}{2.3\times10^{-6}\times AUPP^{0.912}}\right)^{\beta} \quad \textbf{(27)}$$

For the MEPDG under National Cooperative Highway Research Program (NCHRP) 1-37A (ARA, Inc., ERES Consultants Division 2004), researchers began to develop a fatigue cracking model by considering both the Shell and Asphalt Institute models. The resulting research demonstrated that the Asphalt Institute model, represented by equation 20,was the most applicable (El-Basyouny and Witczack 2005). The model was basically recalibrated using long-term pavement performance (LTPP) data. The researchers introduced a new correction factor *K* to account for thinner pavements (<4 in.), and their final model for fatigue design, which considered failure to occur at 50% cracking of the total lane area, is shown in equation 28.

$$N_f = 0.00432 \times K \times 10^{\mathrm{M}} \times {\varepsilon_t}^{-3.9492} \times {\mathrm{E}_1}^{-1.281} \quad \textbf{(28)}$$

where:

$K = \frac{1}{0.000398 + \frac{0.003602}{1+e^{11.02-3.49\times H_{HMA}}}}$ for bottom-up or alligator cracking

$K = \frac{1}{0.01 + \frac{12}{1+e^{15.676-2.8186\times H_{HMA}}}}$ for top-down or longitudinal cracking

H_{HMA} = Thickness of HMA layer, in.

The AASHTO empirical design uses the SN concept to assign a single number to the overall structural requirement needed to sustain a design's traffic loadings. The SN is comprised of the structural contributions from each layer, using a layer coefficient (a_i) and thickness (h_i), where the layer coefficient is a measure of relative stiffness (SN = a1h1+ a2h2+ a3h3+….). Layer coefficients are typically empirically determined based on the performance of the material (i.e., modulus of the materials). Although the layer coefficients used in the SN model are calculated per each given layer in the tool, it was confirmed that an equivalent thickness with a corresponding modulus could also be used to calculate the SNs.

Computation Algorithms for Estimating Structural Capacities of Iowa County Pavements

The previous section shows that there are many algorithms and models for determining more accurate fatigue and rutting failure for a given pavement structure. Almost all these methods have been developed by relating critical pavement responses to specific pavement distresses. In this study, some methods were tested on a developed synthetic database, seeking to determine the best mathematical model. The Illinois DOT, Shell, and the Asphalt Institute's transfer functions were considered as starting points for calculating allowable load repetitions. Of all the mechanistic-based design models evaluated, the Illinois DOT approach for fatigue failure (N_f) and the Asphalt Institute approach for rutting failure (N_r) achieved the greatest accuracy when using the developed diverse synthetic database. The mathematical models for fatigue failure in equation 29 and rutting failure in equation 30 were therefore integrated into the PSAT.

$$\ln(N_f) = -12.206072 - 3 \times \ln(\varepsilon_t) \quad \textbf{(29)}$$

$$\ln(N_r) = -20.412111 - 4.477 \times \ln(\varepsilon_t) \quad \textbf{(30)}$$

Figures 49 and 50 show the plots of allowable load repetitions to fatigue and rutting failures versus strain, respectively. It compares the results computed by MatLEA and predicted by the ANN. As shown in the figures, the ANN results match the MatLEA results.

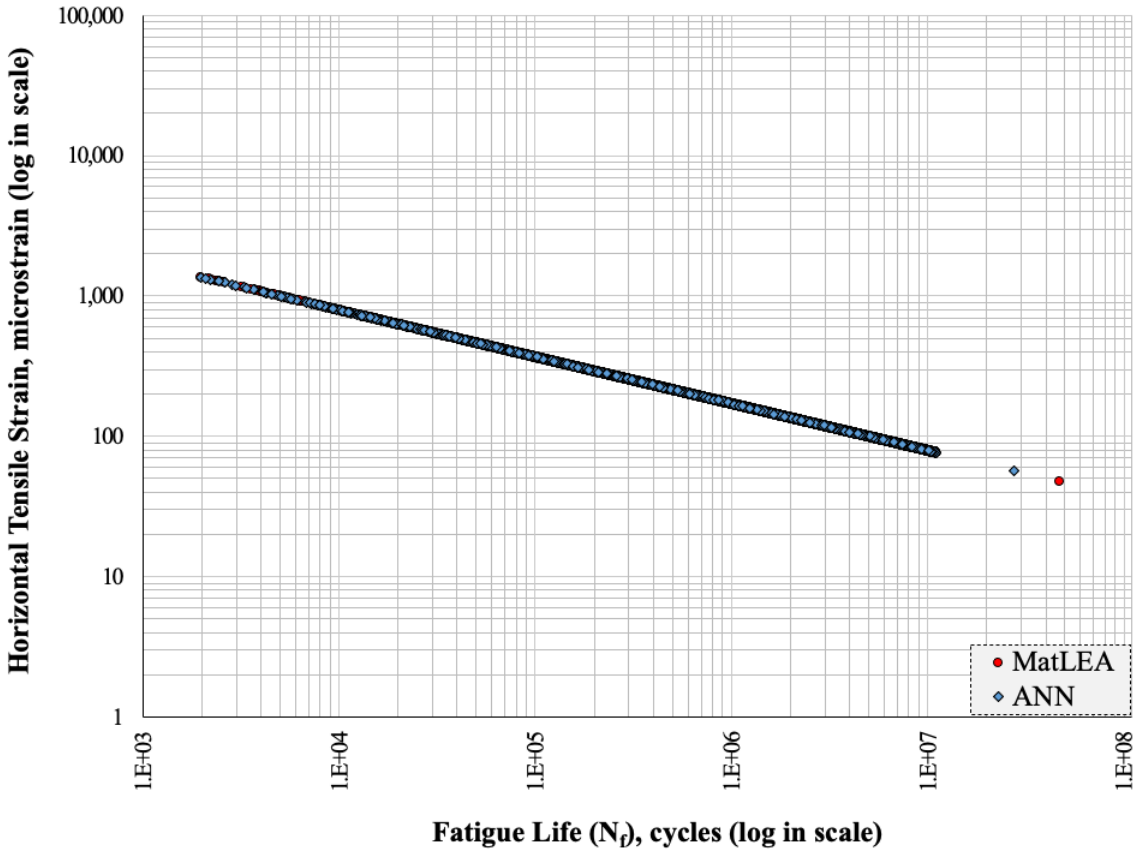

Figure 49. Comparison of MatLEA and ANN for the allowable load repetitions to fatigue failure (N_f) versus horizontal tensile strain

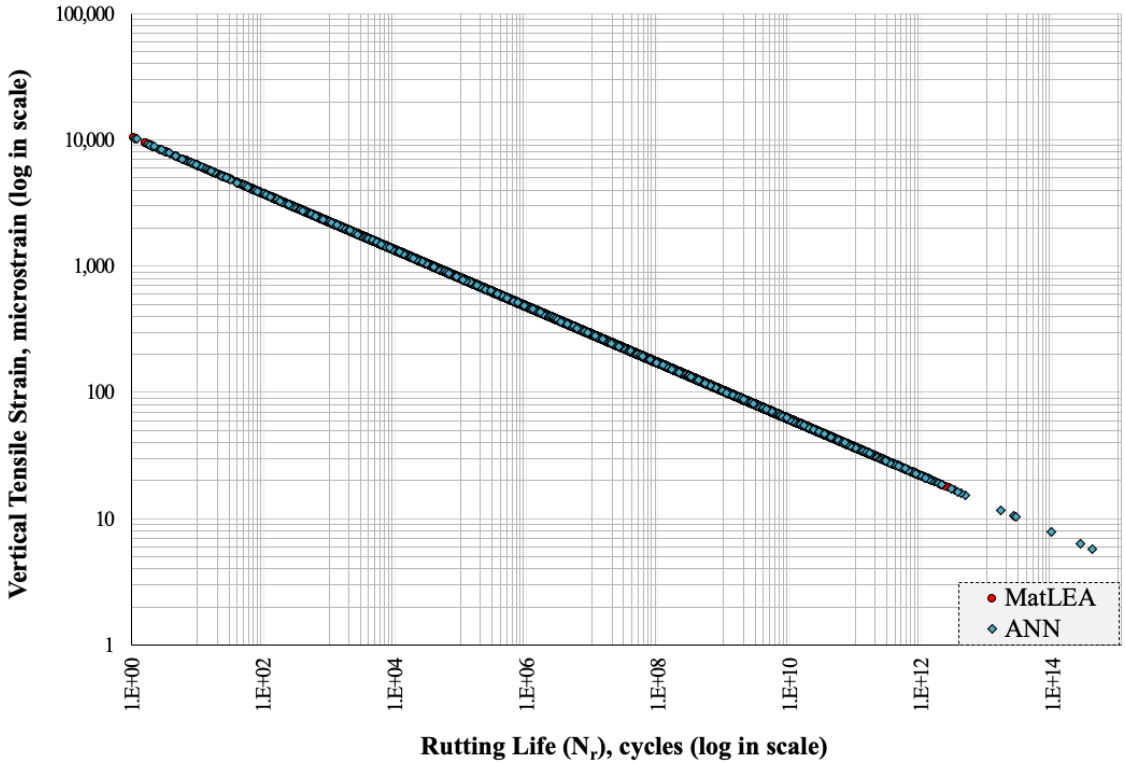

Figure 50. Comparison of MatLEA and ANN for the allowable load repetitions to rutting failure (N_r) versus horizontal tensile strain

Equation 31 lists the layer coefficients adopted in this study and used to calculate SNs.

$a_1 = 0.40 \times \log[E/3000MPa] + 0.44. \implies$ for asphalt layer

$a_2 = 0.52 \times \log[E/3000MPa] + 0.08 \implies$ for stabilized base

$a_3 = 0.23 \times \log[E/160MPa] + 0.15 \implies$ for granular base **(31)**

CHAPTER 6. DEVELOPMENT AND FEATURES OF A PSAT

PSAT Development and Features

The PSAT is a macro-enabled Visual Basic Applications (VBA)-based Microsoft Excel automation tool comprised of the several consecutive subsections shown in Figure 51.

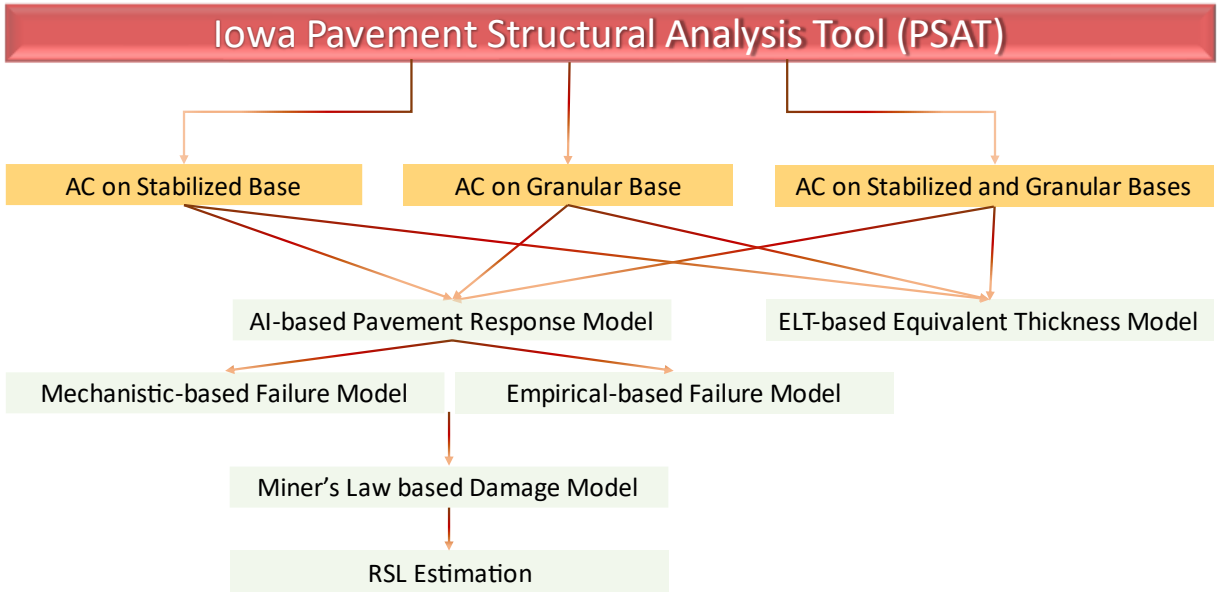

Figure 51. Overview of subsections of the PSAT

The tool has been developed to navigate subsections and analyze three different pavement types: (1) AC on a stabilized base, (2) AC on a granular base, and (3) AC on a stabilized base and granular base. AI-based models have been used to predict critical deflections and strains, and the predicted pavement responses have been used to identify mechanistic-based (fatigue and rutting failures) and empirically based (SN) failures. The damage due to fatigue and rutting has then been calculated for specified traffic levels and results from the failure model. The RSL has been estimated based on current damage.

It should be noted that the PSAT is a macro-enabled automation tool. The question "This workbook contains macros. Do you want to disable macros before opening the file?" may be asked to the user while opening the PSAT. The user should click Enable Macros before proceeding further.

The PSAT has been developed to simultaneously analyze two pavement systems, helping to compare two different pavement sections at the same time, and to analyze them from beginning to end on the same platform, i.e., from predicting critical pavement responses to estimating their RSLs based on major flexible pavement failures.

The subsections of the PSAT are as follows:

- Input Panel
- Pavement Response Prediction Panel
- Equivalent Thickness Calculation Panel
- Traffic Calculation Panel (Conversion from average daily traffic [ADT] to ESAL)
- Failure Identification Panel
- Damage Calculation Panel
- RSL Estimation Panel

Within the PSAT, cell representation is as follows:

- The red-colored cells indicate subsection titles
- The green-colored cells indicate positions for user input
- The white-colored cells indicate either predicted/computed outputs or unit conversions
- The gray-colored boxes indicate macro-based buttons that users should click to make selections
- The other colors in the cells are for labeling inputs or outputs

The user is asked to enter and/or edit data only at green-colored cells and is not allowed to change information in other cells, i.e., all cells except green-colored cells are locked and protected within the tool. While US units were mainly used in developing the models and algorithms, the tool can convert its data to the International System of Units (SI) for illustration purposes, although input parameters must be entered in US units.

The tool first asks users to enter the following project information:

- Project Name: Descriptions for the road, e.g., street name
- County Name
- Project No.: Number (ID) of the project
- BPRJ: Beginning of the project
- EPRJ: Ending of the project

The PSAT source code is provided in the appendix. In addition, details on how to use the PSAT are provided in a standalone user guide that was also developed as part of this project.

CHAPTER 7. CONCLUSIONS

Overall Conclusions

A detailed methodology for developing computational pavement structural analysis models and a tool that analyze AC pavements representing conventional and full-depth flexible pavements has been described and discussed. The methodology included grouping the pavements into three different types used in Iowa: (1) AC on a stabilized base, (2) AC on a granular base, and (3) AC on a stabilized base and granular base. Each major pavement type can be sub-grouped as AC on a base and AC overlay on AC on a base.

This study presented a systematic approach to the generation of a highly realistic annotated synthetic database for training deep neural networks in regression tasks. To begin development of the structural analysis tool, a comprehensive synthetic database including a total of 150,000 different pavement cases was developed for mechanistic-based pavement structural analysis. A synthetic database was specifically used in this study to boost the data set size given more training data for the models were needed; the Iowa county pavement system lacks field data to supply the inputs and outputs required for structural analysis. The approach to generate a synthetic database was characterized as using process-driven and data-driven methods. This study used both a statistical analysis for determining pavement characteristics within the defined range used for machine learning techniques for modeling and a computational LEA for computing pavement responses using MatLEA (Kutay and Lanotte 2020), and it greatly benefitted from using both process- and data-driven techniques.

Using the synthetic database, ANNs were developed to predict critical pavement responses. AI techniques such as ANN-based models have been found to be great tools for modeling pavement structural performance when considering many pavement sections with various ages, thicknesses, stress levels, materials, physical conditions, moduli, and traffic loading. They are also very fast tools that can deal with thousands of pavement scenarios in seconds. Both these features of ANN models make them excellent tools for use in the development of pavement structural performance modeling at the project-level in terms of independent testing and modeling at the network-level in terms of training. Using the ANN approach, critical pavement responses can be easily and accurately predicted, saving a great deal of time and cost compared to using approaches such as NDE techniques that require larger budgets or computationally demanding mechanistic-based elastic layer analysis programs.

Using ANN-based models, algorithms and approaches to estimate current structural capacities of pavement systems were developed. One of these approaches led to development of an ELT-based equivalent thickness model. ELT has been found to be a great approach to provide a simple method of approximation in pavement structural analysis in which overlaid pavement layers with different thicknesses and moduli are combined into a single layer with an equivalent thickness. The concept is based on the principle that a simplified pavement system represented by an equivalent layer has the same stiffness as the original multilayered pavement system, making it easier for an Iowa county engineer to (1) estimate the current structural capacities of

in-service county pavements and (2) determine overlay design options for future cycles of rehabilitation.

Another approach was used to develop computation algorithms for estimating current structural capacities of in-service Iowa county pavements in terms of RSL using both mechanistic- and empirically based design approaches. Using the mechanistic-based pavement design approach, the critical pavement responses predicted by the ANN-based models were related through transfer functions to various type of distresses (e.g., fatigue cracking and rutting for flexible pavements) so that structural capacities of in-service pavements were characterized into an allowable number of load repetitions to fatigue (N_f) and rutting (N_r) failures. The Miner's law-based damage model and RSL estimation approach were presented in this study.

Conclusions for Generating Synthetic Database

Synthetic database generation is described in Chapter 3, and the specific related findings can be summarized as follows:

- Three major groups of pavement systems (i.e., AC on a stabilized base, AC on a granular base, and AC on a stabilized base and granular base) were used in the development of a synthetic database.

- Each group contained 50,000 different pavement scenarios representing a total of 150,000 pavement cases.

- The study presents field data characterizations obtained from the Iowa DOT PMIS and the ICEASB. Ranges of pavement characteristics representing real pavement cases were selected from historical pavement databases and field investigations and based on past experiences.

- Each major group of pavement systems (i.e., 50,000 data points) was comprised of 10 different pavement types, with each type comprised of 5,000 different pavement scenarios (e.g., a 3-layered pavement system, 4-layered pavement system, 5-layered pavement system, ..., 13-layered pavement system).

- For each pavement layer in each scenario, three parameters were used to describe the HMA layers on the stabilized and/or granular base/subbase layers above the subgrade layer: (1) elastic modulus, (2) Poisson's ratio, and (3) thickness, except the subgrade layer was assumed to have an infinite depth and so no thickness was used. A total of 35 parameters for the pavement systems of AC on a stabilized base and AC on a granular base and 38 parameters for the pavement system of AC on a stabilized base and granular base were selected as input variables in the synthetic database.

- A high-performance linear-elastic analysis program, MatLEA (Kutay and Lanotte 2020), was used to compute pavement responses. Because tensile strain at the bottom of the asphalt layer

and compressive strain at the top of the subgrade layer are commonly related to fatigue and rutting failures, three critical locations per each pavement scenario with bonded layers were defined for prediction using the mechanistic-based design approach of deflections and strains at the surface, at the bottom of the asphalt layer (or the bottom of the stabilized base layer), and the top of the subgrade layer. A total of six parameters for the pavement systems of AC on a stabilized base and AC on a stabilized base and granular base and five parameters for the pavement system of AC on a granular base were set as output variables in the synthetic database. The six output variables include deflections at the surface, at the bottom of the asphalt, and at the top of the subgrade, along with horizontal tensile strains at the bottom of the asphalt and the bottom of the stabilized base and compressive strains at the top of the subgrade; the five output variables for AC on a granular base are the same as the other output variables only the horizontal strain at the bottom of the stabilized base was not included due to the pavement system having a granular base.

- Essential statistical evaluations to investigate the quality of the input variables and their relationships (e.g., correlation analysis, test hypothesis) were successfully performed on the developed synthetic database.

Conclusions for ANN Model Development for Pavement Response Prediction

The development of ANN models for predicting pavement responses is described in Chapter 4, and the specific related findings can be summarized as follows:

- A total of six different ANN-based models were successfully developed for the three major groups of pavement systems.

- Among the six models, three were used for predicting the following three outputs: deflections (1) on the surface, (2) on the bottom of the asphalt, and (3) at the top of the subgrade. The remaining three models were used for predicting the following two or three outputs, as applicable: strains (1) at the bottom of the asphalt, (2) the bottom of the stabilized base, and (3) at the top of the subgrade.

- The ANN model architectures included the following:
  - One input layer with 35 neurons for cases where the pavements had a single base and 38 neurons for cases where the pavements had 2 bases.
  - Two hidden layers with 96 neurons for deflection prediction models and 128 neurons for strain prediction models.
  - One output layer with three neurons for deflection models, and two or three neurons for strain models developed for cases where the pavements had a single base or cases where the pavement had two bases, respectively.

- The data were split so that 85% of the entire database was used for ANN model development, and the remaining 15% was used to test the ANN model independently and prove the robustness of the developed models.

- Accuracy of the pavement response prediction models in mimicking pavement critical responses computed by MATLEA was measured using statistical measurements such as R^2, AAE, and SEE. Higher R^2 and lower AAE and SEE values are reflective of model prediction accuracy.

- When the ANN predictions are compared with the MatLEA results, all the deflection models have R^2 values greater than 0.9961, AAE values less than 0.000346 in., and SEE values less than 0.000724 in. based on the training, validation, and independent testing accuracy results. All strain models predicting horizontal strains have R^2 values greater than 0.9908, AAE values less than 6.28 microstrain, and SEE values less than 11.97 microstrain. The models predicting vertical strains have R^2 values greater than 0.9961, AAE values less than 21.05 microstrain, and SEE values less than 42.04 microstrain based on the training, validation, and independent testing accuracy results. It was therefore proven that ANN-based models predicted pavement responses with a high accuracy.

- The developed ANN-based models have been integrated into a macro-enabled Microsoft Excel and VBA-based PSAT using the model parameters (e.g., weight and biases) and data transformation and scaling parameters, moving the models into a user-friendly environment that can significantly reduce runtime for predicting critical pavement responses for up to two different pavement systems simultaneously.

Conclusions for Algorithm Development for Structural Capacity Estimation

The development of algorithms and approaches for predicting the current structural capacities of pavement systems is described in Chapter 1 and Chapter 5, and the specific related findings can be summarized as follows:

- The simplification approach was applied to a three-layered pavement structure consisting of an asphalt layer, base, and subgrade layer, and the critical pavement responses of the simplified three-layered pavement structure were very similar to the pavement responses of the multilayered pavement structures.

- Of all the equivalent layer thickness models evaluated, Pronk's model was found to perform best in terms of applicability and accuracy in calculating deflections and strains on the surface, at the bottom of the asphalt, and on top of the subgrade. Based on model assumptions, the equivalent thickness was calculated using a mathematical model in which the equivalent layer modulus would be equal to the modulus of the lower original layer. The model based on these assumptions was integrated into the PSAT.

- For pavement systems of "AC on a stabilized base" and "AC on a granular base," the AC layers are simplified into one layer equivalent to a three-layered pavement system. For the pavement system of "AC on a stabilized base and granular base," the AC layers and stabilized base are simplified into one layer equivalent to a three-layered pavement system.

- Many mechanistic-based design approaches were investigated, and the Illinois DOT, Shell, and Asphalt Institute's transfer functions were ultimately considered as starting points for calculating the number of allowable load repetitions. Of all the mechanistic-based design models evaluated, the Illinois DOT approach for calculating fatigue failure (N_f) and the Asphalt Institute approach for calculating rutting failure (N_r) provided the best accuracy when using the developed diverse synthetic database. These models were thus integrated into the PSAT.

- As an empirically based design approach, the SN concept of AASHTO empirical design was utilized to provide a single number per asphalt surface layer and base that indicates the overall structural requirement needed to sustain the design's traffic loadings. This mathematical model was integrated into the PSAT. Although the layer coefficients used in the SN model are calculated in the tool per the given layers, it was confirmed that the equivalent thickness with a corresponding modulus could also be used to calculate the SNs.

CHAPTER 8. RECOMMENDATIONS FOR IMPLEMENTATION AND FUTURE RESEARCH

This study developed a PSAT for use by Iowa county engineers to help them understand their current structural capacity by predicting critical pavement responses within the pavement structure, calculating equivalent thickness, identifying fatigue/rutting failures and corresponding damages, and ultimately estimating RSL. The tool provides successive subsections for estimating RSL through different approaches and models, and such estimations will help county engineers distinguish between two pavement sections thought to have the same current condition (i.e., the same current international roughness index [IRI]). This can be an ideal approach to addressing transportation planning and performance management criteria requirements of the Moving Ahead for Progress in the 21st Century Act (MAP-21). Such damage and RSL estimations in terms of fatigue and rutting failures will allow county engineers to distinguish between two pavement sections using multiple cycles of pavement construction and renewal.

Figure 52 shows the pavement asset management procedures recommended by the Iowa Highway Research Board (IHRB) project TR-740 (Citir et al. 2021b), adapted for the current project, describing how the developed tool could be integrated into Iowa county pavement asset management procedures.

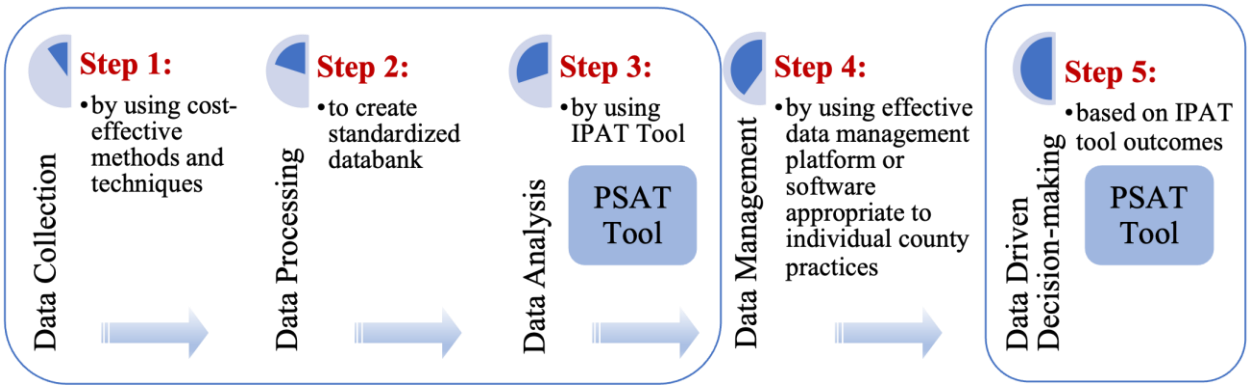

Adapted from Citir et al. 2021b

Figure 52. Pavement asset management procedures

The procedure is comprised of consecutive steps of (1) data collection, (2) data processing, (3) data analysis, (4) data management, and (5) data-driven decision-making.

A major part of the asset management procedure was satisfied by generating a comprehensive synthetic database using ranges of pavement characteristics from both field data and an historical pavement database (i.e., data collection), preprocessing the data using statistical techniques (i.e., data processing), developing ANN-based models to analyze the preprocessed data for ultimately estimating structural performance and RSL of county pavements (i.e., data analysis), and using the PSAT predictions to prioritize and allocate resources for future pavement preservation and rehabilitation needs.

Future guidelines for the next phase(s) of this work have been developed, and they propose to fulfill county engineers' needs by fully implementing the recommended steps in Iowa county pavement asset management practices, as well as advancing the PSAT capabilities. These guidelines can be divided into two categories: short-term and long-term actions.

Short-term actions include the following:

- **Develop a structural performance tool for rigid (concrete) pavements:** Implementing a second version of the PSAT for structurally analyzing concrete pavements would promote use of a complementary structural analysis tool providing local road agencies with greater capability for managing the entire pavement network system. The approach and techniques developed and proposed in this study could easily be pursued and employed for developing models and a tool for use on concrete pavements by considering mechanistic-based concrete design and analysis approaches.

- **Develop structural overlay design tool:** The outcomes from the PSAT and models represent only a first step in estimating the current structural capacity of pavements. The next step would be to estimate the overlay thickness required to overcome identified failures. A structural overlay design tool could facilitate better decision-making for future maintenance cycles and more effective project prioritization.

Long-term actions include the following:

- **Develop an approach for relating mechanistic-based failures to pavement distresses:** Developing algorithms with an additional layer of transfer functions to convert the identified damage—the outcome of the present PSAT—into field distresses would provide better information about the structural capacity and condition of a pavement system. The approach could find relationships between pavement structural performance and pavement condition and distresses (e.g., relating fatigue failure to the number of fatigue cracks in cases where there is insufficient data for use in the Iowa Pavement Analysis Techniques [IPAT] tool's fatigue cracking prediction models). The revised algorithms could be delivered as a complementary addition to the PSAT to automate a series of steps ranging from pavement structural evaluation to pavement performance evaluation.

- **Develop a smartphone application version of the PSAT:** Developing a smartphone application version of the PSAT and integrating it into a geographic information system (GIS) platform and/or software as an officially recognized application (app) under the ICEASB AppSuite would provide better data management practices.

- **Develop a platform integrating IPAT, PSAT, and CyROID tools:** The CyROID tool, the outcome of an ongoing IHRB project titled Development of a Smartphone-Based Road Performance Data Collection Tool that standardizes nonproprietary collection tools (i.e., a smartphone-based road performance data collection tool and a smart vehicle black box) with automatic vehicle location (AVL) technology; the IPAT tool, the outcome of a completed

IHRB project titled Development of Iowa Pavement Analysis Techniques (IPAT) (Kaya et al. 2020, Citir et al. 2021a, Citir et al. 2021b, Kaya et al. 2023) that estimates pavement performance and RSL; and the PSAT, the outcome of this study that evaluates the current structural capacity of pavement systems, can all be provided on the same platform, providing Iowa county engineers with greater ease in managing a project from data collection through decision-making. It would allow engineers to evaluate a pavement system both functionally and structurally.

- **Develop a functional overlay design tool:** A functional overlay design tool would assist engineers in identifying potential pavement preservation opportunities and evaluating the impact of such preservation techniques on pavement life.

REFERENCES

AASHTO. 1993. *Guide for the Design of Pavement Structures*. American Association of State Highway and Transportation Officials, Washington, DC.

AASHTO. 2008. *Mechanistic-Empirical Pavement Design Guide, Interim Edition: A Manual of Practice*. American Association of State Highway and Transportation Officials, Washington, DC.

Adil Mutlag, S. 2012. Effect Of binder layer properties on flexible pavement in Iraq. *Al-Qadisiyah Journal for Engineering Sciences*, Vol. 5, No. 4, pp. 466–476.

Albayati, A. H., H. Al-Mosawe, A. T. Fadhil, and A. A. Allawi. 2018. Equivalent modulus of asphalt concrete layers. *Civil Engineering Journal*, Vol. 4, No. 10, pp. 2264–2274.

ARA, Inc., ERES Consultants Division. 2004. *NCHRP 1-37A: Guide for Mechanistic-Empirical Design of New and Rehabilitated Pavement Structures*. National Cooperative Highway Research Program, Washington, DC.

Asphalt Institute. 1982. *Research and Development of the Asphalt Institute's Thickness Design Manual (MS-1)*. Ninth Edition. Research Report No. 82-2. Asphalt Institute, Lexington, KY.

Brunton, J. M., S. F., Brown, and P. S. Pell. 1987. Development to the Nottingham analytical design method for asphalt pavements. *Proceedings of the Sixth International Conference on the Design of Asphalt Pavements, July 13–17, Ann Arbor, Michigan, Volume 1*. International Society for Asphalt Pavements, Lino Lakes, MN. pp. 366–377.

Ceylan, H. 2002. *Analysis and Design of Concrete Pavement Systems Using Artificial Neural Networks*. PhD dissertation. University of Illinois at Urbana-Champaign, Urbana, IL.

Ceylan, H., M. B. Bayrak, and K. Gopalakrishnan. 2014. Neural networks applications in pavement engineering: A recent survey. *International Journal of Pavement Research and Technology*, Vol. 7, No. 6, pp. 434–444.

Ceylan, H., and A. Guclu. 2005. Effects of combined temperature and gear loading on the response of concrete airfield pavements serving the Airbus A380-800 aircraft. First European Airport Pavement Workshop, May 11–12, Amsterdam, Netherlands.

Ceylan, H., E. Tutumluer, and E. J. Barenberg. 1999. Artificial neural networks for analyzing concrete airfield pavements serving the Boeing B-777 aircraft. *Transportation Research Record*, Vol. 1684, pp. 110–117.

Chabot, A., O. Chupin, L. Deloffre, and D. Duhamel. 2010. Viscoroute 2.0: A tool for the simulation of moving load effects on asphalt pavement. *Road Materials and Pavement Design*, Vol. 11, No. 2, pp. 227–250.

Citir, N., H. Ceylan, and S. Kim. 2020. Neural network models for flexible pavement structural evaluation. *Advances in Materials and Pavement Performance Prediction II*. CRC Press, Boca Raton, FL, pp. 28–32.

Citir, N., H. Ceylan, S. Kim, and O. Kaya. 2021a. Incorporating the effectiveness of preservation and rehabilitation techniques on flexible pavement service life predictions using machine learning approach. *Airfield and Highway Pavements 2021: Pavement Materials and Sustainability*. American Society of Civil Engineers, Reston, VA, pp. 365–377.

Citir, N., O. Kaya, H. Ceylan, S. Kim, D. Waid, and B. P. Moore. 2021b. *Development of Iowa Pavement Analysis Techniques (IPAT)*. Institute for Transportation, Ames, IA.

Craus, J., R. Yuce, and C. L. Monismith. 1984. Fatigue behavior of thin asphalt concrete layers in flexible pavement structures. *Association of Asphalt Paving Technologists, Proceedings*, Vol. 53, pp. 559–582.

Claessen, A. I. M., J. M. Edwards, P. Sommer, and P. Uge. 1977. Asphalt pavement design—the Shell method. *Proceedings of the Fourth International Conference on the Design of Asphalt Pavements, August 22–26, Ann Arbor, Michigan, Volume 1*. International Society for Asphalt Pavements, Lino Lakes, MN. pp. 39–74.

Davies, T. G., and M.S. Mamlouk. 1985. Theoretical response of multilayer pavement systems to dynamic nondestructive testing. *Transportation Research Record*, Vol. 1022, pp. 1–7.

Das, A., and B. B. Pandey. 1999. Mechanistic-empirical design of bituminous roads: an Indian perspective. *Journal of Transportation Engineering*, Vol. 125, No. 5, pp. 463–471.

De Barros, S. T. 1966. Deflection factor charts for two- and three-layer elastic systems. *Highway Research Record*, Vol. 145.

Chou, Y. T. 1987. *Probabilistic and Reliability Design Procedures for Flexible Airfield Pavements-Elastic Layered Method*. U.S. Army Waterways Experiment Station Geotechnical Laboratory, Vicksburg, MS.

El-Badawy, S. M., and M. A. Kamel. 2011. Assessment and improvement of the accuracy of the Odemark transformation method. *International Journal of Advanced Engineering Sciences and Technologies*, Vol. 5, No. 2, pp. 105–110.

El-Basyouny, M., and M. Witczak. 2005. Development of the fatigue cracking models for the 2002 design guide. *Transportation Research Board 84th Annual Meeting, January 9–13, Washington, DC, Compendium of Papers*. Transportation Research Board, Washington, DC.

Fakhri, M., and A. R. Ghanizadeh. 2014. Modelling of 3D response pulse at the bottom of asphalt layer using a novel function and artificial neural network. *International Journal of Pavement Engineering*, Vol. 15, No. 8, pp. 671–688.

Ghazavi, M., A. Seitllari, and M. E. Kutay. 2020. Performance evaluation of long-life pavements using the Mechanistic-Empirical Asphalt Pavement Analysis (MEAPA) web application. *Proceedings of the Ninth International Conference on Maintenance and Rehabilitation of Pavements*. Springer, Cham, Cham, Switzerland. pp. 79–89.

Goncalves, A., P. Ray, B. Soper, J. Stevens, L. Coyle, and A. P. Sales. 2020. Generation and evaluation of synthetic patient data. *BMC Medical Research Methodology*, Vol. 20, No. 1, pp. 1–40.

Gopalakrishnan, K., H. Ceylan, and N. O. Attoh-Okine (Eds). 2009. *Intelligent and Soft Computing in Infrastructure Systems Engineering*. Studies in Computational Intelligence Series, Vol. 259. Springer-Verlag, Inc., Berlin, Germany.

Haykin, S. 1999. *Neural Networks: A Comprehensive Foundation*. Prentice Hall, Upper Saddle River, NJ.

Hecht-Nielsen, R. 1990. *Neurocomputing*. Addison-Wesley, Boston, MA.

Highway Research Board. 1973. *Structural Design of Asphalt Concrete Pavements to Prevent Fatigue Cracking*. Special Report 140. Highway Research Board, Washington, DC.

Huang, Y. H. 2004. *Pavement Analysis and Design*. Volume 2. Prentice Hall, Upper Saddle River, NJ. pp. 401–409.

Hossain, M., and Z. Wu. 2002. *Estimation of Asphalt Pavement Life*. K-TRAN: KSU-97-6. Kansas State University, Manhattan, KS.

ICEA. 2022. About Secondary Roads. Iowa County Engineers Association. https://www.iowacountyroads.org/about-secondary-roads#general-information.
Kaya, O., H. Ceylan, S. Kim, D. Waid, and B. P. Moore. 2020. Statistics and artificial intelligence-based pavement performance and remaining service life prediction models for flexible and composite pavement systems. *Transportation Research Record*, Vol. 2674, No. 10, pp. 448–460.
Kaya, O., N. Citir, H. Ceylan, S. Kim, and D. Waid. 2023. Development of pavement performance and remaining service life prediction tools for Iowa jointed plain concrete pavement systems. *Journal of Transportation Engineering, Part B: Pavements*, Vol. 149, No. 1.
Khazanovich, L., and Q. Wang. 2007. MnLayer: High-performance layered elastic analysis program. *Transportation Research Record*, Vol. 2037, pp. 63–75.
Kleizienė, R., A. Vaitkus, D. and Čygas. 2016. Influence of asphalt visco-elastic properties on flexible pavement performance. *The Baltic Journal of Road and Bridge Engineering*, Vol. 11, No. 4, pp. 313–323.
Kutay, M. E., and M. Lanotte. 2020. *Formulations of the Pavement Performance Prediction Models in the Mechanistic-Empirical Asphalt Pavement Analysis (MEAPA) Web Application*. Michigan Economic Development Corporation and Michigan State University, Lansing, MI. https://paveapps.com/meapaapp2/images/MEAPADocumentation_V3.pdf.
Lav, A. H., A. B. Goktepe, and M. A. Lav. 2009. Backcalculation of flexible pavements using soft computing. 2009. *Intelligent and Soft Computing in Infrastructure Systems Engineering*. Studies in Computational Intelligence Series, Vol. 259. Springer-Verlag, Inc., Berlin, Germany. pp. 67–106.
Li, G., Y. Li, J. B. Metcalf, and S. S. Pang. 1999. Elastic modulus prediction of asphalt concrete. *Journal of Materials in Civil Engineering*, Vol. 11, No. 3, pp. 236–241.
Majidzadeh, K., F. Bayomy, and S. Khedr. 1978. Rutting evaluation of subgrade soils in Ohio. *Transportation Research Record*, Vol. 671, pp. 75–84.
Muniandy, R., E. Aburkaba, and N. Thamer. 2013. Comparison of flexible pavement performance using KENLAYER and CHEVPC software program. *Australian Journal of Basic and Applied Sciences*, Vol. 7, No. 9, pp. 112–119.
Nijboer, L. W. 1955. *Dynamic Investigations of Road Constructions*. Shell Bitumen Nomograph No. 2. London, UK.
Odemark, N. 1949. *Investigations as to the Elastic Properties of Soils and Design of Pavements According to the Theory of Elasticity*. Statens Vaeginstitute, Stockholm, Sweden.
Owende, P. M., A. M. Hartman, S. M. Ward, M. D. Gilchrist, and M. J. O'Mahony. 2001. Minimizing distress on flexible pavements using variable tire pressure. *Journal of Transportation Engineering*, Vol. 127, No. 3, pp. 254–262.
Park, H. M., and Y. R. Kim. 2003. Prediction of remaining life of asphalt pavement with falling weight deflectometer multiload-level deflections. *Transportation Research Record*, Vol. 1860, pp. 48–56.
Parker, D. B. 1985. *Learning Logic*. Technical Report TR-47. Center for Computational Research in Economics and Management Science, Massachusetts Institute of Technology, Cambridge, MA.

Powell, W. D., J. F. Potter, H. C. Mayhew, and M. E. Nunn. 1984. *The Structural Design of Bituminous Roads*. TRRL Laboratory Report 1132. Transport and Road Research Laboratory, Crowthorne, Berkshire, UK.

Priest, A. 2005. *Calibration of Fatigue Transfer Functions for Mechanistic-Empirical Flexible Pavement Design*. PhD dissertation. Auburn University, Auburn, AL.

Pronk, A. C. 1993. The Pasternak Foundation: An attractive alternative for the Winkler Foundation. *Fifth International Conference on Concrete Pavement Design and Rehabilitation, Volume 1*. Purdue University, West Lafayette, IN.

Pronk, A. C. 1994. *Equivalent Layer Theories: State of the Art Report*. DWW Werkdocument W-DWW-94-904. Dienst Weg-En Waterbouwkunde (DWW), Delft, Netherlands.

Qiu, Y., N. Dennis, and R. Elliott. 2000. Design criteria for permanent deformation of subgrade soils in flexible pavements for low-volume roads. *Soils and Foundations*, Vol. 40, No. 1, pp. 1–10.

Raad, L., and J. L. Figueroa. 1980. Load response of transportation support systems. *Journal of Transportation Engineering*, Vol. 106, No. 1, pp. 111–128.

Rakesh, N., A. K. Jain, M. A. Reddy, and K. S. Reddy. 2006. Artificial neural networks—genetic algorithm-based model for backcalculation of pavement layer moduli. *International Journal of Pavement Engineering*, Vol. 7, No. 3, pp. 221–230.

Reddy, M. A., K. S. Reddy, and B. B. Pandey. 2004. Selection of genetic algorithm parameters for backcalculation of pavement moduli. *International Journal of Pavement Engineering*, Vol. 5, No. 2, pp. 81–90.

Rezaei-Tarahomi, A., H. Ceylan, K. Gopalakrishnan, S. Kim, O. Kaya, and D. R. Brill. 2019. Artificial neural network models for airport rigid pavement top-down critical stress predictions: Sensitivity evaluation. *Airfield and Highway Pavements 2019: Innovation and Sustainability in Highway and Airfield Pavement Technology*. American Society of Civil Engineers, Reston, VA. pp. 302–312.

Rind, T. A., A. A. Jhatial, A. R. Sandhu, I. A. Bhatti, and S. Ahmed. 2019. Fatigue and rutting analysis of asphaltic pavement using KENLAYER software. *Journal of Applied Engineering Sciences*, Vol. 90, No. 2.

Rodway, B. 1995. The impact of new-generation large aircraft on the structural design of flexible pavements. *Proceedings, Airports 95*, October 9–11, Sydney, Australia.

Rumelhart, D. E., G. E. Hinton, and R. J. Williams. 1986. Learning representations by back-propagating errors. *Nature*, Vol. 323, pp. 533–536.

Saleh, M. 2016. A mechanistic-empirical approach for the evaluation of the structural capacity and remaining service life of flexible pavements at the network level. *Canadian Journal of Civil Engineering*, Vol. 43, No. 8, pp. 749–758.

Salles, L. S., Z. Wan, and L. Khazanovich. 2022. Tire footprint analysis of agricultural vehicles for rural pavements. *Eleventh International Conference on the Bearing Capacity of Roads, Railways, and Airfields, Volume 2*. CRC Press, Boca Raton, FL. pp. 360–369

Saltan, M., M. Tiğdemir, and M. Karaşahin. 2002. Artificial neural network application for flexible pavement thickness modeling. *Turkish Journal of Engineering and Environmental Sciences*, Vol. 26, No. 3, pp. 243–248.

Southgate, H. F., R. C. Deen, J. H. Havens, and W. B. Drake. 1976. *Kentucky Research: A Flexible Pavement Design and Management System*. Research Report 455. Kentucky Transportation Cabinet, Lexington, KY.

Sun, L. 2016. The precise design of asphalt pavement. *Structural Behavior of Asphalt Pavements.* Butterworth-Heinemann, Oxford, UK. pp. 923–940.

Srikanth, M. R. 2015. Study on effect of surface course thickness and modulus of elasticity on performance of flexible pavement using a software tool. *International Journal of Engineering Research & Technology*, Vol. 4, No. 8, pp. 771–774.

Thompson, M. R. 1987. ILLI-PAVE based full-depth asphalt concrete pavement design procedure. *Proceedings of the Sixth International Conference on the Design of Asphalt Pavements, July 13–17, Ann Arbor, Michigan, Volume 1*. International Society for Asphalt Pavements, Lino Lakes, MN. pp. 13–22.

Timm, D., B. Birgisson, and D. Newcomb. 1998. Development of mechanistic-empirical pavement design in Minnesota. *Transportation Research Record*, Vol. 1629, pp. 181–188.

Tsai, B. W., J. T. Harvey, and C. L. Monismith. 2009. Case studies of asphalt pavement analysis/design with application of the genetic algorithm. *Intelligent and Soft Computing in Infrastructure Systems Engineering*. Studies in Computational Intelligence Series, Vol. 259. Springer-Verlag, Inc., Berlin, Germany. pp. 205–238.

Ullidtz, P., and K. R. Peattie. 1982. Programmable calculators in the assessment of overlays and maintenance statistics. *Proceedings of the Fifth International Conference on the Design of Asphalt Pavements, August 23–26, Delft University of Technology, Netherlands, Volumes 1 and 2*. International Society for Asphalt Pavements, Lino Lakes, MN.

Ullidtz, P. 1987. *Pavement Analysis*. Elsevier, Amsterdam, Netherlands.

Werbos, P. 1974. *Beyond Regression: New Tools for Prediction and Analysis in the Behavioral Sciences*. PhD dissertation. Harvard University, Cambridge, MA.

Van Gurp, C. A. P. M. 1995. *Characterization of seasonal influences on asphalt pavements with the use of falling weight deflectometers*. PhD dissertation. Delft University of Technology, Delft, Netherlands. http://resolver.tudelft.nl/uuid:596d5b28-308d-4c74-a3b8-cad632a93619.

Verstraeten, J., Veverka, V. and Francken, L. 1982. Rational and practical designs of asphalt pavements to avoid cracking and rutting. *Proceedings of the Fifth International Conference on the Design of Asphalt Pavements, August 23–26, Delft University of Technology, Netherlands, Volumes 1 and 2*. International Society for Asphalt Pavements, Lino Lakes, MN.

Ziyadi, M., and I. L. Al-Qadi. 2017. Efficient surrogate method for predicting pavement response to various tire configurations. *Neural Computing and Applications*, Vol. 28, No. 6, pp. 1355–1367.

APPENDIX. PROGRAMMING CODE OF PSAT

Example of Source Code by Python Software to Develop ANN Models

```
import matplotlib.pyplot as plt
import numpy as np
import pandas as pd
from sklearn.model_selection import train_test_split
from sklearn.model_selection import cross_val_score
from sklearn.neural_network import MLPRegressor
from sklearn.model_selection import GridSearchCV


#################### Import Input and Output files ####################
x= pd.read_excel('../Input.xlsx') # train inputs
y= pd.read_excel('../Output.xlsx') # train outputs

######################## Train the ANN model ######################
regr = MLPRegressor(random_state=1, activation = 'relu',
                    hidden_layer_sizes=(50,),
                    learning_rate='adaptive', max_iter=500,
                    solver = 'adam', alpha = 0.0001,
                    batch_size = 16, verbose=True,
                   momentum = 0.9, learning_rate_init=0.001)

X=x
Y=y

activn = ['tanh']
hiddenLayers = [(128, 128)]
slvrs = ['sgd']
alphaS = [0]
btchSize = [1]
mmnts = [0.9]
lrInit = [0.001]

param_grid = dict(hidden_layer_sizes=hiddenLayers,
                  activation=activn, solver=slvrs,
                 alpha = alphaS, batch_size = btchSize,
                 momentum = mmnts, learning_rate_init = lrInit)
grid = GridSearchCV(estimator=regr, param_grid=param_grid, cv=10, scoring='r2',
return_train_score=True)
grid_result = grid.fit(X, Y)

print("Best: %f using %s" % (grid_result.best_score_, grid_result.best_params_))
means = grid_result.cv_results_['mean_test_score']
```

```
stds = grid_result.cv_results_['std_test_score']
params = grid_result.cv_results_['params']
for mean, stdev, param in zip(means, stds, params):
    print("%f (%f) with: %r" % (mean, stdev, param))


###################### Export the ANN model ######################
print("best index=" , grid_result.best_index_)
print("best score=" ,grid_result.best_score_)
print("best estimator=" ,grid_result.best_estimator_)

gridcvresults = pd.DataFrame(grid_result.cv_results_)
gridcvresults.to_excel("Model_gridcv_results.xlsx")

bestparams=np.transpose(pd.DataFrame(pd.DataFrame(grid_result.best_estimator_.get_params()
).iloc[0,:]))
bestparams.to_excel("Model_gridcv_bestparams.xlsx")

# If there is 1 hidden layer
# Extract weights
weights_layer1=pd.DataFrame(grid_result.best_estimator_.coefs_[0])
weights_layer2=pd.DataFrame(grid_result.best_estimator_.coefs_[1])

weights_layer1.to_excel("Model_gridcv_weights_layer1.xlsx")
weights_layer2.to_excel("Model_gridcv_weights_layer2.xlsx")

# Extract bias
bias_layer1=pd.DataFrame(grid_result.best_estimator_.intercepts_[0])
bias_layer2=pd.DataFrame(grid_result.best_estimator_.intercepts_[1])

bias_layer1.to_excel("Model_gridcv_bias_layer1.xlsx")
bias_layer2.to_excel("Model_gridcv_bias_layer2.xlsx")
```

Example of Script by VBA in Excel to Develop PSAT

```
'Macro for Predicting Deflection
Sub Deflection()
Unhide_Deflection
'Sheet1.protect UserInterfaceOnly:=False
'Unprotect

Dim Cell As Range
Dim Paste As Range
Dim CellsEmpty As Boolean
CellsEmpty = True

"""""""""""""""""""""""""""""""""""" General Check""""""""""""""""""""""""""""""""""""
"""""""""" If Both HMA Is Empty:
'If first HMA layer for PS-1 is empty, continue;
If Sheet1.Application.WorksheetFunction.CountBlank(Range("B48:B50")) = 3 Then
   If Sheet1.Application.WorksheetFunction.CountBlank(Range("D48:D50")) = 3 Then
   'If first HMA layer for PS-2 is empty, exit;
      Sheet1.Select
      Range("B64:B66").Select
      Selection.ClearContents
      Sheet1.Select
      Range("D64:D66").Select
      Selection.ClearContents
      MsgBox "Please enter first layer HMA information"
      GoTo EndSub
   End If
Else
GoTo NextStep
End If
NextStep:
EndSub:

"""""""""" If PS-1 Is Empty:
'If first HMA layer for PS-1 is full, exit;
If Sheet1.Application.WorksheetFunction.CountBlank(Range("B48:B50")) = 0 Then
   GoTo NextStep1
Else
   Sheet1.Select
   Range("B64:B66").Select
   'Selection.ClearContents
   GoTo EndSub1
End If
NextStep1:
EndSub1:
```

```
''''''''''''''' If PS-2 Is Empty:
'If first HMA layer for PS-2 is full, exit;
If Sheet1.Application.WorksheetFunction.CountBlank(Range("D48:D50")) = 0 Then
   GoTo NextStep2
Else
   Sheet1.Select
   Range("D64:D66").Select
   'Selection.ClearContents
   GoTo EndSub2
End If
NextStep2:
EndSub2:

'''''''''''''''''''''''''''''''''''''''''''''''''''''' Specific Check''''''''''''''''''''''''''''''''''''''''''''''''''''''
'''''''''''''' ANN Model for PS with Stabilized Base – PS-1 ''''''''''''''
'If stabilized base layer is empty, exit;
If Sheet1.Application.WorksheetFunction.CountBlank(Range("B51:B53")) = 3 Then
   Sheet1.Select
   Range("B64:B66").Select
   Selection.ClearContents
   GoTo NextStep3
'If granular base layer -also- is full, exit;
ElseIf Sheet1.Application.WorksheetFunction.CountBlank(Range("B54:B56")) = 0 Then
   Sheet1.Select
   Range("B64:B66").Select
   Selection.ClearContents
   GoTo NextStep3a
'If stabilized base layer is full, continue;
Else
   Sheet1.Select
   Range("B64:B66").Select
   Selection.ClearContents

   Sheet21.Select
   Range("B41:B43").Select   'Deflections
   Application.CutCopyMode = False
   Selection.Copy
   Sheet1.Select
   Range("B64:B66").Select
   ActiveSheet.Paste Link:=True
   GoTo NextStep2222:

End If
NextStep3:
NextStep3a:
```

```
""""""""""""""" ANN Model for PS with Granular Base – PS-1 """""""""""""""
'If granular base layer is empty, exit;
If Sheet1.Application.WorksheetFunction.CountBlank(Range("B54:B56")) = 3 Then
   Sheet1.Select
   Range("B64:B66").Select
   Selection.ClearContents
   GoTo NextStep4
'If stabilized base layer -also- is full, exit;
ElseIf Sheet1.Application.WorksheetFunction.CountBlank(Range("B51:B53")) = 0 Then
   Sheet1.Select
   Range("B64:B66").Select
   Selection.ClearContents
   GoTo NextStep4a
'If granular base is full, continue;
Else
   Sheet1.Select
   Range("B64:B66").Select
   Selection.ClearContents

   Sheet28.Select
   Range("B41:B43").Select  'Deflections
   Application.CutCopyMode = False
   Selection.Copy
   Sheet1.Select
   Range("B64:B66").Select
   ActiveSheet.Paste Link:=True
   GoTo NextStep2222:
End If
NextStep4:
NextStep4a:

""""""""""""""" ANN Model for PS with Stabilized Base and Granular Base – PS-1 """""""""""""""
'If stabilized base and granular base layers are empty, exit;
If Sheet1.Application.WorksheetFunction.CountBlank(Range("B51:B56")) = 6 Then
   Sheet1.Select
   Range("B64:B66").Select
   Selection.ClearContents
   GoTo NextStep5
'If stabilized base and granular base layers are full, continue;
ElseIf Sheet1.Application.WorksheetFunction.CountBlank(Range("B51:B56")) = 0 Then
   Sheet1.Select
   Range("B64:B66").Select
   Selection.ClearContents

   Sheet30.Select
   Range("B44:B46").Select  'Deflections
```

```
    Application.CutCopyMode = False
    Selection.Copy
    Sheet1.Select
    Range("B64:B66").Select
    ActiveSheet.Paste Link:=True
    GoTo NextStep2222:
'Other any condition, exit;
Else
    Sheet1.Select
    Range("B64:B66").Select
    Selection.ClearContents
    GoTo NextStep5a
End If
NextStep5:
NextStep5a:
NextStep2222:
""""""""""""""" ANN Model for PS with Stabilized Base – PS-2 """""""""""""""
'If stabilized base layer is empty, exit;
If Sheet1.Application.WorksheetFunction.CountBlank(Range("D51:D53")) = 3 Then
    Sheet1.Select
    Range("D64:D66").Select
    Selection.ClearContents
    GoTo NextStep6
'If granular base layer -also- is full, exit;
ElseIf Sheet1.Application.WorksheetFunction.CountBlank(Range("D54:D56")) = 0 Then
    Sheet1.Select
    Range("D64:D66").Select
    Selection.ClearContents
    GoTo NextStep6a
'If stabilized base layer is full, continue;
Else
    Sheet1.Select
    Range("D64:D66").Select
    Selection.ClearContents

    Sheet21.Select
    Range("B349:B351").Select   'Deflections
    Application.CutCopyMode = False
    Selection.Copy
    Sheet1.Select
    Range("D64:D66").Select
    ActiveSheet.Paste Link:=True
    'protect
    Hide_Deflection
    Exit Sub
End If
```

```
NextStep6:
NextStep6a:
""""""""""""""" ANN Model for PS with Granular Base – PS-2 """""""""""""""
'If granular base layer is empty, exit;
If Sheet1.Application.WorksheetFunction.CountBlank(Range("D54:D56")) = 3 Then
   Sheet1.Select
   Range("D64:D66").Select
   Selection.ClearContents
   GoTo NextStep7
'If stabilized base layer -also- is full, exit;
ElseIf Sheet1.Application.WorksheetFunction.CountBlank(Range("D51:D53")) = 0 Then
   Sheet1.Select
   Range("D64:D66").Select
   Selection.ClearContents
   GoTo NextStep7a
'If granular base is full, continue;
Else
   Sheet1.Select
   Range("D64:D66").Select
   Selection.ClearContents

   Sheet28.Select
   Range("B349:B351").Select  'Deflections
   Application.CutCopyMode = False
   Selection.Copy
   Sheet1.Select
   Range("D64:D66").Select
   ActiveSheet.Paste Link:=True
   'protect
   Hide_Deflection
   Exit Sub
End If
NextStep7:
NextStep7a:
""""""""""""""" ANN Model for PS with Stabilized Base and Granular Base – PS-2 """""""""""""""
'If stabilized base and granular base layers are empty, exit;
If Sheet1.Application.WorksheetFunction.CountBlank(Range("D51:D56")) = 6 Then
   Sheet1.Select
   Range("D64:D66").Select
   Selection.ClearContents
   GoTo NextStep8
'If stabilized base and granular base layers are full, continue;
ElseIf Sheet1.Application.WorksheetFunction.CountBlank(Range("D51:D56")) = 0 Then
   Sheet1.Select
   Range("D64:D66").Select
   Selection.ClearContents
```

```
    Sheet30.Select
    Range("B352:B354").Select 'Deflections
    Application.CutCopyMode = False
    Selection.Copy
    Sheet1.Select
    Range("D64:D66").Select
    ActiveSheet.Paste Link:=True
    'protect
    Hide_Deflection
    Exit Sub
'Other any condition, exit;
Else
    Sheet1.Select
    Range("D64:D66").Select
    Selection.ClearContents
    GoTo NextStep8a
End If
NextStep8:
NextStep8a:
'protect
Hide_Deflection
End Sub

'Sub Unprotect()
'Sheet1.Unprotect Password:=…
'End Sub

'Sub protect()
'Sheet1.protect Password:=…
'End Sub

Sub Unhide_Deflection()
Sheet21.Visible = xlSheetVisible
Sheet28.Visible = xlSheetVisible
Sheet30.Visible = xlSheetVisible
Sheet4.Visible = xlSheetVisible
End Sub

Sub Hide_Deflection()
Sheet21.Visible = xlSheetVeryHidden
Sheet28.Visible = xlSheetVeryHidden
Sheet30.Visible = xlSheetVeryHidden
Sheet4.Visible = xlSheetVeryHidden
End Sub
```

THE INSTITUTE FOR TRANSPORTATION IS THE FOCAL POINT FOR TRANSPORTATION AT IOWA STATE UNIVERSITY.

InTrans centers and programs perform transportation research and provide technology transfer services for government agencies and private companies;

InTrans contributes to Iowa State University and the College of Engineering's educational programs for transportation students and provides K–12 outreach; and

InTrans conducts local, regional, and national transportation services and continuing education programs.

IOWA STATE UNIVERSITY

Visit **InTrans.iastate.edu** for color pdfs of this and other research reports.